January 2022

Thermal Stability And Decomposition Of Per- And Polyfluoroalkyl Substances (PFAS) Using Granular Activated Carbon And Other Porous Materials

Pavankumar Challa Sasi

THERMAL STABILITY AND DECOMPOSITION OF PER- AND POLYFLUOROALKYL SUBSTANCES (PFAS) USING GRANULAR ACTIVATED CARBON AND OTHER POROUS MATERIALS

by

Pavankumar Challa Sasi
Bachelor of Engineering, Anna University, India, 2011
Master of Engineering, University of North Dakota, 2015

A Dissertation

Submitted to the Graduate Faculty

of the

University of North Dakota

in partial fulfillment of the requirements

for the degree of

Doctor of Philosophy

Grand Forks, North Dakota

August 2022

Name: Pavankumar Challa Sasi

Degree: Doctor of Philosophy

This document, submitted in partial fulfillment of the requirements for the degree from the University of North Dakota, has been read by the Faculty Advisory Committee under whom the work has been done and is hereby approved.

DocuSigned by:
Dr. Feng (Frank) Xiao
Dr. Feng (Frank) Xiao

DocuSigned by:
Taufique H Mahmood
Dr. Taufique Mahmood

DocuSigned by:
Howe Lim
Dr. Howe Lim

DocuSigned by:
Dr. Daba Gedafa
Dr. Daba Gedafa

DocuSigned by:
Dr. Michael Mann
Dr. Michael Mann

This document is being submitted by the appointed advisory committee as having met all the requirements of the School of Graduate Studies at the University of North Dakota and is hereby approved.

DocuSigned by:
Chris Nelson
Chris Nelson
Dean of the School of Graduate Studies

7/19/2022
Date

PERMISSION

Title Thermal Stability and Decomposition of Per- And Polyfluoroalkyl Substances (PFAS) Using Granular Activated Carbon and Other Porous Materials

Department Civil Engineering

Degree Doctor of Philosophy

In presenting this dissertation in partial fulfillment of the requirements for a graduate degree from the University of North Dakota, I agree that the library of this University shall make it freely available for inspection. I further agree that permission for extensive copying for scholarly purposes may be granted by the professor who supervised my dissertation work or, in his absence, by the Chairperson of the department or the dean of the School of Graduate Studies. It is understood that any copying or publication or other use of this dissertation or part thereof for financial gain shall not be allowed without my written permission. It is also understood that due recognition shall be given to me and the University of North Dakota in any scholarly use which may be made of any material in my dissertation.

Pavankumar Challa Sasi

07/18/2022

ACKNOWLEDGMENTS

I wish to express my sincere appreciation to my advisor, Dr. Feng “Frank” Xiao, and all other members of the committee for their guidance and support during my time in the Doctoral program at the University of North Dakota (UND). Further I would also like to acknowledge the support of the Civil Engineering department for providing me with the appropriate resources for research and conducting experiments. Acknowledgment also extends to the North Dakota Water Resources and Research Institute and United State Geological Survey for providing fellowship grant and additional federal grants from my advisor, Dr. Xiao. I would also like to thank my fellow team members Ali Alinezhad, Dr. Bin Yao, Mansurat Abdulmalik Ali, Runze Sun, and Shwetha Mallula for their constant support and help.

My education and research would not be possible without the moral and emotional support of my mom (Madhavi Challa), dad (Satyanarayana Challa) and sister (Dr. Sathya Challa). They gave me the necessary freedom to pursue my dream and remain to be my pillars of support in all endeavors of my life. Finally, the acknowledgments would not be complete without a heart-felt thanks to my friends Karthik Balaji and Anai Caparo Bellido who made sure I never wavered from my goals.

TABLE OF CONTENTS

LIST OF FIGURES

ABSTRACT

Per- and polyfluoroalkyl substances (PFAS) are anthropogenic chemicals that have been produced for decades as either processing aids or individual ingredients in many industrial and commercial products, including aqueous film-forming foams (AFFFs), non-stick cookware, and fast-food packaging. PFOA and PFOS have been reported in >95% of blood samples collected during multiple U.S. national surveys at concentrations that are a risk to human health. Thermal treatment is routinely used to reactivate the spent granular activated carbon (GAC) from water purification facilities. The aims of this study were: (1) to improve our understanding of the thermal stability of per- and polyfluoroalkyl substances; (2) to investigate their decomposition mechanisms on spent granular activated carbon (GAC) during thermal reactivation; and (3) present a detailed investigation of the fate of per- and polyfluoroalkyl substances (PFAS) and one PFAS alternative (GenX) in thermal processes, focusing on the effect of GAC. We studied seven perfluoroalkyl carboxylic acids (PFCAs), three perfluoroalkyl sulfonic acids (PFSAs), and one perfluoroalkyl ether carboxylic acid (PFECA) in different atmospheres (N_2, O_2, CO_2, and air). We found that the destabilization of studied compounds during thermal treatment followed first-order kinetics. The temperature needed for thermally destabilizing PFCAs increased with the

number of perfluorinated carbons (n_{CF2}). Decomposition of PFCAs such as perfluorooctanoic acid (PFOA) on GAC initiated at temperatures as low as 200 °C. The PFECA was even more readily decomposed than PFCA with the same n_{CF2}. PFSAs such as perfluorooctanesulfonic acid (PFOS), on the other hand, required a much higher temperature (≥450 °C) to decompose. Volatile organofluorine species were the main thermal decomposition product of PFOA and PFOS at low to moderate temperatures (≤600 °C). Efficient mineralization to fluoride ions (>80%) of PFOA and PFOS on GAC occurred at 700 °C or higher, accompanied by near complete PFOA and PFOS decomposition (>99.9%). We demonstrate that the thermolysis of perfluoroalkyl carboxylic acids (PFCAs), including perfluorooctanoic acid (PFOA), and GenX can occur at temperatures of 150–200 °C. Three temperature zones were discovered for PFOA, including a stable and nonvolatile zone (≤90 °C), a phase-transfer and thermal decomposition zone (90–400 °C), and a fast decomposition zone (≥400 °C). The thermal decomposition began with the homolysis of a C–C bond next to the carboxyl group of PFCAs, which formed unstable perfluoroalkyl radicals. Dual decomposition pathways seem to exist. The addition of a highly porous adsorbent, such as GAC or a copolymer resin, compressed the intermediate sublimation zone of PFCAs, changed their thermal decomposition pathways, and increased the decomposition rate constant by up to 150-fold at 250 °C. The results indicate that the observed thermal decomposition acceleration was linked to the adsorption of gas-phase PFCA molecules on GAC. Overall, the results indicate that (1) decomposition of PFCAs and GenX in thermal water/wastewater/sludge/waste treatments is very likely provided sufficiently high temperatures are used, and (2) the presence or addition of GAC or other highly porous materials can accelerate thermal PFAS decomposition.

1. CHAPTER 1: Introduction and Overview

1.1. Background on Per- and Polyfluoroalkyl Substances

With the advent of chemicals, our day to day lives became simpler which paved the way to develop technological marvels without which the current world would not operate. Due to lack of foresight and accountability harmful substances are released into our delicate ecosystem. One such invention is these synthetic organic compounds called per- and polyfluoroalkyl substances (PFAS) by DuPont in the 1940s. In 1950s, developed Teflon and Scotchgard using perfluorooctanoic acid (PFOA) and perfluorooctanesulfonic acid (PFOS) for the manufacture of nonstick cookware and other products. Their ability to repel water, dirt and oils meant they could be used in a plethora of commercial and household products such as stain repellents, surface coatings, fire-fighting foams, and cleaners (Paul et al., 2009). As is often the case with industrial chemicals, PFAS did not remain solely in their intended places. By late 1990s, the scientific community regarded them as global contaminants due to them being highly stable, persistent, bioaccumulative, toxic, and ubiquitously present in the environment, biota and humans (Conder et al., 2008; Ericson et al., 2009; Lindstrom et al., 2011; Nabb et al., 2007; Prevedouros et al., 2006; Strynar et al., 2015). For more than 50 years PFAS compounds were released into our environment, polluting rivers, lakes, forests and groundwater. Due to increased awareness of the harmful health effects, companies voluntarily phased out production in the early 2000s in the United States however production continued in the rest of the world. The two most commonly detected classes of PFASs are perfluoroalkylsulfonic acids (PFSAs) and perfluorocarboxylic acids (PFCAs). The total emissions of PFOS between 1958 and 2015 were estimated as 1228-4930 tons and for PFOS precursors as 1230-8738 tons (Armitage

et al., 2009). In a recent study, it is estimated that an additional 8-153 tons of PFOS will be released during the years 2016-2030 (Wang et al., 2017). For perfluorohexanesulfonic acid (PFHxS), perfluorodecanesulfonic acid (PFDS) it is 120-1022 and 38-378 tons, respectively. Similarly, an additional 2-89 and 0-2 tons are expected to be released during the years 2016-2030 (Boucher et al., 2019) for PFHxS and PFDS respectively. In the case of PFCAs, estimates suggest that 2610-21400 tons of C_4-C_{14} PFCAs were released between 1951-2015 and projects an additional 20-6420 tons during the years 2015-2030 (Wang et al., 2014). Due to the phase out of legacy PFAS compounds, shorter-chain alternatives such as perfluoroether carboxylic acids (PFECAs) are being adopted. Hexafluoropropylene oxide dimer acid (HFPO-DA) or the trade name GenX is a popular alternative for PFOA has been widely detected in the environment and recent studies suggest these alternatives may be as toxic if not more than their predecessors.

1.2. Toxicity:

The exceptional properties that make PFAS highly useful for manufacturing products also make them highly persistent and toxic in the environment. PFAS compounds have been detected in the surface water (Banzhaf et al., 2017; D'Agostino and Mabury, 2017; Lindstrom et al., 2011), groundwater (Moody et al., 2003) and even the remotest regions, such as the High Arctic (Young et al., 2007). PFAS substances were found in the Norwegian arctic marine food web which showed significant amounts in seabirds, fish, and ice amphipods in which PFOS displayed the highest concentrations (Haukas et al., 2007). PFAS accumulation was also shown in agricultural plants where they can transfer to humans through the food web. Long-chain PFAS such as PFOA and PFOS were less accumulated in potatoes and cereal seeds while short-chain compounds showed higher

levels of accumulation in leafy vegetables and fruits (Ghisi et al., 2019). Data from the National Health and Nutrition Examination Survey (NHANES) showed that >98% of blood samples collected in the U.S. detected PFAS in the blood serums (Calafat et al., 2007). Exposure to PFAS has been linked to several health problems (Fenton et al., 2021; Grandjean and Clapp, 2015), including cancer (Sunderland et al., 2019), elevated cholesterol (Nelson Jessica et al., 2010), obesity, immune suppression, and endocrine disruption. The earliest studies on adverse effects to human health due to PFAS exposure were conducted by 3M in the 1980s. The factory workers had organic fluorine concentrations 10 times higher than the general population (Sunderland et al., 2019). In a 90-day study conducted in 1988 on monkeys to determine the carcinogenic nature of N-ethyl perfluorooctane sulfonamidoethanol (N-EtFOSE), all the monkeys in different treatment groups died after just 20 days with a dosage of 10mg/kg/day (Goldenthal et al., 1979). In humans, young children are more vulnerable to PFAS exposures and studies have positively correlated to health risks such as dyslipidemia, immunity, renal function and age at menarche (Rappazzo et al., 2017). In children between 5 and 7 years old, elevated exposures to PFAS were associated with reduced humoral immune response to routine childhood immunizations (Granum et al., 2013). In breastfeeding toddlers, the total PFAS concentrations were higher than their mothers and, in some cases, it was more than 10 times higher. The PFAS concentrations increased 3-5% every month during the breastfeeding duration (Mogensen et al., 2015; Sagiv et al., 2015). More recently, PFAS was found in fast-food packaging, women's beauty products and in pesticides, which could be an additional source of exposure to humans.

While the legacy long-chain PFAS have been phased out of production manufacturers have replaced them with shorter-chain versions of the legacy compounds. These alternative compounds such as GenX, 4,8-dioxa-3H-perfluorononanoate (ADONA), chlorinated polyfluorinated ether sulfonic acid (6:2 Cl-PFESA) and its hydrogen substituted analogue (6:2 H-PFESA) are frequently detected in countries across the world (Pan et al., 2018). Cl-PFESAs were detected in >98% of the individuals from a metal working plant in China and it was estimated that the median half-life for renal clearance is 280 years (Shi et al., 2016). They are more -soluble and hydrophilic than the long-chain compounds, making them more mobile and persistent (Ateia et al., 2019; Li et al., 2020). Groundwater from non-industrial regions in China were analyzed and short-chain compounds were detected at an alarming 62.75-100% of the samples compared to only 40% detection of long-chain compounds (Wei et al., 2018). Studies indicate that these alternatives have systemic multiple organ toxicities similar to their predecessors, if not more harmful (Wang et al., 2019). Depending on the serum concentrations, short-chain compounds such as PFHxS had a considerably longer half-life compared to the longer-chain counterparts PFOA and PFOS. The estimated average half-lives were reported to be 3.4 - 5.4 years for PFOS, 5.3 - 8.5 years for PFHxS and 2.7 - 3.8 years for PFOA in humans (Li et al., 2018; Olsen et al., 2007).

1.3. Exposure Pathways

Human exposure to PFAS occurs through contaminated drinking water, dietary intake, indoor air, dust, clothing, personal care products and other contaminated media (Sunderland et al., 2019). Drinking water is the major source of PFAS exposure to the general population (De Silva et al., 2021) followed by dust inhalation and dermal

adsorption (Poothong et al., 2020). In the United States, drinking water is the primary source of PFAS exposure with more than 6 million US residents with drinking water supplies exceed US EPA's old health advisory levels (HAL) of 70 parts per trillion (ppt) for PFOA and PFOS (Hu et al., 2016).

Other exposure pathways such as dietary intake was estimated to be 250 ng/day for PFCAs and PFOS according to samples from 1992 - 2004 where subjects were consuming seafood, meat, poultry, frozen entrees, fast food and microwave popcorn (Tittlemier et al., 2007). The legacy compounds PFOA and PFOS were the most frequently detected among all food sources. A common trend across the world shows that seafood and fish contain the highest concentration of PFAS (Jian et al., 2017; Domingo and Nadal, 2017) and the exposure through dietary intake was the highest for children due to dosage factor (Domingo et al., 2012).

Biosolids generated from the wastewater treatment plants are often used for land application or for fertilizer in agriculture in the United States, presenting another vector for human exposure. In a nationwide study of biosolids ten out of thirteen PFAS analyzed were consistently detected and PFOS was the most abundant PFAS detected at a dry weight of 403 ± 127 ng/g (Venkatesan and Halden, 2013). Out of the annual biosolids load, 60% is applied to agricultural land as fertilizers, 17% is shipped to landfills and 20% to incineration facilities (Venkatesan and Halden, 2013). Unlined landfills are another source of PFAS release to the environment and likely represent a significant source of PFAS to the groundwater aquifers (Hepburn et al., 2019). It was estimated for the year 2013, 563 – 638 kg of PFAS was measured in landfill leachate across the nation (Lang et al., 2017).

PFAS and their precursor compounds have been detected in the indoor air of children's bedrooms (Harris et al., 2017; Winkens et al., 2017). The most frequently detected compound was 8:2 fluorotelomer alcohol (8:2 FTOH) even though the industries have transitioned to other compounds. Other PFAS compounds such as N-ethylperfluorooctane sulfonamidoethanol (EtFOSE), N-methylperfluorooctane sulfonamidethylacrylate (MeFOSEA) concentrations in the indoor were detected to be 10 – 20 times greater than the outdoor concentrations (Morales-Mcdevitt et al., 2021; Zheng et al., 2020). Another recent development in PFAS exposure and release is through cosmetics products such as foundations, mascaras and lip products (Schultes et al., 2018). Similar to indoor air samples 6:2 and 8:2 FTOHs were the most frequently detected in these cosmetic products which are a known precursor to harmful PFCAs (Whitehead et al., 2021). These compounds could easily build up in the wastewater streams and accumulation at landfills present an indirect exposure to the environment.

1.4. Regulations:

After the increased awareness in the early 2000s regarding potential harmful health impacts, large PFAS manufacturers voluntarily phased out PFOA and PFOS. In 2016 USEPA released a health advisory level which is not enforceable for PFOA and PFOS combined at a conservative 70 ppt. Due to the lack of national regulations, the U.S. saw an increasing number of states implementing policies or enacted laws to control and prevent further PFAS pollution (Brennan et al., 2021). The policies range from restricting PFAS in consumer products to action plans that aim to phase out PFAS chemicals. Connecticut and Maine have passed legislation to phase out the use of PFAS from consumer products as of 2021 (Legislature, 1989; Doll, 2021). California recently released a notification level of

6.5 ppt for PFOS and 5.1 ppt for PFOA in drinking water, following other states like New Jersey, New York, Vermont, New Hampshire, Michigan, Massachusetts, all proposing levels much lower than the USEPA's health advisory level. Many states are mandating testing and/or disclosure of PFAS in water (Doll, 2021).

In 2021, USEPA initiated the process to regulate PFOA and PFOS through the National Primary Drinking Water Regulation process (Kurwadkar et al., 2022). This process aims to review and gather feedback on health effects, strategies to reduce exposure by reducing the contaminations in drinking water and to determine Maximum Contaminant Level Goals (Agency, 2021). As part of this process, on June 21st, 2022, EPA updated lifetime HALs for PFOA, PFOS, GenX and PFBS at 4 parts per quadrillion (ppq), 20 ppq, 10 ppt and 2000 ppt respectively (EPA, 2022). Based on the 2016 HALs, nearly 60 million residents were under the risk of PFAS exposure from drinking water and if the levels were reduced to 1 ppt an estimated 200 million are exposed to PFAS (Andrews and Naidenko, 2020).

The Bipartisan Infrastructure Bill announced $10 billion towards PFAS cleanup of environment, drinking water and for small and disadvantages communities (EPA, 2021).

1.5. Treatment Technologies:

The conventional drinking water treatment technologies such as coagulation, flocculation and disinfection do not effectively remove PFAS from water (Rahman et al., 2014; Xiao et al., 2013b). In certain cases, during drinking water disinfection by ozone or chlorine, PFOA and PFOS were generated from their cationic/zwitterionic compounds (Xiao et al., 2018c). Advanced adsorption technologies such as GAC, Ion Exchange resins, reverse osmosis or nanofiltration have to be implemented to attain sufficient removal of

PFAS compounds (Appleman et al., 2013). Several innovative treatment technologies are under development to remove these compounds from our drinking water sources. Due to their persistent nature, toxicity and mobility, simply removing them from our water sources is not sufficient. Technologies that can degrade or destroy PFAS are needed however breaking the C-F bonds is an energy-intensive process. A more approachable solution would be to remove these compounds from the aqueous media using adsorption followed by a destruction technique.

1.5.1. Separation processes:

1.5.1.1. Surface Active Foam Fractionation:

Foam fractionation is a separation technique used for removing detergents, protein separation, downstream processing of biotechnological waste, metal industry and fish farms (Leonard and Lemlich, 1965). Although this technology was developed in the 1960s it was not that widely adopted in the water or wastewater treatment industry. However due to the recent awareness of PFAS contamination researchers began conducting studies on PFAS removal using foam fractionation technique. Due to their surface-active properties, PFAS compounds are ideal candidates for adsorption at gas-liquid interfaces (Tharapiwattananon et al., 1996). Several commercial scale trials have been conducted and reports show ≥99.5% PFOS, PFHxS and PFOA from the contaminated groundwaters at Army Aviation Centre Oakey, Australia (Burns et al., 2021). Similar results were observed in Sweden where ≥98.7% PFOS, ≥99.7% PFOA and ≥98.8% PFHxS were removed from landfill leachate (Burns et al., 2022). However, due to the low adsorption coefficients of short-chain compounds to air-bubble interface <50% removals were attributed to short-chain PFAS species including PFBA, PFPeA, PFBS and PFHxA (Burns et al., 2022; Burns

et al., 2021). In addition, it still produces a waste stream which has to be further treated using a destructive technique (Ross et al., 2018).

1.5.1.2. Ion exchange Resins:

Ion exchange (IX) resins are used in water treatment systems for water softening, heavy metal removal, wastewater, removal of inorganic ions and natural organic matter. The ion exchange process is a reversible exchange of ions from the surface of polymeric resin and a solution containing ions with the same charge. Based on the charge carried by the polymeric resin it is classified into two types, anion, and cation exchange resins. For PFAS removal, anion exchange resins have proven to be more effective than GAC, particularly for short-chain PFAS compounds (McCleaf et al., 2017; Zaggia et al., 2016; Yu et al., 2009b). A clear relationship is found between the hydrophobicity of the functional group of resin used (Zaggia et al., 2016), the perfluorocarbon chain length (McCleaf et al., 2017) and removal efficiency. Also, the presence of natural organic matter (NOM) can impact the removal efficiency of the resins (Gagliano et al., 2020). Regeneration of anion exchange resins using simple salt solutions is not effective in releasing PFAS but organic solvents offer better regeneration (Liu and Sun, 2021). However, using organic solvents on a commercial scale is not practical and hence resins used for PFAS removal are considered single use-and-dispose resins (Dixit et al., 2019). Although improvements in resin regeneration are underway a viable regenerant is yet to be found. Proper treatment and handling of the exhausted resins must be considered when opting IX resins for PFAS treatment. IX treatment studies are being coupled with destruction technologies such as electrochemical oxidation, plasma treatment, incineration, thermal destruction and supercritical oxidation.

1.5.1.3. Granular Activated Carbon (GAC):

GAC can remove various taste- and odor-producing compounds, natural organic matter, volatile organic compounds (VOCs), synthetic organic compounds, pesticides and disinfection byproduct precursors. GAC particles are manufactured from carbonaceous raw materials such as wood, bituminous coal, coconut shells etc., and has an extremely high internal surface area suitable to remove target contaminants to concentrations below 1 ug/L. It has been used in the drinking water production for decades due its reliability, low cost, versatility and it has been widely used to sorb various compounds (Merino et al., 2016). Naturally several studies were conducted to study the efficiency of PFAS removal using GAC. Initial studies focused on the two trademark compounds, PFOA, PFOS and found that GAC is effective at removing them at favorable loading capacities (Appleman et al., 2013; Belkouteb et al., 2020; Carter and Farrell, 2010; McCleaf et al., 2017; McNamara et al., 2018). The removal efficiency is dependent on the functional group and perfluorocarbon chain length. PFAS containing sulfonic groups and longer chain lengths were more readily adsorbed by GAC compared to the carboxylic group compounds and their shorter chained alternatives. Another concern with GAC is the problem with saturated GAC which in most cases ends up at landfills or incineration units where there is a possibility for PFAS compounds to desorb from the GAC and be released back into the environment. In case of incineration there is concern on PFAS being released in the atmosphere.

A unique advantage of GAC is its ability to be regenerated using a process called reactivation. Reactivation of GAC is performed under the presence of gases such as nitrogen, air or steam at temperatures ranging from 700 – 900 ºC, depending on the manufacturer and their specific proprietary product. Research has shown that in certain

cases the reactivated GAC is more effective at removing organic compounds due to an increase in microporous surface area.

1.5.2. Destructive Treatments:

1.5.2.1. Bioremediation:

The current state of research on the bioremediation of PFAS is limited and does not offer any promising results that can be implemented for PFAS remediation. Bioremediation is a very sensitive process with a narrow set of conditions and time-intensive. (Huang and Jaffe, 2019) showed that *acidimicrobium Sp. Strain A6* under acidic pH, iron-rich soil environment can promote the degradation of PFOS and PFOA. Under very high concentrations of 100 mg/L, 60% removal was observed during a 100-day incubation period. Major byproducts included fluoride ions, short-chain compounds, and acetate.

1.5.2.2. Electrochemical oxidation:

Electrochemical oxidation (EO) for PFAS decomposition has been studied using boron doped diamond (BDD) electrode, Ti/SnO2, PbO2 from lead acid battery and Ce/PbO2. The most efficient and successful technique seems to be using BDD electrode where studies have shown up to 99.7% removal of several PFAS compounds from different water matrices. This process has been widely studied on field-scale studies in tandem with other separation processes to achieve zero waste at end of the remediation process. Only 60% fluoride recovery has been observed suggesting PFAS decomposition generates short-chain intermediates. Even though BDD thin film electrode provides higher removal rates, the manufacturing process is expensive and complicated to build. Some limitations of EO include oxidation of precursor compounds lead to PFCAs and FASAs being generated, high energy consumption, leakage of heavy metals, hydrogen fluoride gas and strategies for disposing exhausted electrodes has to be taken in to account.

1.5.2.3. Plasma treatment:

Plasma treatment uses electricity to convert water into a mixture of highly reactive species including hydroxyl radicals, ozone, oxygen and hydrogen radicals (Merino et al., 2016; Singh et al., 2019). An inert gas such as argon is pumped through the submerged diffusers to generate bubbles. PFAS being surface active compounds adsorb at the air water liquid interface of the bubbles and form a thin layer on the liquid surface. Studies have shown 90% removal of PFOA and PFOS using different energy-based reactors while operating high energy resulted in faster decomposition of PFAS compounds, for example, PFOA and PFOS took 30 min and 8 min to decompose 90% respectively (Singh et al., 2019). While plasma treatment is an innovative technology there are some limitations such as the production of intermediate short-chain compounds. It is also imperative consider the costs involved in construction and implementation of this technology for a large-scale water treatment system.

1.5.2.4. Thermal treatments:

Thermal treatment processes are widely available, scalable and often used to manage contaminated solids, liquids or gases (Wang et al., 2022). Thermal treatment processes include incineration, thermal desorption, hydrothermal treatment, GAC reactivation and smoldering. Typically thermal treatment processes operate at temperatures >500 C and often reported to decompose >99.9% of PFAS compounds (Xiao et al., 2021a). From a remediation perspective, Crownover et al., 2019 examined the decontamination of soil containing perfluoroalkyl substances by heating the soil to a specific temperature to vaporize the chemicals (i.e., thermal desorption) (Crownover et al., 2019). A reduction of up to 99.998% of perfluoroalkyl substances in soil was observed after 10–14 days of heating at 200–400 °C under an airflow (Crownover et al., 2019). Gerhard and co-workers

treated soil and granular activated carbon laden with perfluoroalkyl substances by smoldering combustion at much higher temperatures (>900 °C) (Duchesne et al., 2020a). The authors observed a substantial PFOS removal of up to >99.9995% from the treated media (Duchesne et al., 2020a). Strathmann and co-workers recently developed a hydrothermal treatment (Hao et al., 2021; Wu et al., 2019a) that can effectively decompose a variety of PFASs at near-critical temperature and pressure (350 °C; 16.5 MPa) within 15–30 min (Hao et al., 2021). However, there are certain uncertainties associated with thermal treatment processes. Incomplete decomposition and potential recombination to form new compounds, the ability to effectively measure the efficiency of treatment and recovery of off gases using industrial scrubbers (EPA, 2020).

1.6. Current gaps in research

Although innovative and advanced treatment technologies are showing promise in lab-scale studies GAC continues as the most-frequently used approach for treating PFAS contaminated water however, saturated GAC needs further treatment. Spent GAC can be regenerated using thermal reactivation where the saturated GAC is heated for ~30 min at temperatures ranging from 700 – 800 °C. Previous studies investigated the decomposition of legacy compounds such as PFOA and PFOS at temperatures >700 °C. The decomposition efficiencies for other types of PFAS and at lower temperatures is not available. Investigate the fate of PFAS during thermal processes and determining mechanisms involved would lead to designing better informed treatments and helpful when proposing regulations.

1.7. Main goals and objectives of this research

The main goals of this research are to systematically investigate the fate of PFAS in thermal treatment processes such as GAC reactivation and evaluate different parameters involved in decomposing PFAS. The specific objectives of the research are to:

1) Evaluate the thermal stability of PFAS compounds which are deemed "thermally stable".
2) Thermal decomposition efficiency of PFAS on spent GAC.
3) Investigate the temperatures required to achieve sufficient mineralization.
4) Investigate the effects of functional groups and chain-length on thermal treatment.
5) Study the effects GAC and other porous carbonaceous materials like biochar on the amount and rate of decomposition of PFAS.
6) Evaluate the decomposition of PFAS without porous compounds.
7) Investigate the byproducts and intermediate compounds generated during thermal treatment.
8) Develop thermal decomposition pathways for PFAS compounds.

1.8. Organization of the Dissertation

Chapter 2 is a journal paper published in ACS ES&T Letters titled "Thermal Stability and Decomposition of Perfluoroalkyl Substances on Spent Granular Activated Carbon". In this chapter, we discuss the temperatures required to destabilize different PFAS and determine their decomposition efficiencies on GAC when heated at temperatures ranging from 150 – 900 °C.

Chapter 3 discusses thermal decomposition of PFCAs and one PFECA at low – moderate (150 – 300 °C) temperatures. The effect of GAC and other carbonaceous

materials during thermal treatment is determined. The kinetics of such reactions are also presented in this chapter. This chapter is the first part of a journal paper published in Water Research.

Chapter 4 discusses the mechanisms involved in thermal decomposition of PFAS. Based on the results obtained from thermal decomposition experiments, identified short-chain intermediate compounds and the yield of F- a detailed decomposition pathway is proposed. This chapter is the second part of a journal paper published in Water Research.

Chapter 5 provides a brief summary of the chapters and discusses the key findings of this dissertation.

2. CHAPTER 2: Thermal Stability and Decomposition of Perfluoroalkyl Substances on Spent Granular Activated Carbon

Feng Xiao, **Pavankumar Challa Sasi**, Bin Yao, Alena Kubátová**,** Svetlana A. Golovko, Mikhail Y. Golovko, Dana Soli, 2020. Thermal stability and decomposition of perfluoroalkyl substances on spent granular activated carbon. ***Environmental Science and Technology Letters*** (published) DOI: https://doi.org/10.1021/acs.estlett.0c00114

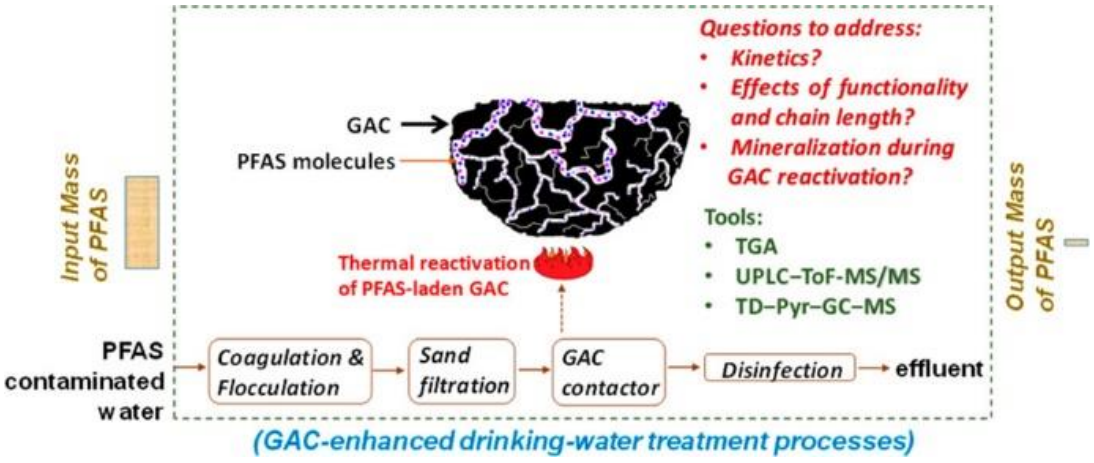

2.1. Introduction

Per- and polyfluoroalkyl substances (PFAS) are synthetic organic chemicals, widely used for a range of consumer and industrial products, including nonstick cookware, aqueous film-forming foams (AFFFs), and paint materials (Paul et al., 2009; Prevedouros et al., 2006). Once released to the natural environment (Xiao et al., 2012a; Xiao et al., 2012b; Xiao et al., 2015), long-chain PFAS (≥7 perfluorocarbons), including perfluorooctanoic acid (PFOA) and perfluorooctanesulfonic acid (PFOS), can bioaccumulate and biomagnify through food webs (Bischel et al., 2010; Houde et al., 2006; Smithwick et al., 2005; Xiao et al., 2013a). PFOA and PFOS have been reported in >95% of blood samples collected during multiple U.S. national surveys (NHANES, 2014) at concentrations that are a risk to human health (DeWitt et al., 2018; Grandjean et al., 2012; Melzer et al., 2010; Steenland et al., 2010). PFOA/PFOS-contaminated drinking water is an important source of exposure for the general population (Boiteux et al., 2012; Ericson et al., 2009; Hoffman et al., 2011; Post et al., 2012; Vestergren and Cousins, 2009). The U.S. EPA recently set a drinking water advisory on the combined level of PFOA and PFOS at 0.070 μg/L, making the removal of these compounds from drinking water a health priority (Anumol et al., 2016; Appleman et al., 2014; Xiao et al., 2013b).

Presently, PFOA and PFOS cannot be easily removed from water during conventional drinking water treatment (Appleman et al., 2014; Eschauzier et al., 2012; Rahman et al., 2014; Yang et al., 2019). For example, coagulation and flocculation processes achieve only up to 25% of PFOA/PFOS removal (Xiao et al., 2013b). Both chemicals are recalcitrant to degradation because of the strong carbon–fluorine bond (Eschauzier et al., 2012; Schröder and Meesters, 2005; Takagi et al., 2011). In fact, (Xiao

et al., 2018c) demonstrated that PFOA and PFOS are generated from cationic/zwitterionic polyfluoroalkyl compounds during drinking-water disinfection by chlorine or ozone (Xiao et al., 2018c). Others have shown that certain advanced technologies can degrade PFOA and PFOS in water but under specialized conditions, including B_{12}-mediated reduction (Lee et al., 2017), photocatalysis (Hori et al., 2005; Sahu et al., 2018), electrochemical approaches (Yang et al., 2019; Zhou et al., 2011), reduction by hydrated electrons under completely anaerobic conditions (Bentel et al., 2019; Song et al., 2013), hydrothermal decomposition at alkaline pH (Wu et al., 2019b), and plasma treatment (Singh et al., 2019). Although progress is continually being made for these advanced treatment technologies, at pilot- and full-scale operations granular activated carbon (GAC) adsorption continues as the most frequently used approach for treatment of PFAS-contaminated water (Rahman et al., 2014). The predominant residual from GAC systems is spent or exhausted carbon which contains PFAS. Further treatment of PFAS on spent GAC is required.

Commercial GAC is a highly porous pyrogenic carbonaceous material, produced from bituminous coal, wood, or coconut shell which is activated at 700 °C and above in CO_2 or steam. Spent GAC can be thermally reactivated or regenerated, used as a fuel for combustion, or landfilled depending on whether the spent GAC is deemed nonhazardous (Council, 2009). During thermal reactivation, the exhausted carbon is heated for ~30 min with hot inert gases (e.g., N_2), CO_2, or steam (Marsh and Rodríguez-Reinoso, 2006). Air may be inadvertently or intentionally introduced during the reactivation process to cool the reactor (Xiao et al., 2018a; Xiao and Pignatello, 2016). The fate of PFAS in thermal processes such as those occurring during GAC reactivation and combustion is poorly understood. Filling this key knowledge gap will accomplish the following: (1) promote the

development of effective and sustainable thermal decomposition technologies for PFAS on GAC; and (2) enhance our understanding of PFAS fate in other relevant thermal processes, including heating and baking of cookware which may contain PFAS, use of PFAS-containing AFFFs for fire suppression, and incineration of PFAS-containing biosolids and municipal solid wastes.

2.2. Materials and Methods

2.2.1. Chemicals

We studied seven perfluoroalkyl carboxylic acids (PFCAs) and three perfluoroalkyl sulfonic acids (PFSAs): perfluorobutyric acid (PFBA), perfluoropentanoic acid (PFPeA), perfluoroheptanoic acid (PFHpA), PFOA, perfluorononanoic acid (PFNA), perfluorodecanoic acid (PFDA), perfluoroundecanoic acid (PFUnDA), and potassium salts of perfluorobutanesulfonic acid (PFBS), perfluorohexanesulfonic acid (PFHxS), and PFOS (Appendix A, Table A1). The test set also included one perfluoroalkyl ether carboxylic acid, hexafluoropropylene oxide dimer acid (HFPO-DA). The ammonium salt of HFPO-DA (trade name, GenX (Xiao, 2017)) is a new alternative to PFOA/PFOS.

2.2.2. Sample collection and pretreatment

The test solution was surface water collected from the Red River (Grand Forks, ND) (dissolved organic carbon = 7.8 mg/L; specific ultraviolet absorbance = 3.2 L/mg/cm; pH = ~7.8; turbidity = 14.3 NTU). The water sample was spiked with PFAS to a known concentration, equilibrated for 48 h at room temperature (~22 °C). Pretreatment included 1-min coagulation with alum (Al_2 $(SO_4)_3 \cdot 18H_2O$) at a dose of 40 mg/L, 20-min flocculation, 30-min settling, and filtration through a Whatman paper filter (Grade 5) to remove remaining fine particles/flocs (Xiao et al., 2018c).

2.2.3. Determination of porosity and surface area of GAC

The porosity and pore size distribution of GAC particles were measured by means of N_2 porosimetry at 77 K (Autosorb-iQ, Quantachrome, Boynton Beach, FL) as detailed previously (Cao et al., 2019; Xiao et al., 2018a; Xiao et al., 2018b). The specific surface area of GAC was calculated by the 11-point Brunauer−Emmett−Teller (BET) method. The micro- and meso-porosities and pore size distributions of GAC were determined by quenched solid density functional theory from the N_2 adsorption isotherm at 77 K (Cao et al., 2019; Xiao et al., 2018a; Xiao et al., 2018b).

2.2.4. PFAS-laden GAC preparation

Adsorption of PFAS in the pretreated water to GAC (Filtrasorb 200, Calgon Carbon Corporation, PA) (BET surface area, 691.4 m2/g; microporosity, 0.3 cm^3/g; mesoporosity, 0.07 cm^3/g; see Figure A1) was performed in 50-mL Thermo Scientific Nunc™ sterile polypropylene vials that were rotated end-over-end at 40 rpm for four days at ~22 ˚C. Apparent adsorption equilibrium was reached within one day. After adsorption, the PFAS-laden GAC particles were freeze dried and split into two portions, one for extractions screening tests and the other portion for thermal treatment experiments.

2.2.5. Extraction screening tests

In these tests, GAC particles (0.07 g) in pre-cleaned polypropylene vials were spiked with a known volume of 1×10^{-3} mol/L PFAS stock solution in methanol. Then 10 mL of methanol, methanol with 100 mmol/L NaOH, or methanol with 100 mmol/L NH_4Ac was added to the tubes. The mixture was then ultrasonicated at room temperature or at 60 °C for 30 min and subsequently centrifuged. Afterwards, the liquid phase was sampled and microfiltered (0.45 µm nylon filter; Thermo Scientific™ Target2™). The concentration of

PFAS in the filtrate was determined and the mass was calculated to compared with the spiked mass in order to calculate the recoveries.

The PFAS-laden freeze-dried GAC particles were weighed, and extracted using methanol (V_{extr}, mL) with 100 mmol/L ammonium acetate (NH_4Ac) to determine the PFAS mass on GAC before thermal treatment ($M_{PFAS,GAC,initial}$) by eq 2.1.

$$M_{PFAS,GAC} = (C_{extr} \times V_{extr})/E \quad (2.1)$$

where E (%) is the extraction efficiency and C_{extr} (μmol) is the concentration of PFAS in the extract measured using a Waters Acuity ultrahigh pressure liquid chromatograph (UPLC) coupled with a Waters QToF-MS/MS (Synapt G2-S, Waters Corporation, Milford, MA, USA).

2.2.6. Thermal Treatment experiments

The quartz tube was washed thoroughly after every thermal treatment of PFAS-containing GAC samples. In selected tests (at HTTs of 200, 300, 500, and 700 °C), after the thermal treatment and cool down, we rinsed the tube with 100 mL F-free deionized (DI) water and measured PFAS in the rinsate; no measurable concentrations of target PFAS were found.

Furthermore, triplicate unspiked controls were prepared in sorbate-free vials with only GAC in the unspiked pretreated surface water to examine possible contamination of samples by PFAS and F^- from laboratory apparatus. GAC particles collected from control vials were freeze-dried and heated at a HTT up to 900 °C. F and remaining PFAS in off-gas and on GAC particles after the thermal treatment were measured in the procedures as described in the text. No measurable F^- and PFAS were found in these control samples.

The other portion of PFAS-laden freeze-dried GAC particles was transferred to a porcelain crucible and heated in a temperature-programmable two-zone quartz tube furnace (MTI Corporation, CA) under a flow of N_2 or CO_2 (200 mL/min) to simulate the industrial reactivation process of spent GAC. The sample was heated at the rate of 10 °C/min to the desired final heat treatment temperature (HTT = room temperature (non-heating control) to 900 °C) and held for 30 min. Off-gas from the furnace was passed through a series of six beakers containing 50-mL fluorine ions (F^-)-free deionized water (DW) (#1–5) and methanol (#6). After the thermal treatment and cool down, the crucible was placed in a known volume of DW (#7) and ultrasonicated for 30 min. Concentrations of F^- in DW samples and residual PFAS in DW and methanol samples were determined and their mass ($M_{F^-,total}$ and $M_{PFAS,liquid,residual}$, μmol) were calculated. Concentrations of F^- were determined by the standard SPADNS method (Rice et al., 2012). To verify the results obtained in the tube furnace (an open system under a flow of N_2 or CO_2) and to investigate the effect of O_2, certain reactivation experiments were also performed in a closed system in an air atmosphere.

The above-mentioned adsorption and heating experiments were repeated. After thermal treatment, GAC was extracted by methanol with 100 mmol/L NH_4Ac added to determine the residual concentration of PFAS on GAC ($C_{extr,GAC,residual}$) and remaining mass ($M_{PFAS,GAC,residual}$, μmol) by eq 2.1.

The thermal decomposition efficiency was calculated by

$$\text{Decomposition (\%)} = \left[1 - \frac{(C_{extr} \times V_{extr}/E)_{PFAS,GAC,residual} + M_{PFAS,liquid,residual}}{(C_{extr} \times V_{extr}/E)_{PFAS,GAC,initial}}\right] \times 100\% \qquad (2.2)$$

After thermal treatment, if no measurable residual PFAS was detected on GAC and in liquid samples #1–#7, the values of $C_{\text{extr,GAC,residual}}$ and $M_{\text{PFAS,liquid,residual}}$ in eq 2.2 were assigned to zero or the decomposition efficiency was assigned to 100%.

The yield of F^- from a PFAS with $(2n + 1)$ F atoms during thermal decomposition was calculated with the following equation

$$\text{Yield } (F^-) = \frac{M_{F-,\text{total}}}{(2n+1)\left[M_{\text{PFAS,GAC,initial}} - M_{\text{PFAS,GAC,residual}} - M_{\text{PFAS,liquid,residual}}\right]} \times 100\% \qquad (2.3)$$

Furthermore, we conducted dynamic and isothermal thermogravimetric analyses (TGA) of PFAS chemical powders and identified decomposition products of PFOA using a thermal desorption–pyrolysis system (CDS Analytical) connected to a gas chromatograph with an MS detector (TD–Pyr–GC–MS) (Agilent GC 7890 and 5975C MS; Santa Clara, CA).

2.2.7. Thermal treatment in a closed system with air

Certain reactivation experiments were also performed in an air atmosphere in a muffle furnace (Neytech., Vulcan 3-550, USA) at a predetermined HTT. For these experiments, PFAS-loaded GAC particles were placed in borosilicate biochemical oxygen demand (BOD) bottles with glass pennyhead stoppers and heated in an air atmosphere in the muffle furnace at a predetermined HTT (ranging from room temperature to 500 °C). After heat treatment and cool down, 50 mL F-free DI water or 10 mL methanol (amended with 100 mmol/L ammonium acetate) was added to the bottle and ultrasonicated for 30 min. Then, we measured concentrations of PFAS and F^- in the aqueous solution as well as PFAS in methanol.

To test the extent to which BOD bottles were leakproof, we spiked known volumes of sodium fluoride stock solution (10 mg/L) to three groups of raw GAC particles, freeze-

dried the GAC particles, placed them in triplicate BOD bottles, and heated them in the muffle furnace at a HTT of 400, 450 and 500 °C. After heat treatment and cool down, 50 mL F-free DI water was added to the bottle and ultrasonicated for 30 min. Then, we determined concentration and mass of F^- in solution and compared with the spiked mass. The difference varied by <14%, generally considered to be within the range of analytical variability. In some cases, cracks on the stopper occurred after moving the bottle from the muffle furnace at 450 or 500 °C (suddenly) to room temperature. Even with these cracks, we did not observe apparent loss of F from the bottle.

2.2.8. UPLC–QToF-MS/MS method

The analysis was carried out on a Waters Acquity ultrahigh pressure liquid chromatography (UPLC) system coupled with a Waters QToF-MS/MS(Xiao et al., 2018c) (Synapt G2-S, Waters Corporation, Milford, MA, USA) available in the Department of Biomedical Sciences of University of North Dakota. Chromatography was performed using a Waters Acquity UPLC BEH Shield RP18 column (100 × 2.1 mm; 130 Å; 1.7 μm) with a Waters Acquity UPLC BEH Shield RP18 VanGuard pre-column (5 × 2.1 mm; 130 Å; 1.7 μm). The mobile phase consisted of eluent A (2 mM ammonium formate in Optima™ water; LC/MS grade) and eluent B (2 mM ammonium formate in Optima™ methanol; LC/MS grade). The elution started at 20% B for 0.5 min and then was linearly increased to 85% B in 5 min, further increased to 98% B in 0.1 min and kept isocratic for 1.5 min. At 7.1 min, the A/B ratio changed back to the initial value of 80/20 over 0.1 min to re-equilibrate the column for another 1.3 min. Analytes were eluted using a Waters Acquity UPLC pump equipped with a well-plate autosampler that was maintained at 8 ˚C. The flow rate was

maintained at 0.45 mL/min, and the column temperature was 55 ˚C. The UPLC retention times were 4.6, 4.7, and 4.8 min for PFOAAmS, PFOA, and PFOAB, respectively.

Mass spectrometry analysis was performed using the Synapt G2-S QToF-MS with an ESI source operated in a negative ion mode. MS operating conditions were as follows: cone voltage, 20 V; capillary voltage, 1.8 kV; source temperature, 110 ˚C; desolvation temperature, 350 ˚C; cone gas flow rate, 10 L/h; and desolvation gas flow, 1,000 L/h. The analyzer was operated with an extended dynamic range at 10,000 resolution (fwhm at *m/z* 554) with an acquisition time of 0.1s. The Synapt G2-S ToF MS^E mode was used to collect data with the T-wave element alternated between a low energy of 2V (MS) and high energy (MS^E) states in which the transfer T-wave element voltage ranged from 10–25 V. Leucine enkephalin (400 pg/μL) was infused at a rate of 10 μL/min for mass correction. MassLynx V4.1 software (Waters) was used for instrument control, acquisition, and mass analysis. The structural information of the degradation products was obtained by the state-of-the-art MS^E function that allows the simultaneous acquisition of both MS and MS/MS fragmentation during a single chromatographic run(Waters., 2011; Xiao et al., 2017).

Quantification of all target PFAAs were made using extracted ion currents (10 ppm mass window) and were based on their *m/z* values and UPLC retention times relative to a six-point external calibration standard curves.

2.2.9. Thermogravimetric analysis (TGA)

We also conducted TGA of PFAS chemical powders using a thermal analyzer system (TGA/STD Q600, TA Instrument, DE) in an atmosphere of N_2, CO_2, or O_2. In one instance, we performed *dynamic* TGA scans from room temperature to a predetermined temperature. The other TGA experiment was devoted to calculation of the weight loss of

PFAS under *isothermal* conditions. In brief, we conducted a scan from room temperature to the predetermined temperature in which the sample was kept under isothermal conditions.

2.2.10. TD–Pyr–GC–MS methods

PFOA thermal decomposition products were analyzed by a thermal desorption–pyrolysis system (CDS Analytical) connected to a gas chromatograph–mass spectrometer system (Agilent GC 7890 and 5975C MS; Santa Clara, CA) (TD–Pyr–GC–MS). The TD-Py program consisted of single or sequential thermal steps with the pyroprobe heated for 30 sec at thermal desorption temperatures of 200, 300 °C, and pyrolysis temperatures of 400, 500, and 10 sec at 890 °C with the interface heated to 300 °C and 350 °C, respectively. For each temperature the interface was opened for 2.5 min to transfer the analytes (products) through the heated transferline, a GC injector port (in 10:1 split) kept at 300 °C onto the column held at 40 °C, this was then followed by GC analysis. The GC temperature program started at 40 °C for 1 min followed by a gradient of 40 °C/min to 80 °C, and then 25 °C/min to 320 °C, and held for 4 min. The GC was equipped with a 52.5 m HP-5MS column (0.25 µm film thickness and 0.25 mm i.d.). The MS analysis was performed with electron ionization in mass range 35-850 m/z. Ultra-pure helium (99.999%) was used as the carrier gas with a constant flow rate of 1.1 mL min^{-1}.

2.3. Results and discussion

2.3.1. Extraction of PFAS from GAC particles

Pure methanol, whether heated (at 60 °C) or not, resulted in low recoveries (30.0–67.8%) of PFAS from GAC (Figure 2.1). Methanol that was amended with NaOH yielded improvement in extraction for PFSAs (71.6–82.5%) but consistently had recoveries greater

than 130% for PFCAs. On the other hand, methanol added with NH_4Ac achieved recoveries ranging from 79.2 to 111.8% for most of the PFAS.

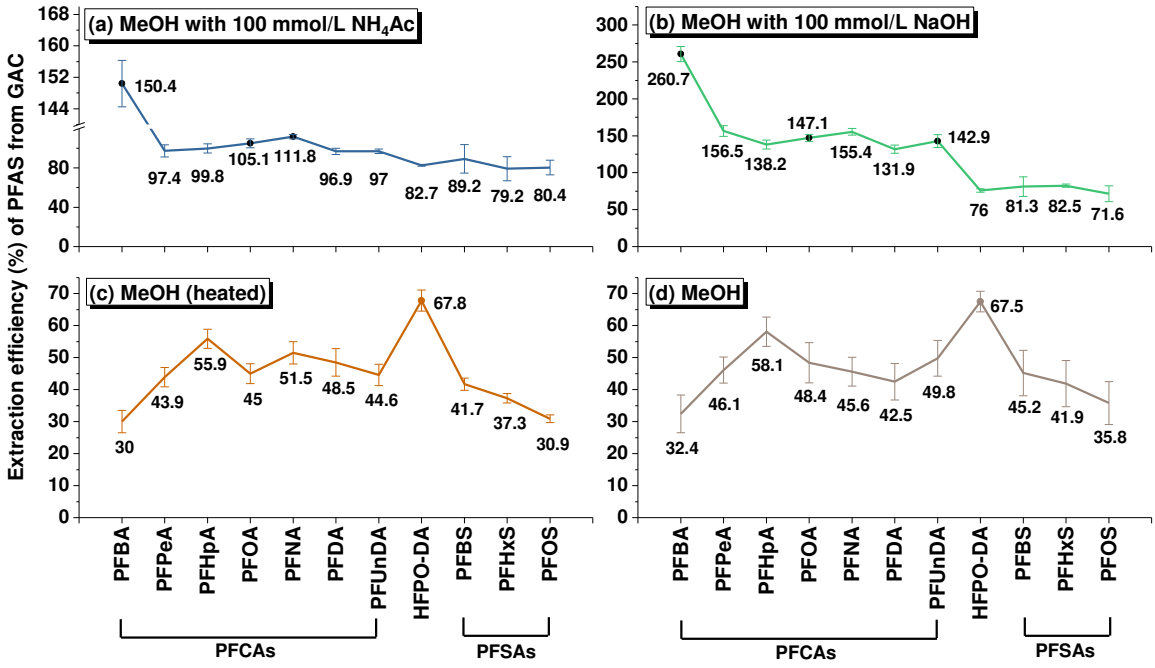

Figure 2.1. *Recovery of PFCAs, PFECA (i.e., HFPO-DA), and PFSAs from GAC by selected methanol (MeOH) extraction conditions.*

2.3.2. Thermal stability of PFAS.

According to the results of TGA (Figure 2.2) and thermal decomposition of PFAS during GAC reactivation (Figure 2.4), PFAS exhibited the following order of thermal stability: PFSAs >> PFUnDA > PFDA > PFNA > PFOA > PFBA > HFPO-DA. TGA curves of PFCAs shifted to a higher temperature when the number of perfluorinated carbons (n_{CF2}) increases (Figures 2.2a–2.2c).

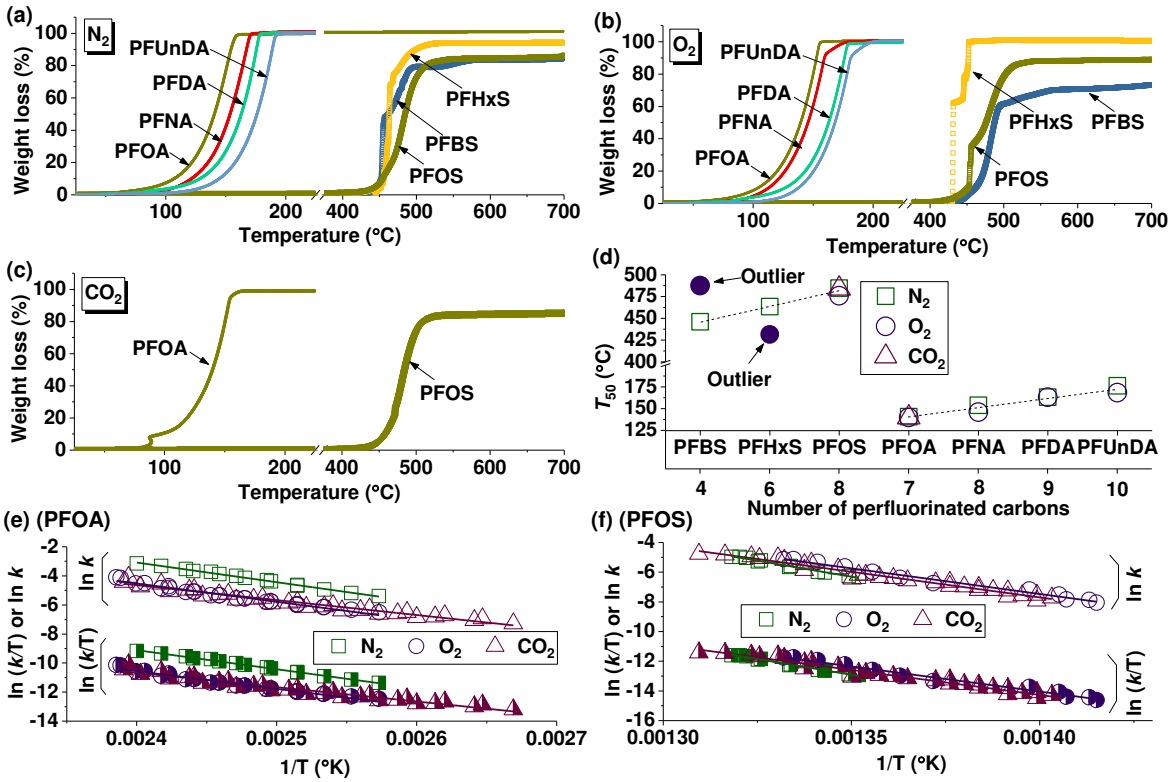

Figure 2.2. *(a)– (c): Dynamic TGA scan curves of PFAS in different atmospheres. (d): Correlation between T50 and the number of perfluorinated carbons in PFAS. (e) and (f): Arrhenius- (ln k vs 1/T) and Eyring-like (ln k/T vs 1/T) plots for PFOA and PFOS based on isothermal TGA scan data.*

The temperature (T_{50}; °C) corresponding to 50% weight loss of a PFAS in dynamic TGA scans (Figures 2.2a–2.2c) correlates well with n_{CF2} (Figure 2.2d):

$T_{50} = 11 \times n_{CF2} + 63$; $R^2 = 0.96$ (four PFCAs in Fig 2.2d) (2.4)

$T_{50} = 9 \times n_{CF2} + 410$; $R^2 = 0.96$ (three PFSAs in Fig 2d without including two outliers) (2.5)

An increase in one perfluorinated carbon unit (–CF_2–) leads to a rise of T_{50} by approximately 11 and 9 °C for PFCAs and PFSAs, respectively. T_{50} varied insignificantly between different atmospheric environments (N_2, CO_2, O_2) (Figure 2.2d).

Analysis of isothermal TGA data revealed that the weight loss (destabilization) of PFAS follows first-order kinetics (Figure 2.2). Figures 2.2e and 2.2f show Arrhenius- and Eyring-like plots for first-order thermal destabilization rate constants (k) of PFOS and PFOA. The thermal destabilization half-lives ($t_{1/2}$) of PFOA and PFOS calculated from k decreased exponentially with increasing temperature, for example, from 26 min at 439 °C to 0.65 min at 500 °C for PFOS (Figure A2). Khan et al. calculated the theoretical thermal decomposition half-life of PFOS to be only 1 sec at 727 °C based on quantum chemistry(Khan et al., 2020).

2.3.3. Thermal decomposition of PFAS laden in GAC

Figures 3 and 4 show that the minimum temperatures leading to thermal decomposition of PFOA and PFOS are 150 and 450 °C, respectively. Therefore, the significant weight loss of PFOA below 150 °C in dynamic TGA scans (Figures 2.2a–2.2c) should be primarily caused by sublimation. While perfluoroalkyl acids (PFAAs) such as PFOA are nonvolatile at room temperature, they become more volatile with increasing temperature owning to the rising vapor pressure (Kaiser et al., 2005). The decomposition and mineralization rates of PFAS in the open system (tube furnace under a flow of N_2 or CO_2) were similar to those measured in the closed (air) system (Figures 2.3 and 2.4). Taken together, the results indicate that PFAS molecules thermally destabilized and transferred from GAC to the gas phase were decomposed in the gas phase provided sufficiently high temperatures are used.

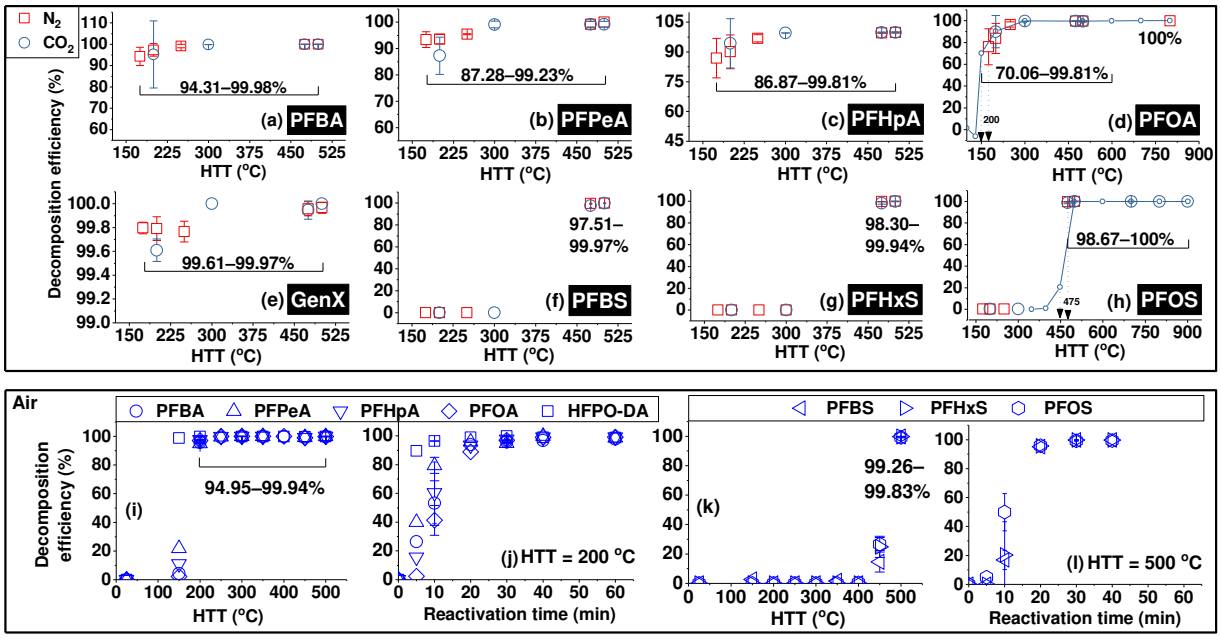

Figure 2.3. *(a–h) Decomposition of PFAS on GAC during 30-min GAC thermal reactivation performed in a tube furnace under a flow of N_2 or CO_2. The solid lines in (d) and (h) represent independent experiments. (i–l) Decomposition of PFAS on GAC in a closed system with air at different HTTs (i; k) or durations (j; l). The adsorption of PFAS on GAC in these experiments was carried out in pretreated surface water. The decomposition efficiency was assigned to 100% if no measurable PFAS was found on GAC after thermal treatment and in samples #1–#7 (see eq 2.2).*

As shown in Figures 2.3j and 2.3l, a 20-min thermal treatment achieved >90% decomposition of PFCAs and PFSAs on GAC at 200 and 500 °C, respectively. A 30-min thermal treatment of spent GAC at ≥300 °C in either N_2, CO_2, or air achieved ≥99.9% removal of HFPO-DA and ≥99% removal of PFCAs (e.g., PFOA) (Figure 2.4). HFPO-DA was more readily decomposed than PFCA with the same n_{CF2} (i.e., PFBA) (Figure 2.3), indicating that the perfluorinated chain becomes less thermally stable with the inclusion of an ether group. A much higher heat treatment temperature (or HTT) (≥500 °C) is needed

to achieve ≥99% decomposition of PFSAs (e.g., PFOS) on GAC during a 30-min thermal treatment (Figure 2.3).

Shorter-chained PFAAs (e.g., PFPeA and PFHpA), generated during chemical(Hori et al., 2005; Song et al., 2013) and biological(Huang and Jaffe, 2019) degradation of PFOA, were not found in this study. Instead, we observed a number of gaseous products. The sequential TD–Pyr–GC–MS chromatograms and mass spectra of PFOA at 200–890 °C are illustrated in Figure 2.4. As shown, the decomposition of PFOA had already started at 200 °C. The broad peak at a GC retention time (2.142–2.270 min) in Figures 2.5a–2.5c represents small organic fluorine compounds/fragments(Wang et al., 2013) (e.g., $\cdot C_5F_9$; see Figures 2.4f–2.4i). The single sharp peak (*m*/*z* 395.1) observed at 200 °C at a GC retention time of 5.172 min (Figure 2.4a) corresponds to the radical of 2H polyfluorocarboxylic acid (2HPFOA)(Washington et al., 2015) or PFOA itself(NIST, 2018). This sharp peak disappeared when the temperature increased from 200 to 300 °C (Figure 2.4). The broader peak at 2.142–2.270 min also became much smaller with increasing temperature and almost invisible at 500 °C or higher (Figures 2.4d and 2.4e) as a result of mineralization to F^- (Figure 2.5).

According to the measured yields of F^- (Figure 2.5), significant mineralization of PFOA/PFOS requires a HTT of ≥700–800 °C (Figure 2.5). For example, the mineralization rate of PFOA on GAC increased sharply to 92.4 mol% at 700 °C from 9.4–28.8 mol% at 150–600 °C. Similarly, the yield of F^- from PFOS on GAC gradually increased with HTT, reaching a maximum of 86.8 mol% at 800 °C. The mineralization rate in CO_2 (tube furnace; open system) was not significantly different from that in air (closed system) at a given HTT (Figure 2.5). Thermal decomposition pathways of PFOA (Figure 2.5 (c)) were proposed

based on the organic fluorine species identified by TD–Pyr–GC–MS (Figure 2.4). The proposed mechanism indicates 73.3–80 mol% mineralization yield to F (Figure 2.5 (a & b).

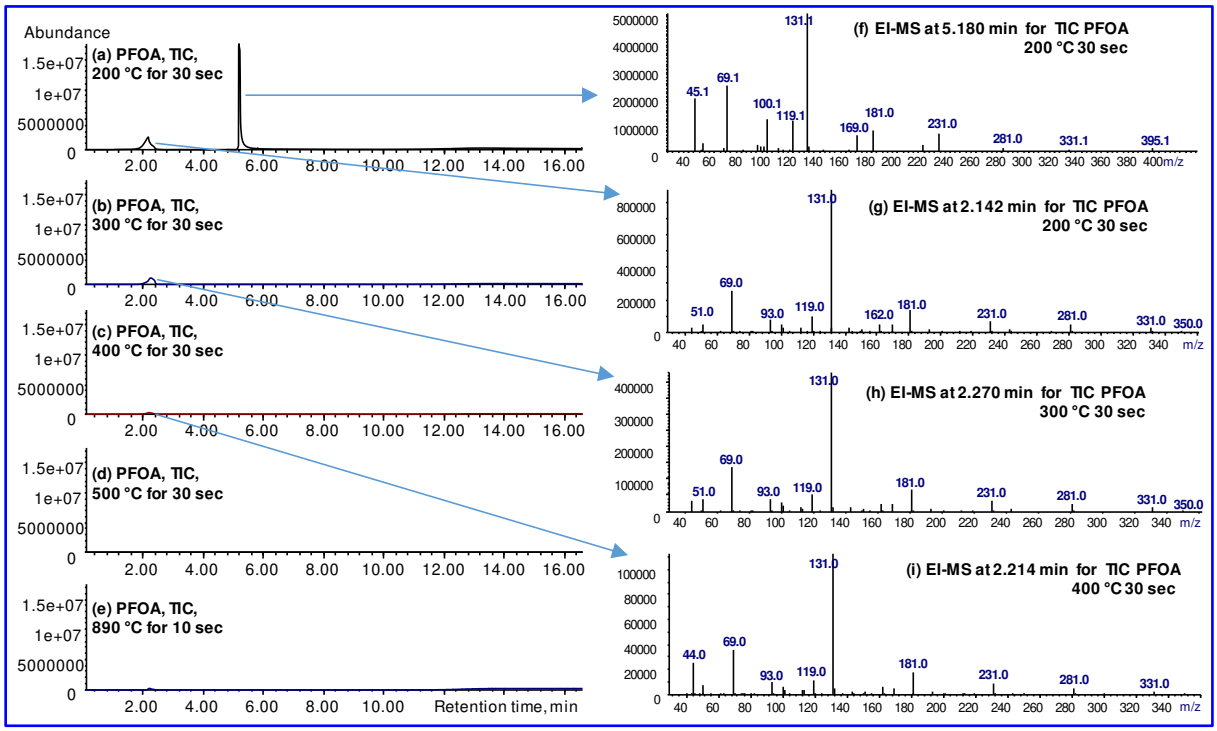

Figure 2.4. *TD–Pyr–GC–MS chromatograms (a–e) and mass spectra (f–i) of thermal decomposition products of PFOA at different temperatures and predetermined durations.*

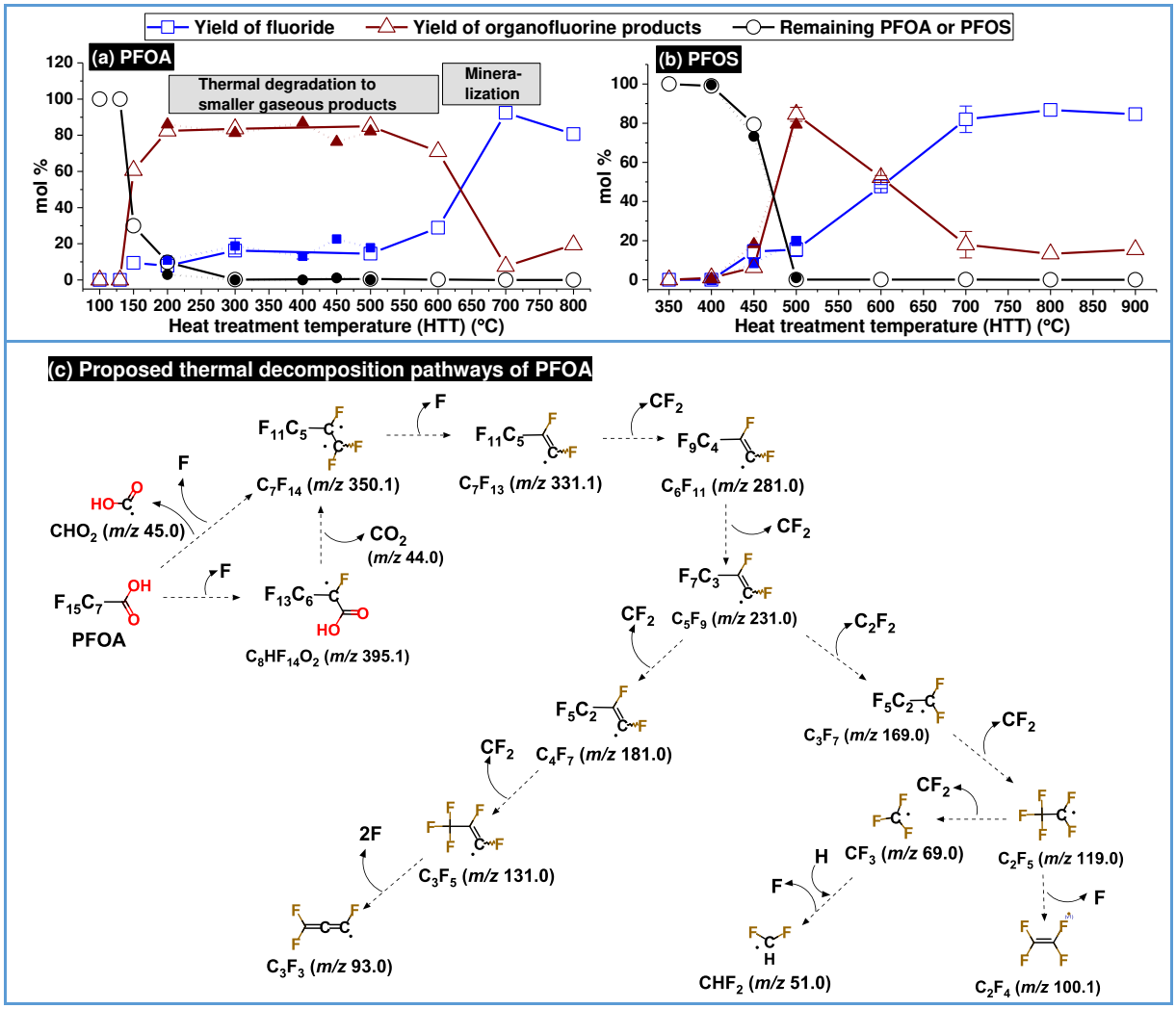

Figure 2.5. *Measured yields of F from (a) PFOA and (b) PFOS during GAC thermal reactivation performed in an open system under a flow of CO_2 (open symbols) and in a closed system with air (closed symbols). (c) Proposed thermal decomposition pathways of PFOA in an inert atmosphere on the basis of thermal decomposition products of PFOA identified by TD–Pyr–GC–MS.*

3. CHAPTER 3: Effect of Granular Activated Carbon and Other Porous Materials on Thermal Decomposition Of PFAS

Pavankumar Challa Sasi, Ali Alinezhad, Bin Yao, Alena Kubátová, Svetlana A. Golovko, Mikhail Y. Golovko, Feng Xiao. 2021. Effect of granular activated carbon and other porous materials on thermal decomposition of per- and polyfluoroalkyl substances: mechanisms and implications for water purification. ***Water Research*** (published)

DOI: https://doi.org/10.1016/j.watres.2021.117271

3.1. Introduction

Per- and polyfluoroalkyl substances (PFAS) are anthropogenic chemicals that have been produced for decades as either processing aids or individual ingredients in many industrial and commercial products, including aqueous film-forming foams (AFFFs) (Barzen-Hanson et al., 2017; Houtz et al., 2013), non-stick cookware (Begley et al., 2005; Sajid and Ilyas, 2017), and fast-food packaging (Schaefer et al., 2017). Perfluoroalkyl substances comprise compounds such as perfluorooctanoic acid (PFOA) and perfluorooctanesulfonic acid (PFOS) in which C–F bonds have replaced C–H bonds in nonfluorinated counterparts. Perfluoroalkyl substances are chemically and biologically recalcitrant (Schröder and Meesters, 2005; Sinclair and Kannan, 2006; Xiao et al., 2012a), whereas polyfluoroalkyl substances, including cationic or zwitterionic PFAS, are subject to degradation (Houtz et al., 2016; Jin et al., 2020; Lee et al., 2010; Nabb et al., 2007; Xiao et al., 2018c). Once released to the natural environment, long-chain PFAS (≥7 perfluorocarbons) can bioaccumulate and biomagnify through food webs (Houtz et al., 2016; Jin et al., 2020; Langberg et al., 2019; Xiao et al., 2013a). PFOA and PFOS have been reported in >95% of blood samples collected during multiple U.S. national surveys (NHANES, 2014) at concentrations that are a risk to human health (DeWitt et al., 2018; Grandjean et al., 2012; Melzer et al., 2010; Steenland et al., 2010). PFAS-contaminated drinking water is an important source of exposure for the general population (Boiteux et al., 2012; Ericson et al., 2009; Hoffman et al., 2011; Post et al., 2012; Vestergren and Cousins, 2009). PFAS are recalcitrant to degradation at ambient temperature and atmospheric pressure, and are not easily removed in conventional drinking-water and wastewater treatment processes (Anumol et al., 2016; Appleman et al., 2014; Eschauzier

et al., 2012; Liu et al., 2020; Rahman et al., 2014; Xiao et al., 2012a; Xiao et al., 2013b; Yu et al., 2009a). In fact, Xiao et al. demonstrated that PFOA and PFOS are generated from certain cationic/zwitterionic polyfluoroalkyl compounds during drinking water treatment by chlorine or ozone (Xiao et al., 2018c). The U.S. EPA recently set a drinking water advisory on the combined level of PFOA and PFOS at 0.070 µg/L, making the removal of these compounds from drinking water a health priority.

Adsorption by granular activated carbon (GAC) is frequently used to remove PFAS from drinking water at full-scale treatment operations (Belkouteb et al., 2020; Rahman et al., 2014; Yu et al., 2009b). The spent or exhausted GAC can be reactivated or regenerated, used as a fuel for combustion, or deposited in a landfill, depending on whether or not it is nonhazardous (Council, 2009). Information on the fate of PFAS during GAC thermal treatments (regeneration or combustion) is meager. Watanabe et al. studied the decomposition of PFOA, perfluoroheptanoic acid (PFHpA), and PFOS on GAC at 700 ^{o}C (Watanabe et al., 2018). The authors observed a 99% decomposition efficiency of these chemicals at 700 ^{o}C (Watanabe et al., 2018). The decomposition rates at other temperatures were not determined (Watanabe et al., 2018). Gerhard and co-workers found that the thermal treatment of PFAS-loaded GAC at high temperatures (1011–1048 ^{o}C) resulted in near complete degradation of PFAS (e.g., >99.8%) (Duchesne et al., 2020b). Xiao et al. investigated the thermal stability and decomposition of several short- and long-chain PFAS on GAC within a wide temperature range of 25–900 ^{o}C (Xiao et al., 2020). The authors also developed a method for PFAS extraction from GAC (Xiao et al., 2020). The term ‘thermal stable’ has been frequently used to describe PFAS in the literature. However, Xiao et al. observed 94.95–99.99% decomposition of perfluoroalkyl carboxylic acids (PFCAs)

on GAC after a 30-min thermal treatment at low temperatures (200–300 ºC) (Xiao et al., 2020). The authors also found that the degradation of PFAS in GAC varied insignificantly between different atmospheric environments (N_2, CO_2, O_2) (Xiao et al., 2020). This discovery raises the question on the nature of PFAS thermal decomposition. Can perfluoroalkyl substances be thermally degraded at 200 ºC without the presence of GAC? If so, how fast is this process? Does GAC facilitate the thermal degradation of these compounds? If yes, what is the relative importance of the polyaromatic surface and the porosity of GAC? Answering these questions has important implications for understanding the fate of PFAS in thermal water/wastewater/sludge/waste treatment processes.

Two important structural features of porous pyrogenic carbonaceous materials (PCMs), including GAC, are the porosity and polyaromatic units (Kah et al., 2017). An analogy can be drawn between polyaromatic units of porous PCMs and the hexagonal sp^2-carbon ("graphene") sheets that make up the surface of graphite, graphene materials, and carbon nanotubes. The polyaromatic units jumble disorderedly to create nanopore networks. During the activation step of GAC production, oxidative gases enter these networks, remove obstructions such as tarry materials, and open more pore networks.

The PCM family also includes natural charcoals generated during the incomplete combustion, or pyrolysis, of lignocellulosic biomass (Glover et al., 2018; Lehmann and Joseph, 2009; Schmidt and Noack, 2000; Skjemstad et al., 2002). Unlike GAC, charcoal particles have underdeveloped pore structures and show porosity mainly in the ultramicropore region (3.5–7 Å) (Xiao and Pignatello, 2016). Natural charcoals are widespread in soils as a result of historical wildfires (III, 2020), land clearing, and crop residual burning (Lehmann and Joseph, 2009; Schmidt and Noack, 2000; Skjemstad et al.,

2002), contributing to 30–50% of soil organic carbon in certain areas such as Midwest prairie soils (Glaser et al., 2001; Mao et al., 2012). Natural charcoals are similar in many respects to an engineered PCM form, commonly known as 'biochar' that has been modified such as to enhance its performance as an adsorbent in water and wastewater treatment. The polyaromatic surface of both GAC and biochar has been suggested to act as an electron shuttle, accelerating the redox conversion of organic compounds (Kappler et al., 2014; Millerick et al., 2013; Tang et al., 2011). Another question arises whether charcoals/biochars can alter the thermal degradation of PFAS, which has critical implications not only for fate/transport studies of PFAS under natural thermal conditions (e.g., wildfires) but for designing effective carbonaceous adsorbents for PFAS.

This study was conducted to address the above questions and to better understand the thermal decomposition kinetics, products, and pathways of PFAS, focusing on the effect of GAC and charcoals/biochars.

3.2. Materials and methods

3.2.1. PFAS chemicals.

The test chemical set for thermal treatments included PFOS and five PFCAs — perfluorobutyric acid (PFBA), PFOA, perfluorononanoic acid (PFNA), perfluorodecanoic acid (PFDA), and perfluoroundecanoic acid (PFUnDA) (Supplementary data, Table S1). The test set also included one perfluoroalkyl ether carboxylic acid (PFECA) — hexafluoropropylene oxide dimer acid (HFPO-DA). The ammonium salt of HFPO-DA (trade name, GenX) is a new alternative to PFOA/PFOS that has been detected in surface and drinking water (Heydebreck et al., 2015; Strynar et al., 2015; Xiao, 2017). To confirm

decomposition products, reference standards of perfluoropentanoic acid (PFPeA) and PFHpA were also prepared.

3.2.2. Thermal treatments (T#1)

The thermal decomposition of the studied PFAS was performed in a closed borosilicate glass container (Xiao et al., 2020) (see the Supplementary document) in three conditions (T#1, T#2, T#3), as shown in Figure 3.1. Before the thermal treatment in T#1 (thermolysis), a known quantity (1.2×10^{-5} mol or 0.005 g PFOA) of PFAS chemical powders or solution (in the case of PFBA and HFPO-DA) was added into a pre-cleaned container and air-dried at 25 ºC. The measurement of the weight or volume of PFAS chemicals became less accurate below 1.2×10^{-5} mol of PFAS. The container with PFAS was then capped with a ground glass stopper. Next, we set a muffle furnace (Neytech., Vulcan 3-550, USA) to a predetermined temperature (150 ºC, 200 ºC, 250 ºC, 300 ºC, or 400 ºC), and then quickly put the container with PFAS inside the furnace for an isothermal treatment for up to 180 min. After heat treatment and cooldown, the container was added with distilled water (DW) or methanol (amended with 100 mmol/L ammonium acetate) (Xiao et al., 2020) and sonicated for 30 min. Concentrations of fluoride ions (F^-) in DW and residual PFAS in methanol were determined (see the Appendix B) (Xiao et al., 2020), and their masses (M_F and $M_{PFAS,T}$, mol) were calculated in the manner described previously (Xiao et al., 2020). Our extraction method (methanol with ammonium acetate) achieved recoveries ranging from 80.4% to 111.8% for most of the PFAS compounds involved in this study (Xiao et al., 2020). Concentrations of F^- were determined by the standard SPADNS method (Rice et al., 2012). The analysis of PFAS was carried out on a Waters

Acquity ultrahigh pressure liquid chromatography (UPLC) system coupled with a Waters high-definition quantitative time-of-flight mass spectrometer (ToF-MS) (Xiao et al., 2018c) (Synapt G2-S, Waters Corporation, Milford, MA, USA) available in the Department of Biomedical Sciences of University of North Dakota. Figs. S1–S14 show representative chromatographic and spectral data.

The thermal decomposition efficiency was calculated by comparing the residual mass of PFAS in heated samples ($M_{PFAS,T}$, mol) with that in the non-heated controls ($M_{PFAS,i}$, mol).

The yield of F from a PFAS with ($2n$ + 1) F atoms during thermal decomposition was calculated with the equation 3.1:

$$\text{Yield (F)} = \frac{M_F}{(2n+1)[M_{PFAS,i} - M_{PFAS,T}]} \times 100\% \qquad (3.1)$$

The yield of transient intermediates from a parent compound was calculated by

$$\text{Yield (intermediate)} = \frac{M_{intermediate,formed}}{[M_{PFAS,i} - M_{PFAS,T}]} \times 100\% \qquad (3.2)$$

3.2.3. Thermal treatments (T#2)

The thermal treatment in T#2 was performed similarly to that in T#1, except for the addition of a small amount of a porous adsorbent. The mixture in the container was shaken manually for homogenization before thermal treatment. These porous adsorbents included GAC (Filtrasorb 200, Calgon Carbon Corporation, PA), raw charcoals (n = 4), and thermally air oxidized charcoals (n = 4). Two charcoal samples were made from a cellulose-rich feedstock (Maple wood) at a heat treatment temperature of 350 °C (referred as M350) or 600 °C (M600) following a previously published procedure (Xiao and Pignatello, 2015a; b). Another two charcoal samples were produced from a lignin-rich

feedstock (pecan shells) at a heat treatment temperature of 350 °C (P350) or 700 °C (P700). We also prepared porosity-enhanced charcoals by oxidizing raw charcoals in air at 400 °C for 30 min (Cao et al., 2019; Xiao and Pignatello, 2016). The surface areas (SAs) of these PCMs were measured with N_2 at 77 K (Autosorb-iQ, Quantachrome, Boynton Beach, FL) (Xiao et al., 2019), and calculated by the 11-point Brunauer–Emmett–Teller (BET) method. In addition to these carbonaceous materials, we also included a crosslinked polystyrene copolymer resin (Amberlite® XAD-2, Sigma–Aldrich, St. Louis, MO) as an adsorbent in a T#2 experiment. Finally, to examine the possible effect of borosilicate glass, a sample of PFOA was thermally treated along with five 2-mL borosilicate vials (available SA: 0.0027 m^2 per vial) to increase the available SA of the borosilicate glass container (0.025 m^2) by ~50%.

3.2.4. Thermal treatments (T#3)

To prepare the thermal treatment in T#3, a PFAS chemical was pre-adsorbed to a porous adsorbent in water. We could not conduct gas-phase adsorption experiments because the thermal decomposition of PFCA vapor is inevitable with increasing temperature to or above 150 °C. The test solution was prepared with distilled water containing 1.0×10^{-3} mol/L $NaHCO_3$ as a buffer and 1.0×10^{-3} mol/L NaCl. The adsorption experiment was performed in 50-mL Thermo Scientific Nunc™ sterile polypropylene vials rotated end-over-end at 10 rpm for four days at ~22 ˚C. An apparent adsorption equilibrium was reached within four days.

After adsorption, PFAS-laden adsorbent particles were split into two portions. The first portion was freeze-dried, weighed, and extracted using methanol (V_{extr}, mL) amended

with 100 mmol/L ammonium acetate (NH_4Ac) (Xiao et al., 2020) to determine the mass before thermal treatment ($M_{PFAS,i}$). The one-point water–adsorbent distribution coefficient is defined as the ratio of the adsorbed concentration (C_s) to the dissolved concentration at equilibrium (C_w), $K_{d,w-s} = C_s/C_w$. The second portion of the PFAS-laden adsorbent particles were placed in a closed container and heated in an air environment within a muffle furnace (Neytech., Vulcan 3-550, USA) at a predetermined temperature. After heat treatment and cooldown, the sample was processed in the same way as described above for the T#1 experiment.

3.2.5. Other thermal treatments

We also performed thermal decomposition in the atmosphere of N_2. In this experiment, the sample to be heated was first placed into a container, and purged with N_2 for 15 min to remove air. The container was then capped with a ground glass stopper and heated in the muffle furnace at a pre-determined temperature.

In addition to isothermal treatment, we also examined the decomposition of PFAS in a dynamic thermal environment. Briefly, a known quantity of PFOA/PFOS chemical powders was placed in a closed container and heated dynamically in the muffle furnace at a 10 °C/min heating rate. This heating rate was used previously in the thermogravimetric analysis (TGA) (Xiao et al., 2020). After heat treatment and cooldown, the samples were treated in the same manner as the T#1 experiment.

Finally, the thermal decomposition of PFOA (Xiao et al., 2020) and PFOS at low and moderate temperatures (≤500 °C) was also studied by means of a thermal desorption–pyrolysis system (CDS Analytical) connected to a gas chromatograph with an MS detector

(TD–Pyr–GC–MS) (Agilent GC 7890 and 5975C MS; Santa Clara, CA) (see the Appendix B for more details).

3.3. Results and discussion

3.3.1. Thermal decomposition of PFAS in three conditions

We found that the thermal decomposition of PFAS mostly followed first-order kinetics at temperatures of 150–250 °C, in which the residual PFAS mass ($M_{PFAS,T}$) decreased in an exponential manner over heating time (Figure 3.1). At a higher temperature (300 °C), the decomposition of these chemicals can also be described by second-order kinetics, in which a plot of $1/M_{PFAS,T}$ versus heating time is approximately linear. For comparison purposes, we used the first-order decomposition rate constant (k_{1st}, min^{-1}) in the following discussion.

The value of k_{1st} was below 0.005 min^{-1} for PFCAs at 150–250 °C in T#1 (Figure 3.2). PFECA (HFPO-DA) appears to be more easily degraded than the PFCA with the same number of perfluorinated carbons (i.e., PFBA) (Figures 3.1 and 3.2). This is consistent with our previous observation (Xiao et al., 2020) that the perfluorinated chain becomes less thermally stable with the inclusion of a foreign group such as the ether group.

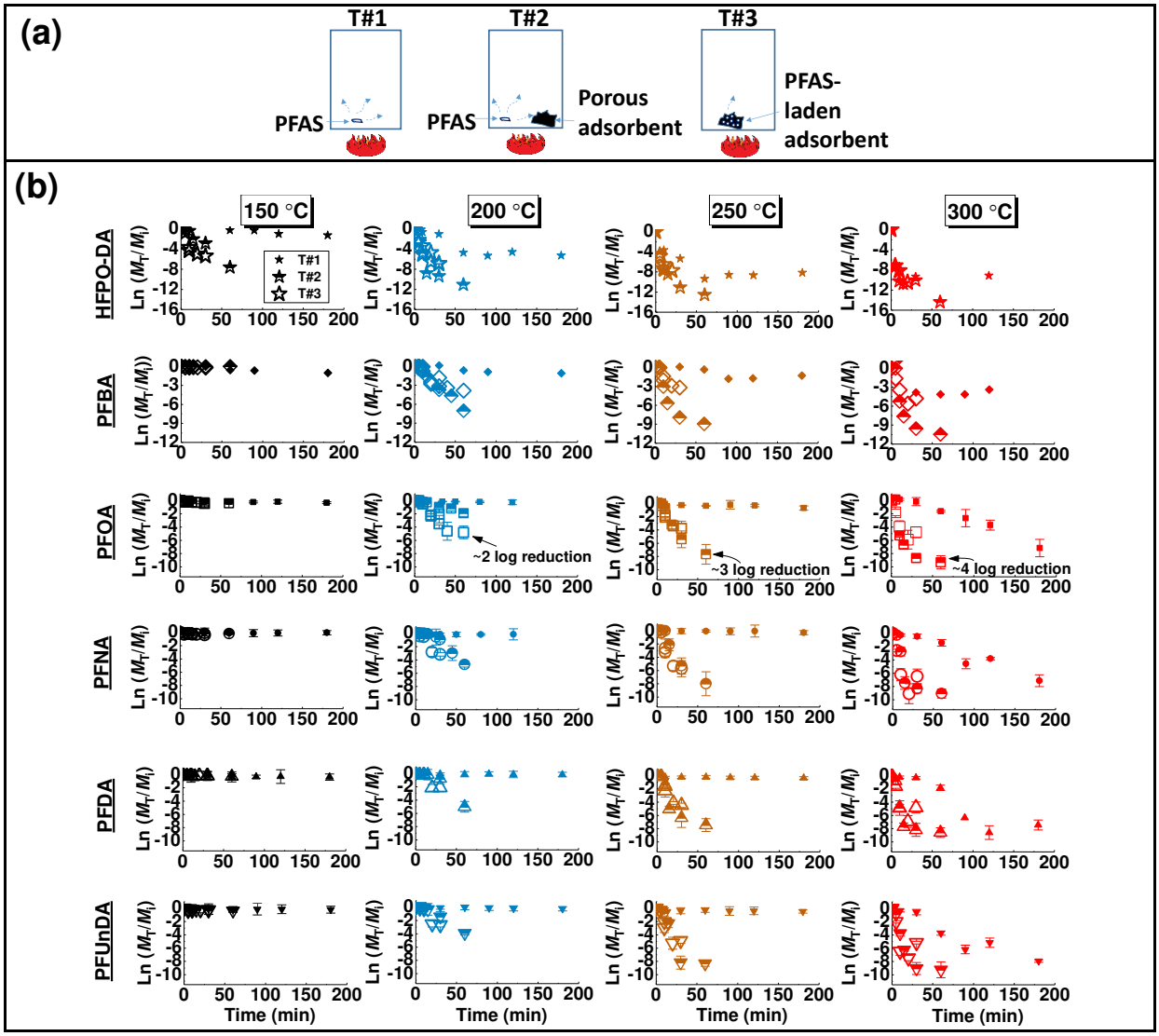

Figure 3.1. *(a) A schematic of PFAS thermal decomposition experiments in a closed system in three conditions (T#1, T#2, T#3). (b) Degradation of studied PFAS and a PFAS alternative (HFPO-DA) at various temperatures. Thermal treatments were triplicated for PFOA, PFNA, PFDA, and PFUnDA. The error bars represent the standard deviation (1-sigma) of three trials. Some points without visible error bars have errors that are smaller than the symbol. T#1 (closed symbols): PFAS only (initial PFAS mass: 1.2 × 10^{-5} mol). T#2 (half-open symbols): PFAS (1.2 × 10^{-5} mol) with the presence of 0.1 g GAC. T#3 (open symbols): 0.1 g of GAC laden with 3.0–4.5 × 10^{-7} mol PFAS. M_T and M_i are the*

residual mass of PFAS in heated samples and the initial mass in non-heated controls, respectively. The degradation of studied PFAS at 150 °C occurred at a slow rate (see Figure 3.2 for decomposition rate constants).

3.3.2. Effect of GAC

As illustrated in Figure 3.2, GAC accelerated the thermal decomposition of HFPO-DA at temperatures as low as 150 °C in T#2 and T#3 conditions. The GAC-induced acceleration was evident for PFCAs at 200 °C, and up to a 60-fold increase in k_{1st} was observed (T#2 and T#3) (Figure 3.2). This acceleration became even more significant at 250 °C, which led to a 150-fold increase in k_{1st} for PFUnDA (Figure 3.2). As displayed in Figure 3.2, the acceleration effect was less pronounced for the short-chain PFAS (PFBA) because the adsorption of PFBA on GAC was much weaker than that of its long-chain homologues (see Figure 3.3 for adsorption isotherms of PFBA, HFPO-DA, and PFOA on GAC). The effect of GAC became less marked at higher temperatures of 300 °C and 400 °C at which the significant thermolysis (T#1) of PFCAs was seen (Figures 3.1 and 3.2). A thermal treatment at 300 °C in T#2 led to near complete decomposition (>99.99%) of PFOA within 60 min. No attempt was made to maximize the thermal decomposition of PFCAs. A similar effect of GAC was observed when the samples were heated anaerobically (Figure 3.4); the k_{1st} of PFOA obtained in air was not significantly different from that obtained in N_2 (Figure 3.4).

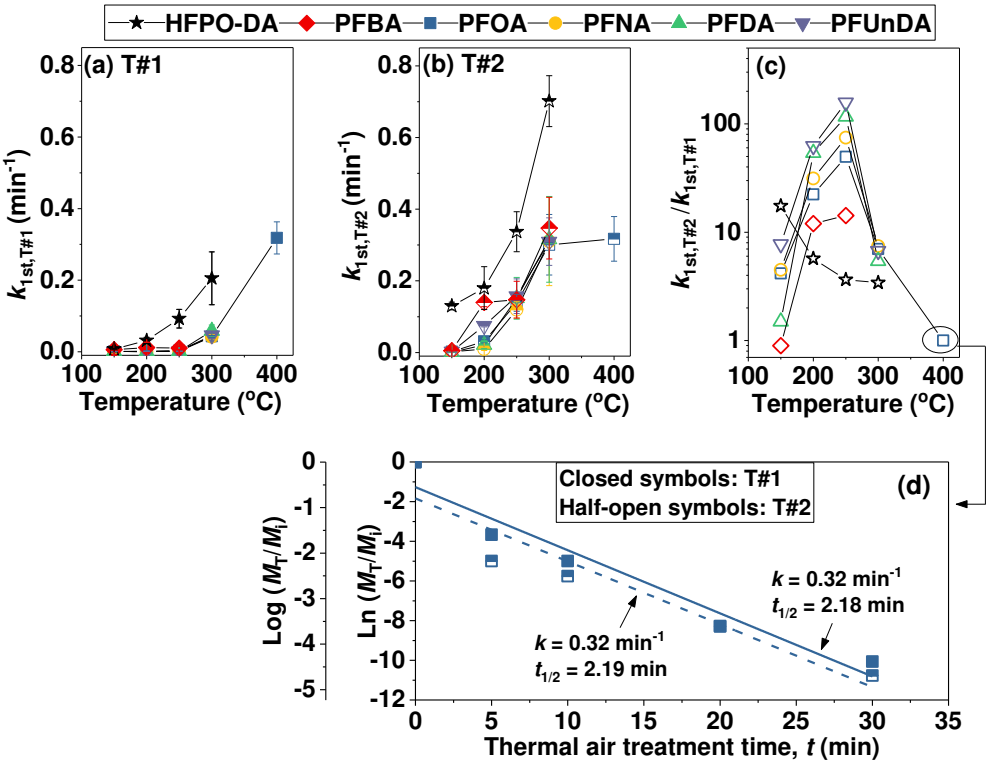

Figure 3.2. *(a–c) First-order decomposition rate constants (k_{1st}, min^{-1}) of PFCAs (1.2×10^{-5} mol) treated at different temperatures in conditions of T#1 (thermolysis; closed symbols) and T#2 (with the presence of 0.1 g of GAC; half-open symbols). (d) Thermal decomposition of PFOA (1.2×10^{-5} mol) in T#1 and T#2 (with the presence of 0.1 g GAC) in a closed container at 400 °C. Lines in (d) represent the best-fit to the decomposition data using the first-order kinetic model.*

Because PFCEA and PFCA molecules were not pre-adsorbed on GAC in T#2 treatments, we hypothesize that the accelerated decomposition was caused by the adsorption of gas-phase PFCEA/PFCA on GAC that is much more thermally conductive (0.4–1.36 W/ (m•K)) than air (<0.032 W/ (m•K) at ≤100 °C) (Jin et al., 2013; Khaliji Oskouei and Tamainot-Telto, 2019). The heat transfer is more efficient on GAC than in air. On the other hand, the thermal conductivity of air increases with temperature. At 400

°C, the effect of GAC amendment on the thermal decomposition rate of PFAS appears to be much less important.

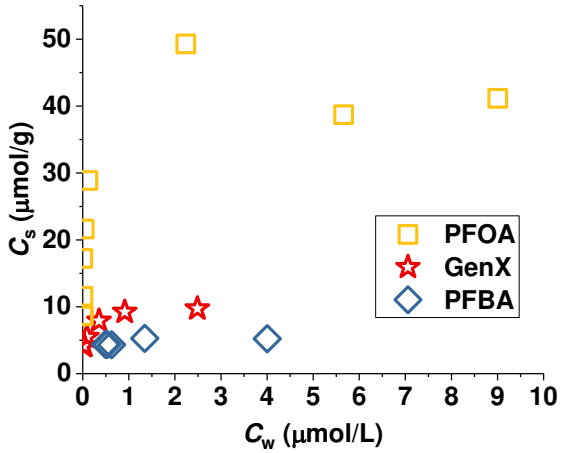

Fits of adsorption isotherms to the Freundlich model ($C_s = K_f \times C_w^n$)			
	GenX	PFBA	PFOA
Log K_f	0.95	0.67	1.48
n	0.21	0.1	0.18
R^2	0.97	0.94	0.73

Figure 3.3. *Adsorption isotherms of three PFAS on GAC (Filtrasorb 200, Calgon Carbon Corporation, PA) in distilled water containing 1.0 × 10^{-3} mol/L $NaHCO_3$ (buffer) and 1.0 × 10^{-3} mol/L NaCl.*

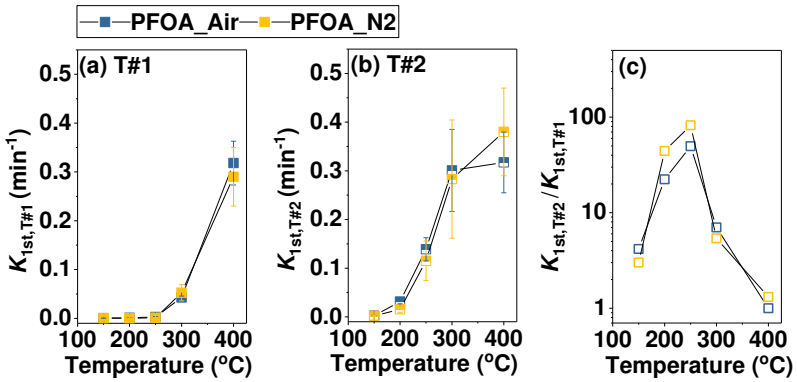

Figure 3.4. *First-order decomposition rate constant (k_{1st}, min^{-1}) of PFOA (1.2 × 10^{-5} mol) treated at different temperature in conditions T#1 (thermolysis; closed symbols) and T#2 (with the presence of 0.1 g of GAC; half-open symbols) in an atmosphere of air or N_2.*

3.3.3. Effect of other PCMs and porous resin

To test this hypothesis, we conducted T#2 experiments with various PCMs and one non-carbonaceous material, XAD-2 resin. The results are plotted as a function of the $K_{d,w-s}$ of PFOA (Figure 3.5). Charcoals have a higher thermal conductivity, 0.08–0.18 W/ (m•K) (Behazin et al., 2016), than air. However, raw charcoals are primarily microporous (≤20 Å) (Xiao and Pignatello, 2016). Steric hindrance can result from narrow pore throats, internal obstructions, or pore blockage by occluded non-covalently bound matter such as pyrolysis tars (Xiao and Pignatello, 2015a; Zhu et al., 2005). The length of PFOA molecules is approximately 10 Å (Xiao et al., 2011). The steric bulk of PFOA molecules may limit their access to the interior micropore SA of raw charcoal that is available to N_2 molecules. Therefore, a low adsorption of PFOA on raw charcoals was observed (Figure 3.5), and the thermal decomposition of PFOA was not accelerated with the addition of a raw charcoal sample (M350, M600, P350, or P700). The thermal air oxidation of raw charcoals caused pore wall etching and/or unclogging of pores bearing tarry deposits generated during the carbonization step (Xiao et al., 2018a; Xiao and Pignatello, 2016). This in turn widened pores of charcoal and created new SA, which helped relieve steric hindrance for adsorption of PFOA molecules (Figure 3.5). As illustrated in Figure 3.5, the thermal decomposition of PFOA increased significantly with the addition of a thermally air oxidized charcoal. Commercial porous materials, GAC (or activated charcoal) and XAD-2 resin, adsorbed PFOA strongly (Figure 3.5) and reduced the thermal decomposition half-life of PFOA from ~400 min to less than 25 min at 200 °C (Figure 3.5). The N_2 B.E.T. SA of the XAD-2 resin (330–370 m^2/g) is lower than that of the thermally air oxidized M600; however, the XAD-2 resin is characterized by a broad pore size distribution and a

mean pore size of 90 Å. Mesopores (20–500 Å) have shown to be important for molecules to access deeper and smaller pores of adsorbents (Xiao and Pignatello, 2015a). Finally, the borosilicate glass appeared to have no significant effect on the thermal decomposition of PFOA (Figure 3.5).

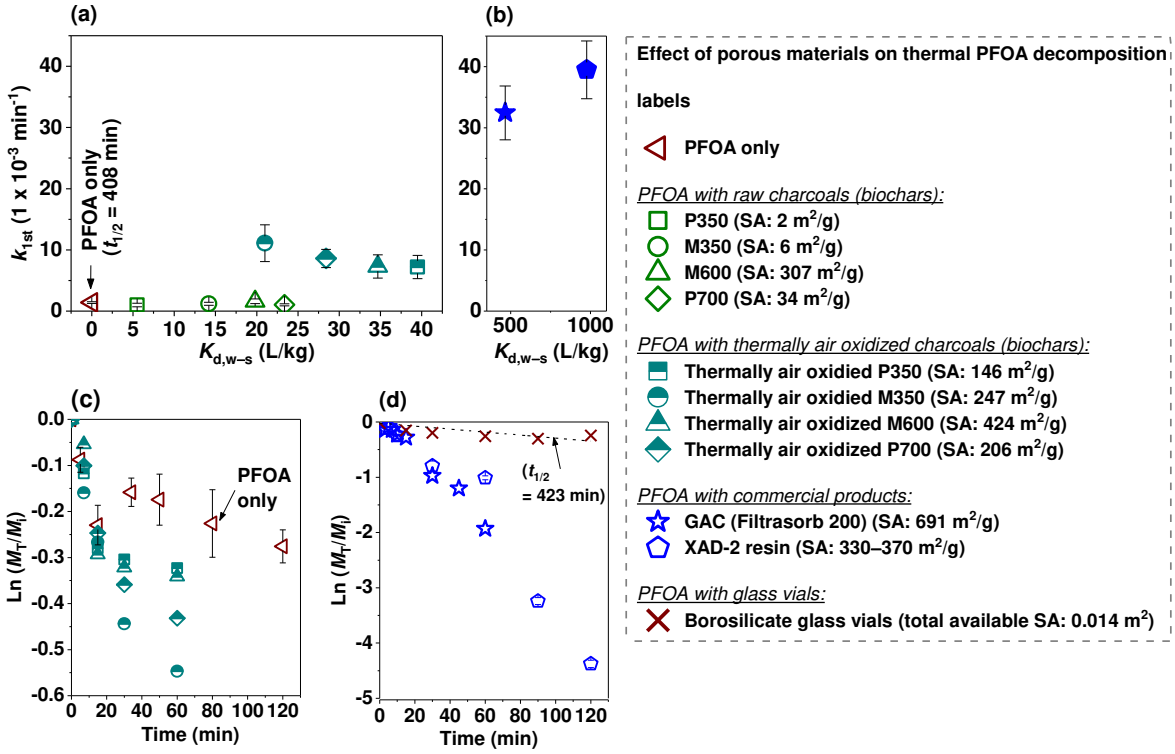

Figure 3.5. *(a) and (b): First-order decomposition rate constants (k_{1st}, 1 × 10^{-3} min^{-1}) of PFOA (1.2 × 10^{-5} mol) treated at 200 °C in T#1 (thermolysis) or in T#2 with the presence of a raw charcoal sample (M350, M600, P350, or P700) (0.5 g), a thermally air oxidized charcoal (0.1 g), GAC (Filtrasorb 200) (0.1 g), a non-carbonaceous porous material (XAD-2 resin) (0.1 g), or five 2-mL borosilicate vials (11.1 ± 0.01 g). (c) and (d): Thermal decomposition of PFOA in different conditions at 200 °C. The dashed line in (d) represents the best-fit to the decomposition data using the first-order kinetic model. The N_2 B.E.T. SA of XAD-2 resin was obtained from the literature (Jung et al., 2001; Tewari and Singh, 2002). The N_2 B.E.T. SAs of nine PCM adsorbents were measured in this study.*

3.3.4. Thermal decomposition pathways

PFCAs yielded several transient PFCA intermediates at temperatures as low as 150 °C (Figures 3.6 and 3.7). For a parent PFCA with *n* perfluorinated carbons, the highest yielding intermediate product is usually the shorter-chained PFCA with (*n* – 1) perfluorinated carbons (Figure 3.6 and 3.7). For example, PFDA yielded shorter-chain PFCAs in the following order, PFNA > PFOA > PFHpA ≈ PFPeA ≈ PFBA. Similarly, the highest yielding byproduct of PFOA was PFHpA, whereas PFBA was a trace intermediate product. This formation pattern seems to agree with the stepwise defluorination mechanism (Pathway II in Figure 4.1) that has been developed for photocatalysis (Wang et al., 2008), reduction by hydrated electrons (Bentel et al., 2019), and plasma (Singh et al., 2019) treatments of PFAS compounds. However, a closer look at the results reveals that it is not the predominant mechanism of the thermolysis of PFAS. First, the yield of intermediate PFCAs is low (<5 mol %) during the T#1 treatment (Figure 3.6). Second, a clear stepwise pattern was not observed because all the short-chain intermediates appeared nearly simultaneously (Figures 3.6 and 3.7).

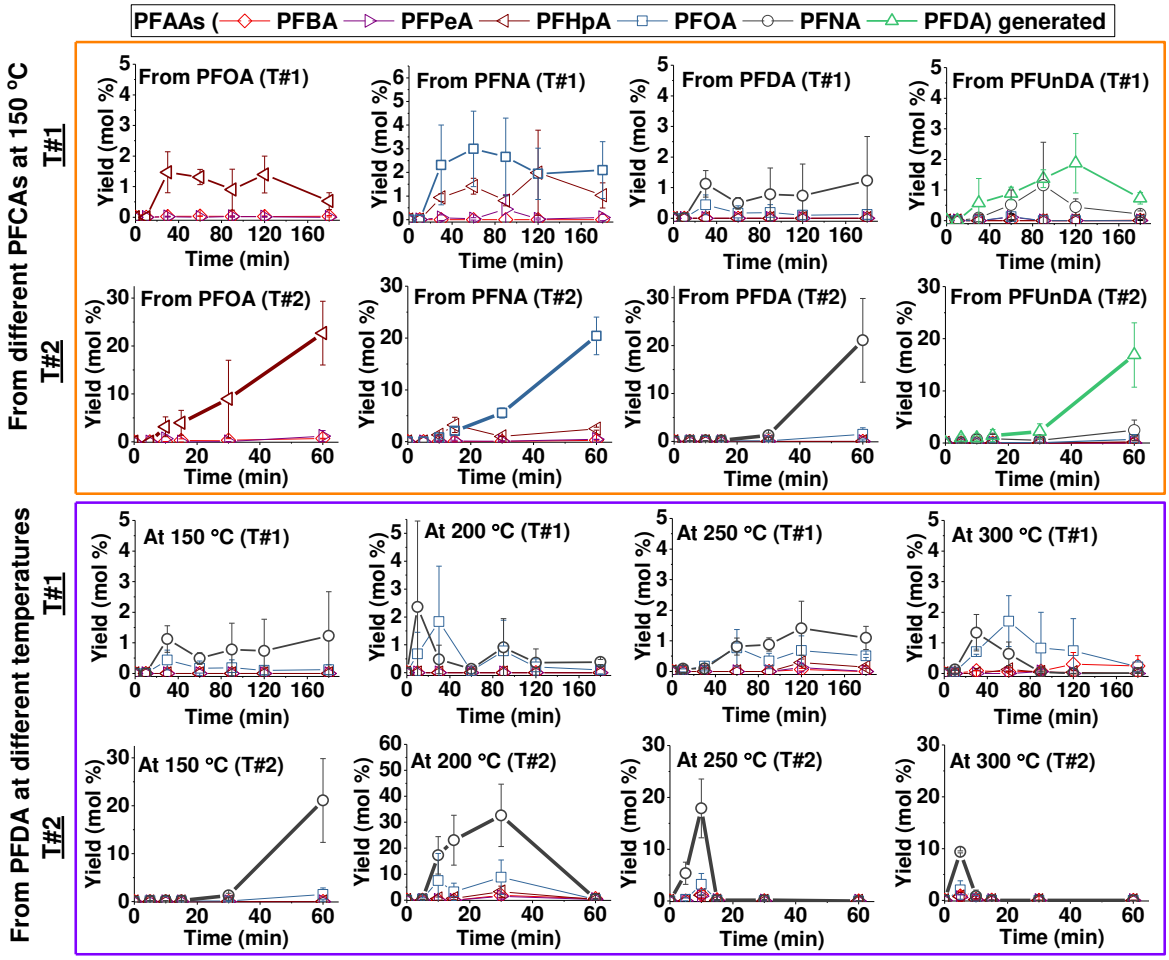

Figure 3.6. *Generation (and subsequent decomposition) of intermediate short-chain PFCAs from parent compounds treated in different conditions (T#1 and T#2; Fig. 1). The intermediates were detected by the UPLC–QToF-MS/MS method as detailed in the Supplementary data. Note the difference in y-axis scales.*

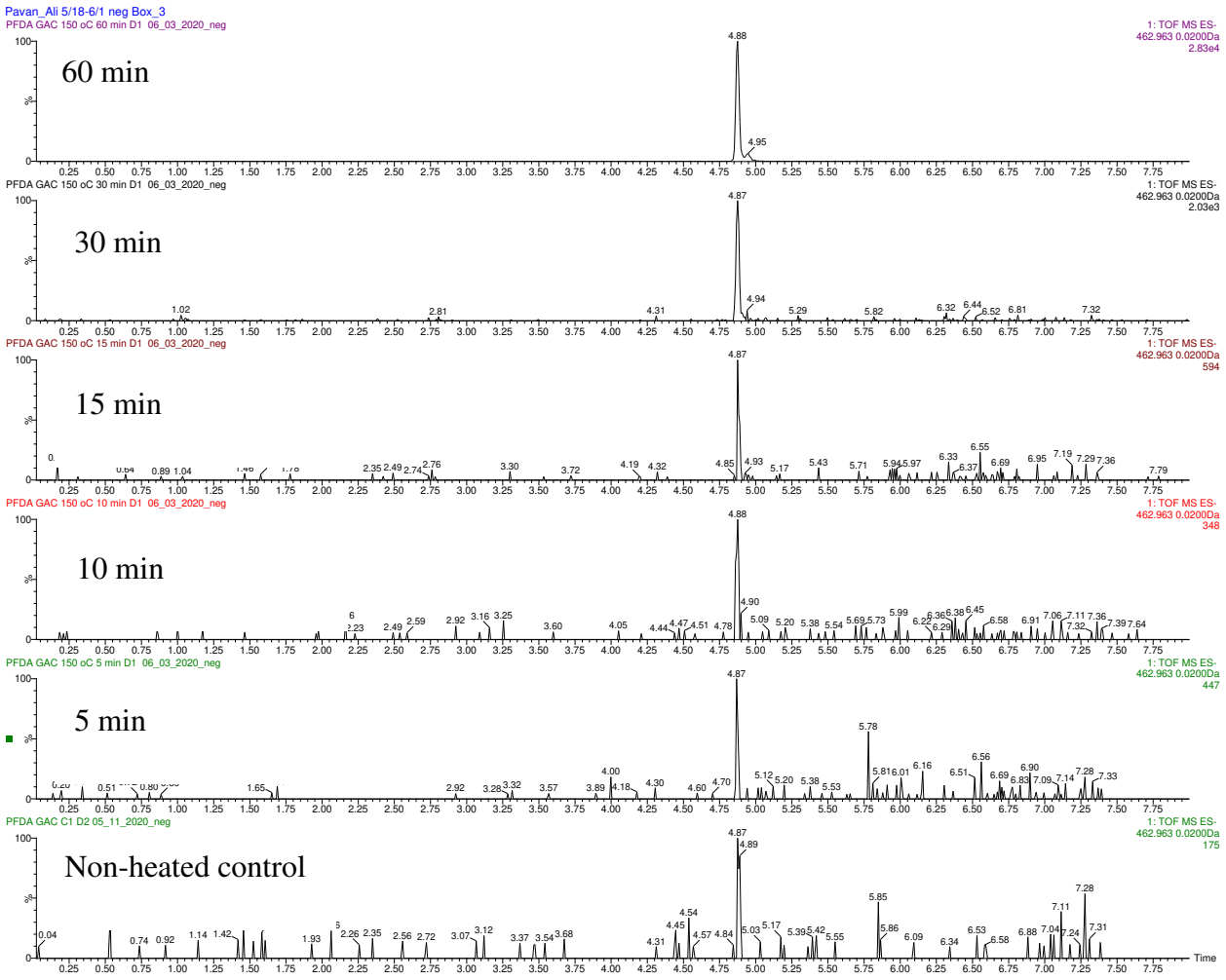

Figure 3.7. *UPLC–ESI⁻-ToF MS selected ion chromatograms on m/z 462.963 of methanol (with 100 mmol/L ammonium acetate) extracts of PFDA after T#2 (with the presence of GAC) thermal treatments at 150 °C for different times.*

4. CHAPTER 4: Mechanisms Involved in Thermal Decomposition of PFAS and Implications to Water Treatment

Pavankumar Challa Sasi, Ali Alinezhad, Bin Yao, Alena Kubátová, Svetlana A. Golovko, Mikhail Y. Golovko, Feng Xiao. 2021. Effect of granular activated carbon and other porous materials on thermal decomposition of per- and polyfluoroalkyl substances: mechanisms and implications for water purification. ***Water Research*** (published)

DOI: https://doi.org/10.1016/j.watres.2021.117271

4.1. Mechanisms

We propose a different thermal decomposition mechanism (Pathway I in Figure 4.1). We believe thermal decomposition of PFAS involves multistep radical chain reactions, including initiation, chain propagation, recombination, and termination (Xiao et al., 2021b). Because of the strong C–F bond, we believe that the thermal decomposition of PFOA was initiated with the homolytic cleavage of the relatively weak C–C bond located next to the carboxyl group of PFOA, or with the C–S bond next to the sulfonate group of PFOS. The C–C or C–S bond splits, forming a nonfluorinated moiety and a perfluoroalkyl biradical such as :C_7F_{14} (*m/z* 350.0) from PFOA or :C_8F_{16} (*m/z* 399.9) from PFOS (Figs. 6 and S4). The perfluoroalkyl radical further undergoes a series of defluorination, or radical chain propagation reactions, generating shorter-chained perfluoroalkyl radicals (Figure 4.1). These perfluoroalkyl radicals may recombine with carboxyl group/radical successively yielding PFCA intermediates. Eventually, these chain propagation reactions are terminated by producing the "dead," or very short, fluorinated units. In Pathway I, transient PFCA intermediates are the minor product. A number of intermediate perfluoroalkyl radicals/species were identified (Figure B13), including ·CF_3 (*m/z* 69.0), ·C_3F_3 (*m/z* 93.0), C_2F_4 (*m/z* 100.0), ·C_2F_5 (*m/z* 119.0), ·C_3F_5 (*m/z* 131.0), ·C_3F_7 (*m/z* 169.0), ·C_4F_7 (*m/z* 181.0), ·C_5F_9 (*m/z* 231.0), ·C_6F_{11} (*m/z* 281.0), ·C_7F_{13} (*m/z* 331.0), and :C_7F_{14} (*m/z* 350.0). Many of these perfluoroalkyl radicals have also been observed in previous studies on the thermal treatment of PFOS (Wang et al., 2013) and perfluorocarbons (Kagramanov et al., 1990). Note that these species were detected by TD–Pyr–GC–MS in an inert atmosphere (helium). At present, our TD–Pyr–GC–MS system is not able to operate in an air atmosphere. However, the general decomposition mechanism (initiation,

chain propagation, termination) illustrated in Figure 4.1 may also apply to the thermal treatment of PFAS under active atmospheres.

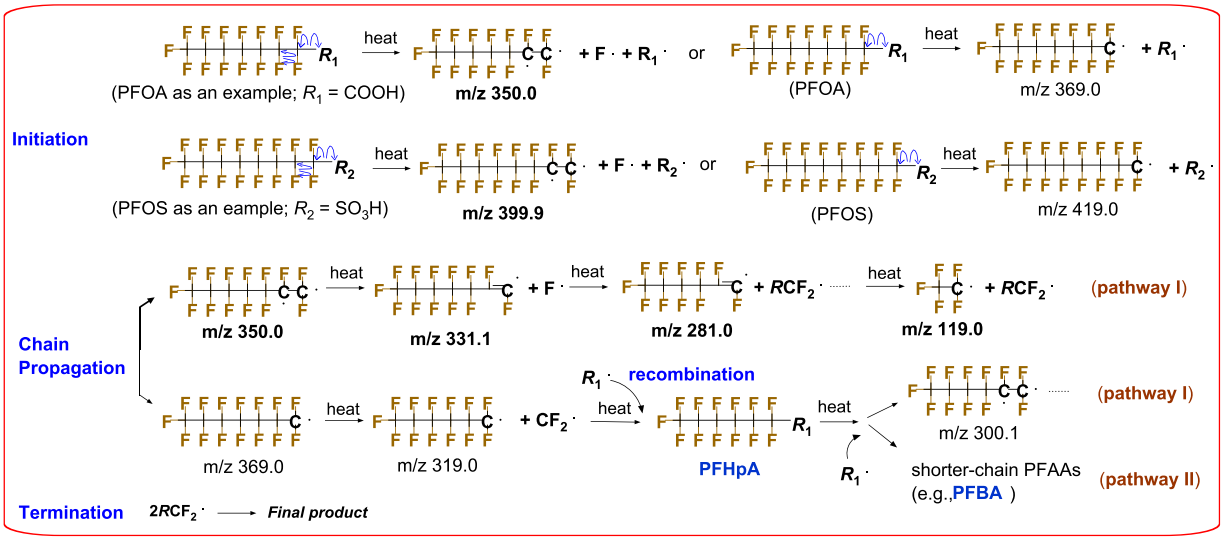

Figure 4.1. *Possible "unzip" decomposition pathways of perfluoroalkyl substances during thermal treatment. Species with m/z 399.9, 350.0, 331.1, 281.0, and 119.0 were shown in TD–Pyr–GC–MS spectra of PFOA (Xiao et al., 2020) and PFOS (Figure B13). We found no MS spectral evidence for :C_7F_{14} (m/z 300.1), ·C_6F_{13} (m/z 319.0), ·C_7F_{15} (m/z 369.0), and ·C_8F_{17} (m/z 419.0), but this does not preclude their formation in small amounts.*

It is evident that the presence of GAC altered the decomposition pathway of PFCAs, significantly increasing yields of shorter-chained PFCA intermediates at 150 °C (Figure 3.6 and 3.7). At 200 °C, the yield of PFNA from PFDA was maximized after a 30-min treatment in T#2, and then disappeared on the same time scale as the parent compound (i.e., PFDA) (Figure 3.6 and 3.7). At a higher temperature (300 °C), the yield of PFNA

from PFDA dropped to <10 mol % after a 5-min treatment (Figure 3.6 and 3.7), and was negligibly low with a longer heating time as PFNA quickly decomposed (Figure 3.1). Previously, no measurable shorter-chained PFCAs were detected after a 30-min thermal treatment of PFOA on GAC at 400 °C (Xiao et al., 2020).

4.2. Effect of GAC on the yield of F from PFOA.

The yield of F from PFOA during low-temperature T#1 thermolysis (≤400 °C) remained less than 2 mol % (Figure 4.2). The addition of GAC (T#2) significantly enhanced the yield of F (Figure 4.2a). We observed a critical mass ratio of PFOA to GAC (620 μmol PFOA/g_{GAC}) above which the effect of GAC is insignificant in T#2 as the GAC may become saturated with gas-phase PFOA molecules (Figure 4.2b). This ratio reflects a dynamic balance between the adsorption and thermal decomposition of gas-state PFOA on the surface of GAC; it is more than one order of magnitude greater than the saturated adsorption amount (~40 μmol PFOA/g_{GAC}), or the maximum adsorption capacity, of the GAC for PFOA in the liquid phase (Figure 3.3).

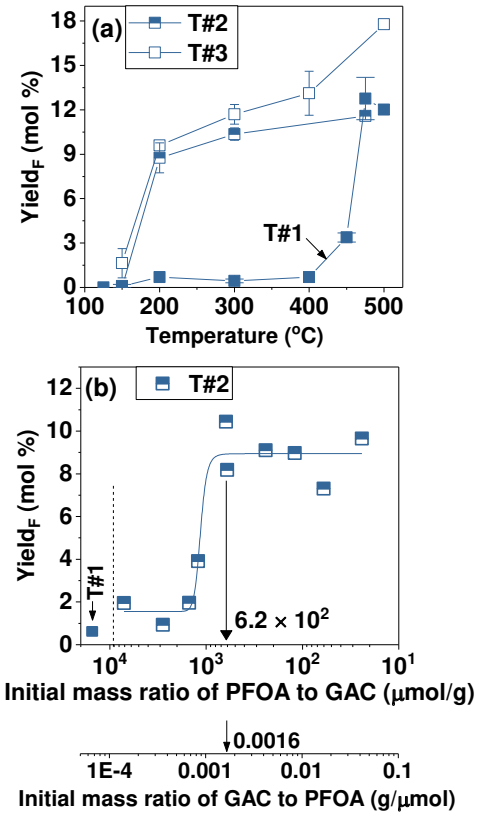

Figure 4.2 *(a) Measured yield of F from PFOA heated at different temperatures in three conditions, T#1 (1.2 × 10^{-5} mol PFOA), T#2 (1.2 × 10^{-5} mol PFOA with 0.1 g GAC), and T#3 (0.1 g of GAC laden with 3.1 × 10^{-7} mol PFOA). (b) Measured yield of F from PFOA heated in T#2 at 200 °C at different initial mass ratios of PFOA to GAC. All the data were obtained after 30-min isothermal heating of PFOA or PFOA with GAC. No measurable F was detected from GAC itself in thermal treatments.*

4.3. Three temperature zones.

According to dynamic decomposition results (Figure 4.3), three temperature zones can be recognized. PFOA is stable and essentially nonvolatile at temperatures below 90 °C (Zone A). A rise in temperature above 90 °C (Zone B) triggers the phase transfer (e.g.,

melting, boiling, sublimation) of PFOA molecules (Xiao et al., 2021b) because of the rising vapor pressure (Kaiser et al., 2005). PFOA molecules started to degrade in Zone B. When the temperature increased to 400 °C or above (Zone C), PFOA molecules were quickly degraded (Figures 3.2d and 4.3). The addition of GAC compressed Zone B and facilitated the thermal decomposition of PFOA. PFOS, on the other hand, is highly nonvolatile until 400 °C (Xiao et al., 2020). The thermal decomposition of PFOS was not significantly affected with the presence of GAC (Figure B14).

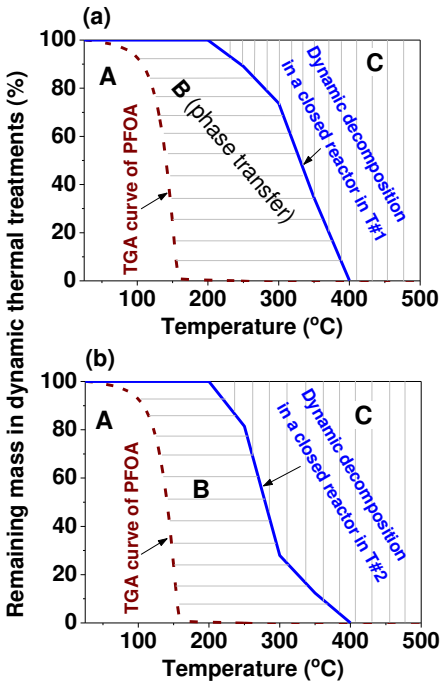

Figure 4.3. *Brown dashed lines: dynamic (10 °C/min) TGA curves of PFOA determined in an open system (Xiao et al., 2020). Blue solid curves: mass loss of PFOA in dynamic (10 °C/min) thermal treatments performed in a closed container in two conditions: (a), T#1 (1.2×10^{-5} mol PFOA); (b), T#2 (1.2×10^{-5} mol PFOA with 0.1 g GAC).*

5. CHAPTER 5: Conclusions and future work

5.1. Conclusions:

PFASs are synthetic organic compounds that are persistent, bioaccumulative and toxic to humans and the environment. Due to their physiochemical properties i.e., the strong carbon-fluorine bond makes these compounds both thermal and chemical stable and remain in the environment forever. Conventional drinking water techniques are not effective in removing them and most new developments have been mainly focused on enhanced removal. However, this does not solve the problem, it moves the contamination from one matrix to another. Hence, there is a need for developing and investigating advanced techniques that not only focus on removal but also destroy them. The fate of PFAS in thermal processes is poorly understood. PFCAs used as surface-active agents in non-stick cookware and fire-fighting foams are generally assumed to be thermally stable at low temperatures (<300 ^{o}C). But previous research on thermal treatment of PFAS is scarce. The objectives of this thesis were to determine the thermal stability, decomposition and the fate of PFAS compounds during thermal treatment using GAC and other porous carbonaceous media.

The key findings of this dissertation are:

1. Investigated extraction methods using amendments to organic solvent. Methanol that was amended with ammonium acetate at 100 mmol/L achieved effective recoveries ranging from 79.2 to 111.8% for most of the PFAS.
2. Demonstrated the thermal stability of 11 PFAS compounds including PFOS, PFOA and GenX under different atmospheric environments. PFAS exhibited the

following order of thermal stability: PFSAs >> PFUnDA > PFDA > PFNA > PFOA > PFBA > HFPO-DA.

3. Based on our data, effective thermal destruction of PFAS during GAC reactivation in CO_2/N_2 or during incineration/combustion of materials laden with PFAS (e.g., municipal solid wastes) is very likely provided high temperatures (≥700 °C) are used.
4. Organofluorine compounds generated from thermal decomposition of PFAS at low to moderate temperatures (≤600 °C) warrant studies on the exposure to these compounds during cooking, baking, firefighting, and other relevant thermal processes involving PFAS.
5. The observed thermal decomposition of PFAS on GAC underscores the importance for more studies that examine the effect of GAC and other porous materials on the thermal stability and mineralization of PFAS. Lastly, this study focuses on PFAAs that represent only a small fraction of the total organic fluorine present in the environment (Miyake et al., 2007; Tan et al., 2014; Xiao, 2017; Yeung et al., 2008).
6. Contradictory to this prevailing view, this study shows that the thermolysis of PFCAs occurs at low temperatures of 150–200 °C (Figures 3.1 and 3.2), albeit slowly.
7. Demonstrated that the low-temperature (150–300 °C) thermal decomposition of PFCAs was accelerated by highly porous adsorbents. The effect of GAC is much less significant at ≥400 °C at which the thermolysis of PFOA was markedly faster.
8. The results also indicate that: (1) the N_2-B.E.T. SA of adsorbents is a poor predictor of the adsorption of PFOA molecules, and (2) the polyaromatic units of PCMs

appear to be unimportant. On the basis of our data, effective removal and decomposition of PFAS thermal processes, such as GAC reactivation, is very likely.

5.2. Future work

Studies are underway to understand the thermal stability of other types of PFAS, including nonionic, cationic and zwitterionic precursor compounds of PFOA and PFOS (Xiao et al., 2019) that have been identified in AFFFs (Barzen-Hanson et al., 2017; D'Agostino and Mabury, 2014), surfactants (Xiao et al., 2017), and the natural environment (Backe et al., 2013; Barzen-Hanson et al., 2017; D'Agostino and Mabury, 2017; Mejia-Avendano et al., 2017; Munoz et al., 2016; Place and Field, 2012). The overall goal of thermal treatment processes is to completely degrade PFAS from aqueous media and mineralize to CO_2 and inorganic fluorine (Wang et al., 2022). Currently there are no standardized measurements methods for quantifying if PFAS or other volatile organofluorine compounds are being released into the air during thermal treatment processes. Development of such methods could potentially answer and help characterize the completeness of thermal treatment of PFAS (EPA, 2020).

6. References

Agency, U.S.E.P. 2021 PFAS Strategic Roadmap: EPA's Commitments to Action 2021-2024.

Andrews, D.Q. and Naidenko, O.V. 2020. Population-wide exposure to per- and polyfluoroalkyl substances from drinking water in the United States. Environ Sci Tech Let 7(12), 931-936.

Anumol, T., Dagnino, S., Vandervort, D.R. and Snyder, S.A. 2016. Transformation of polyfluorinated compounds in natural waters by advanced oxidation processes. Chemosphere 144, 1780-1787.

Appleman, T.D., Dickenson, E.R.V., Bellona, C. and Higgins, C.P. 2013. Nanofiltration and granular activated carbon treatment of perfluoroalkyl acids. Journal of Hazardous Materials 260, 740-746.

Appleman, T.D., Higgins, C.P., Quiñones, O., Vanderford, B.J., Kolstad, C., Zeigler-Holady, J.C. and Dickenson, E.R. 2014. Treatment of poly- and perfluoroalkyl substances in U.S. full-scale water treatment systems. Water Res. 51, 246-255.

Armitage, J.M., Schenker, U., Scheringer, M., Martin, J.W., Macleod, M. and Cousins, I.T. 2009. Modeling the Global Fate and Transport of Perfluorooctane Sulfonate (PFOS) and Precursor Compounds in Relation to Temporal Trends in Wildlife Exposure. Environmental Science & Technology 43(24), 9274-9280.

Ateia, M., Maroli, A., Tharayil, N. and Karanfil, T. 2019. The overlooked short- and ultrashort-chain poly- and perfluorinated substances: A review. Chemosphere 220, 866-882.

Backe, W.J., Day, T.C. and Field, J.A. 2013. Zwitterionic, cationic, and anionic fluorinated chemicals in aqueous film forming foam formulations and groundwater from U.S. military bases by nonaqueous large-volume injection HPLC-MS/MS. Environ. Sci. Technol. 47(10), 5226-5234.

Banzhaf, S., Filipovic, M., Lewis, J., Sparrenbom, C.J. and Barthel, R. 2017. A review of contamination of surface-, ground-, and drinking water in Sweden by perfluoroalkyl and polyfluoroalkyl substances (PFASs). Ambio 46(3), 335-346.

Barzen-Hanson, K.A., Roberts, S.C., Choyke, S., Oetjen, K., McAlees, A., Riddell, N., McCrindle, R., Ferguson, P.L., Higgins, C.P. and Field, J.A. 2017. Discovery of 40 classes of per- and polyfluoroalkyl substances in historical aqueous film-forming foams (AFFFs) and AFFF-impacted groundwater. Environ. Sci. Technol. 51(4), 2047-2057.

Begley, T., Castle, L., Feigenbaum, A., Franz, R., Hinrichs, K., Lickly, T., Mercea, P., Milana, M., O'Brien, A., Rebre, S., Rijk, R. and Piringer, O. 2005. Evaluation of migration models that might be used in support of regulations for food-contact plastics. Food Addit Contam A 22(1), 73-90.

Behazin, E., Ogunsona, E., Rodriguez-Uribe, A., Mohanty, A.K., Misra, M. and Anyia, A.O. 2016. Mechanical, chemical, and physical properties of wood and perennial grass biochars for possible composite application. Bioresources 11(1), 1334-1348.

Belkouteb, N., Franke, V., McCleaf, P., Köhler, S. and Ahrens, L. 2020. Removal of per- and polyfluoroalkyl substances (PFASs) in a full-scale drinking water treatment plant: Long-term performance of granular activated carbon (GAC) and influence of flow-rate. Water Research 182, 115913.

Bentel, M.J., Yu, Y.C., Xu, L.H., Li, Z., Wong, B.M., Men, Y.J. and Liu, J.Y. 2019. Defluorination of per- and polyfluoroalkyl substances (PFASs) with hydrated electrons: Structural dependence and implications to PFAS remediation and management. Environ. Sci. Technol. 53(7), 3718-3728.

Bischel, H.N., MacManus-Spencer, L.A. and Luthy, R.G. 2010. Noncovalent interactions of long-chain perfluoroalkyl acids with serum albumin. Environ. Sci. Technol. 44(13), 5263–5269.

Boiteux, V., Dauchy, X., Rosin, C. and Munoz, J.F. 2012. National screening study on 10 perfluorinated compounds in raw and treated tap water in France. Arch. Environ. Contam. Toxicol. 63(1), 1–12.

Boucher, J.M., Cousins, I.T., Scheringer, M., Hungerbühler, K. and Wang, Z. 2019. Toward a Comprehensive Global Emission Inventory of C_4–C_{10} Perfluoroalkanesulfonic Acids (PFSAs) and Related Precursors: Focus on the Life Cycle of C_6 -and C_{10}-Based Products. Environmental Science & Technology Letters 6(1), 1-7.

Brennan, N.M., Evans, A.T., Fritz, M.K., Peak, S.A. and Von Holst, H.E. 2021. Trends in the Regulation of Per- and Polyfluoroalkyl Substances (PFAS): A Scoping Review. International Journal of Environmental Research and Public Health 18(20), 10900.

Burns, D.J., Hinrichsen, H.M., Stevenson, P. and Murphy, P.J.C. 2022. Commercial‐scale remediation of per‐ and polyfluoroalkyl substances from a landfill leachate catchment using Surface‐Active Foam Fractionation (SAFF®). Remediation Journal 32(3), 139-150.

Burns, D.J., Stevenson, P. and Murphy, P.J.C. 2021. PFAS removal from groundwaters using Surface‐Active Foam Fractionation. Remediation Journal 31(4), 19-33.

Calafat, A.M., Wong, L.-Y., Kuklenyik, Z., Reidy, J.A. and Needham, L.L. 2007. Polyfluoroalkyl chemicals in the U.S. population: data from the National Health and Nutrition Examination Survey (NHANES) 2003-2004 and comparisons with NHANES 1999-2000. Environmental health perspectives 115(11), 1596-1602.

Cao, X.Y., Xiao, F., Duan, P., Pignatello, J.J., Mao, J.D. and Schmidt-Rohr, K. 2019. Effects of post-pyrolysis air oxidation on the chemical composition of biomass chars investigated by solid-state nuclear magnetic resonance spectroscopy. Carbon 153, 173-178.

Carter, K.E. and Farrell, J. 2010. Removal of Perfluorooctane and Perfluorobutane Sulfonate from Water via Carbon Adsorption and Ion Exchange. Separation Science and Technology 45(6), 762-767.

Conder, J.M., Hoke, R.A., De Wolf, W., Russell, M.H. and Buck, R.C. 2008. Are PFCAs bioaccumulative? A critical review and comparison with regulatory lipophilic compounds. Environmental Science & Technology 42(4), 995-1003.

Council, N.R. 2009 Disposal of Activated Carbon from Chemical Agent Disposal Facilities, pp. 1 online resource (xvi, 70 pages), National Academies Press, Washington, D.C.

Crownover, E., Oberle, D., Kluger, M. and Heron, G. 2019. Perfluoroalkyl and polyfluoroalkyl substances thermal desorption evaluation. Remediation Journal 29(4), 77-81.

D'Agostino, L.A. and Mabury, S.A. 2014. Identification of novel fluorinated surfactants in aqueous film forming foams and commercial surfactant concentrates. Environ. Sci. Technol. 48(1), 121-129.

D'Agostino, L.A. and Mabury, S.A. 2017. Certain perfluoroalkyl and polyfluoroalkyl substances associated with aqueous film forming foam are widespread in Canadian surface waters. Environ Sci Technol 51(23), 13603-13613.

De Silva, A.O., Armitage, J.M., Bruton, T.A., Dassuncao, C., Heiger‐Bernays, W., Hu, X.C., Kärrman, A., Kelly, B., Ng, C., Robuck, A., Sun, M., Webster, T.F. and Sunderland, E.M. 2021. PFAS Exposure Pathways for Humans and Wildlife: A Synthesis of Current Knowledge and Key Gaps in Understanding. Environmental Toxicology and Chemistry 40(3), 631-657.

DeWitt, J.C., Blossom, S.J. and Schaider, L.A. 2018. Exposure to per-fluoroalkyl and polyfluoroalkyl substances leads to immunotoxicity: epidemiological and toxicological evidence. J Expo Sci Environ Epidemiol.

Dixit, F., Barbeau, B., Mostafavi, S.G. and Mohseni, M. 2019. PFOA and PFOS removal by ion exchange for water reuse and drinking applications: role of organic matter characteristics. Environmental Science-Water Research & Technology 5(10), 1782-1795.

Doll, S. 2021 2021 Analysis of Upcoming State Legislation on Toxic Chemicals.

Domingo, J.L., Jogsten, I.E., Eriksson, U., Martorell, I., Perello, G., Nadal, M. and van Bavel, B. 2012. Human dietary exposure to perfluoroalkyl substances in Catalonia, Spain. Temporal trend. Food Chemistry 135(3), 1575-1582.

Domingo, J.L. and Nadal, M. 2017. Per- and Polyfluoroalkyl Substances (PFASs) in Food and Human Dietary Intake: A Review of the Recent Scientific Literature. Journal of Agricultural and Food Chemistry 65(3), 533-543.

Duchesne, A.L., Brown, J.K., Patch, D.J., Major, D., Weber, K.P. and Gerhard, J.I. 2020a. Remediation of PFAS-Contaminated Soil and Granular Activated Carbon by Smoldering Combustion. Environmental Science & Technology 54(19), 12631-12640.

Duchesne, A.L., Brown, J.K., Patch, D.J., Major, D., Weber, K.P. and Gerhard, J.I. 2020b. Remediation of PFAS-contaminated soil and granular activated carbon by smoldering combustion. Environ Sci Technol.

Engineering ToolBox, (2003). Thermal Conductivity of Selected Materials and Gases. [online] Available at: https://www.engineeringtoolbox.com/thermal-conductivity-d_429.html [Accessed May 2020].

Engineering ToolBox, (2009). Air - Thermal Conductivity. [online] Available at: https://www.engineeringtoolbox.com/air-properties-viscosity-conductivity-heat-capacity-d_1509.html (accessed May 2020).

EPA 2020 Interim Guidance on the Destruction and Disposal of Perfluoroalkyl and Polyfluoroalkyl Substances and Materials Containing Perfluoroalkyl and Polyfluoroalkyl Substances.

EPA 2021 FACT SHEET: EPA & The Bipartisan Infrastructure Law.

EPA 2022 Lifetime drinking water health advisories for four perfluoroalkyl substances, pp. 36848-36849, Federal Register.

Ericson, I., Domingo, J.L., Nadal, M., Bigas, E., Llebaria, X., van Bavel, B. and Lindstrom, G. 2009. Levels of perfluorinated chemicals in municipal drinking water from Catalonia, Spain: Public health implications. Arch. Environ. Contam. Toxicol. 57(4), 631–638.

Eschauzier, C., Beerendonk, E., Scholte-Veenendaal, P. and de Voogt, P. 2012. Impact of treatment processes on the removal of perfluoroalkyl acids from the drinking water production chain. Environ. Sci. Technol. 46(3), 1708–1715.

Fenton, S.E., Ducatman, A., Boobis, A., Dewitt, J.C., Lau, C., Ng, C., Smith, J.S. and Roberts, S.M. 2021. Per - and Polyfluoroalkyl Substance Toxicity and Human

Health Review: Current State of Knowledge and Strategies for Informing Future Research. Environmental Toxicology and Chemistry 40(3), 606-630.

Gagliano, E., Sgroi, M., Falciglia, P.P., Vagliasindi, F.G.A. and Roccaro, P. 2020. Removal of poly- and perfluoroalkyl substances (PFAS) from water by adsorption: Role of PFAS chain length, effect of organic matter and challenges in adsorbent regeneration. Water Research 171, 31.

Ghisi, R., Vamerali, T. and Manzetti, S. 2019. Accumulation of perfluorinated alkyl substances (PFAS) in agricultural plants: A review. Environmental Research 169, 326-341.

Glaser, B., Haumaier, L., Guggenberger, G. and Zech, W. 2001. The 'Terra Preta' phenomenon: A model for sustainable agriculture in the humid tropics. Naturwissenschaften 88(1), 37–41.

Glover, C.M., Quinones, O. and Dickenson, E.R.V. 2018. Removal of perfluoroalkyl and polyfluoroalkyl substances in potable reuse systems. Water Res. 144, 454-461.

Goldenthal, E.I., Jessup, D.C., Geil, R.G., Mehring, J.S. and Saulog, T.M. 1979 Ninety day subacute Rhesus monkey toxicity study (FM-3422), International Research and Development Corporation.

Grandjean, P., Andersen, E.W., Budtz-Jorgensen, E., Nielsen, F., Molbak, K., Weihe, P. and Heilmann, C. 2012. Serum vaccine antibody concentrations in children exposed to perfluorinated compounds. Jama 307(4), 391–397.

Grandjean, P. and Clapp, R. 2015. Perfluorinated Alkyl Substances. NEW SOLUTIONS: A Journal of Environmental and Occupational Health Policy 25(2), 147-163.

Granum, B., Haug, L.S., Namork, E., Stolevik, S.B., Thomsen, C., Aaberge, I.S., van Loveren, H., Lovik, M. and Nygaard, U.C. 2013. Pre-natal exposure to perfluoroalkyl substances may be associated with altered vaccine antibody levels and immune-related health outcomes in early childhood. Journal of Immunotoxicology 10(4), 373-379.

Hao, S.L., Choi, Y.J., Wu, B.R., Higgins, C.P., Deeb, R. and Strathmann, T.J. 2021. Hydrothermal Alkaline Treatment for Destruction of Per- and Polyfluoroalkyl Substances in Aqueous Film-Forming Foam. Environmental Science & Technology 55(5), 3283-3295.

Harris, M.H., Rifas-Shiman, S.L., Calafat, A.M., Ye, X., Mora, A.M., Webster, T.F., Oken, E. and Sagiv, S.K. 2017. Predictors of Per- and Polyfluoroalkyl Substance (PFAS) Plasma Concentrations in 6–10 Year Old American Children. Environmental Science & Technology 51(9), 5193-5204.

Haukas, M., Berger, U., Hop, H., Gulliksen, B. and Gabrielsen, G.W. 2007. Bioaccumulation of per- and polyfluorinated alkyl substances (PFAS) in selected species from the Barents Sea food web. Environmental Pollution 148(1), 360-371.

Hepburn, E., Madden, C., Szabo, D., Coggan, T.L., Clarke, B. and Currell, M. 2019. Contamination of groundwater with per- and polyfluoroalkyl substances (PFAS) from legacy landfills in an urban re-development precinct. Environ. Pollut. 248, 101-113.

Heydebreck, F., Tang, J., Xie, Z. and Ebinghaus, R. 2015. Alternative and legacy perfluoroalkyl substances: Differences between European and Chinese river/estuary systems. Environ Sci Technol 49(14), 8386-8395.

Hoffman, K., Webster, T.F., Bartell, S.M., Weisskopf, M.G., Fletcher, T. and Vieira, V.M. 2011. Private drinking water wells as a source of exposure to perfluorooctanoic acid (PFOA) in communities surrounding a fluoropolymer production facility. Environ. Health Perspect. 119(1), 92–97.

Hori, H., Yamamoto, A., Hayakawa, E., Taniyasu, S., Yamashita, N., Kutsuna, S., Kiatagawa, H. and Arakawa, R. 2005. Efficient decomposition of environmentally persistent perfluorocarboxylic acids by use of persulfate as a photochemical oxidant. Environ Sci Technol 39(7), 2383-2388.

Houde, M., Martin, J.W., Letcher, R.J., Solomon, K.R. and Muir, D.C. 2006. Biological monitoring of polyfluoroalkyl substances: A review. Environ. Sci. Technol. 40(11), 3463-3473.

Houtz, E.F., Higgins, C.P., Field, J.A. and Sedlak, D.L. 2013. Persistence of perfluoroalkyl acid precursors in AFFF-impacted groundwater and soil. Environ. Sci. Technol. 47(15), 8187–8195.

Houtz, E.F., Sutton, R., Park, J.S. and Sedlak, M. 2016. Poly- and perfluoroalkyl substances in wastewater: Significance of unknown precursors, manufacturing shifts, and likely AFFF impacts. Water Res. 95, 142-149.

Hu, X.C., Andrews, D.Q., Lindstrom, A.B., Bruton, T.A., Schaider, L.A., Grandjean, P., Lohmann, R., Carignan, C.C., Blum, A., Balan, S.A., Higgins, C.P. and Sunderland, E.M. 2016. Detection of Poly- and Perfluoroalkyl Substances (PFASs) in U.S. Drinking Water Linked to Industrial Sites, Military Fire Training Areas, and Wastewater Treatment Plants. Environmental Science & Technology Letters 3(10), 344-350.

Huang, S. and Jaffe, P.R. 2019. Defluorination of perfluorooctanoic acid (PFOA) and perfluorooctane sulfonate (PFOS) by *Acidimicrobium sp.* strain A6. Environ. Sci. Technol. 53(19), 11410-11419.

III 2020. Insurance Information Institute (III). Wildfire statistics. http://www.iii.org/fact-statistic/wildfires (accessed December 2020).

Jian, J.-M., Guo, Y., Zeng, L., Liang-Ying, L., Lu, X., Wang, F. and Zeng, E.Y. 2017. Global distribution of perfluorochemicals (PFCs) in potential human exposure source–A review. Environment International 108, 51-62.

Jin, B., Mallula, S., Golovko, S.A., Golovko, M.Y. and Xiao, F. 2020. In vivo generation of PFOA, PFOS, and other compounds from cationic and zwitterionic per- and polyfluoroalkyl substances in a terrestrial invertebrate (Lumbricus terrestris). Environ Sci Technol 54(12), 7378-7387.

Jin, Z.Q., Tian, B., Wang, L.W. and Wang, R.Z. 2013. Comparison on Thermal Conductivity and Permeability of Granular and Consolidated Activated Carbon for Refrigeration. Chinese J Chem Eng 21(6), 676-682.

Jung, M.W., Ahn, K.H., Lee, Y., Kim, K.P., Paeng, I.R., Rhee, J.S., Park, J.T. and Paeng, K.J. 2001. Evaluation on the adsorption capabilities of new chemically modified polymeric adsorbents with protoporphyrin IX. J. Chromatogr. A 917(1-2), 87-93.

Kagramanov, N.D., Kutin, A.A., Mysov, E.I., Makarov, K.N. and Gervits, L.L. 1990. Mass spectrometric study of the pyrolysis of perfluorinated compounds of composition C_6F_{12}-C_9F_{20}, containing perfluoroisopropyl groups. B Acad Sci Ussr Ch+ 39(5), 925-930.

Kah, M., Sigmund, G., Xiao, F. and Hofmann, T. 2017. Sorption of ionizable and ionic organic compounds to biochar, activated carbon and other carbonaceous materials. Water Research (submitted).

Kaiser, M.A., Larsen, B.S., Kao, C.P.C. and Buck, R.C. 2005. Vapor pressures of perfluorooctanoic, -nonanoic, -decanoic, -undecanoic, and -dodecanoic acids. J. Chem. Eng. Data 50(6), 1841-1843.

Kappler, A., Wuestner, M.L., Ruecker, A., Harter, J., Halama, M. and Behrens, S. 2014. Biochar as an electron shuttle between bacteria and Fe(III) minerals. Environ Sci Tech Let 1(8), 339–344.

Khaliji Oskouei, Z. and Tamainot-Telto, Z. 2019. Investigation of the heat transfer properties of granular activated carbon with R723 for adsorption refrigeration and heat pump. Thermal Science and Engineering Progress 12, 1-12.

Khan, M.Y., So, S. and da Silva, G. 2020. Decomposition kinetics of perfluorinated sulfonic acids. Chemosphere 238, 124615.

Kurwadkar, S., Dane, J., Kanel, S.R., Nadagouda, M.N., Cawdrey, R.W., Ambade, B., Struckhoff, G.C. and Wilkin, R. 2022. Per- and polyfluoroalkyl substances in water and wastewater: A critical review of their global occurrence and distribution. Science of The Total Environment 809, 151003.

Lang, J.R., Allred, B.M., Field, J.A., Levis, J.W. and Barlaz, M.A. 2017. National Estimate of Per- and Polyfluoroalkyl Substance (PFAS) Release to US Municipal Landfill Leachate. Environmental Science & Technology 51(4), 2197-2205.

Langberg, H.A., Breedveld, G.D., Gronning, H.M., Kvennas, M., Jenssen, B.M. and Hale, S.E. 2019. Bioaccumulation of fluorotelomer sulfonates and perfluoroalkyl acids in marine organisms living in aqueous film forming foam (AFFF) impacted waters. Environ. Sci. Technol. 53(18), 10951-10960.

Lee, H., D'eon, J. and Mabury, S.A. 2010. Biodegradation of polyfluoroalkyl phosphates as a source of perfluorinated acids to the environment. Environ. Sci. Technol. 44(9), 3305–3310.

Lee, Y.C., Chen, Y.P., Chen, M.J., Kuo, J. and Lo, S.L. 2017. Reductive defluorination of perfluorooctanoic acid by titanium(III) citrate with vitamin B12 and copper nanoparticles. J Hazard Mater 340, 336-343.

Legislature, M. 1989. An Act To Protect the Environment and Public Health by Further Reducing Toxic Chemicals in Packaging: 32 MRSA § 1731-1747.

Lehmann, J. and Joseph, S. (2009) Biochar for Environmental Management: Science and Technology, Earthscan Publications Ltd., London, UK.

Leonard, R.A. and Lemlich, R. 1965. A STUDY OF INTERSTITIAL LIQUID FLOW IN FOAM .I. THEORETICAL MODEL AND APPLICATION TO FOAM FRACTIONATION. Aiche Journal 11(1), 18-&.

Li, F., Duan, J., Tian, S., Ji, H., Zhu, Y., Wei, Z. and Zhao, D. 2020. Short-chain per- and polyfluoroalkyl substances in aquatic systems: Occurrence, impacts and treatment. Chemical Engineering Journal 380, 122506.

Li, Y., Fletcher, T., Mucs, D., Scott, K., Lindh, C.H., Tallving, P. and Jakobsson, K. 2018. Half-lives of PFOS, PFHxS and PFOA after end of exposure to contaminated drinking water. Occupational and Environmental Medicine 75(1), 46-51.

Lindstrom, A.B., Strynar, M.J., Delinsky, A.D., Nakayama, S.F., McMillan, L., Libelo, E.L., Neill, M. and Thomas, L. 2011. Application of WWTP biosolids and resulting perfluorinated compound contamination of surface and well water in Decatur, Alabama, USA. Environ. Sci. Technol. 45(19), 8015–8021.

Liu, F., Hua, L. and Zhang, W. 2020. Influences of microwave irradiation on performances of membrane filtration and catalytic degradation of perfluorooctanoic acid (PFOA). Environ Int 143, 105969.

Liu, Y.L. and Sun, M. 2021. Ion exchange removal and resin regeneration to treat per- and polyfluoroalkyl ether acids and other emerging PFAS in drinking water. Water Research 207.

Mao, J.D., Johnson, R.L., Lehmann, J., Olk, D.C., Neves, E.G., Thompson, M.L. and Schmidt-Rohr, K. 2012. Abundant and stable char residues in soils: Implications for soil fertility and carbon sequestration. Environ. Sci. Technol. 46(17), 9571–9576.

Marsh, H. and Rodríguez-Reinoso, F. (2006) Activated Carbon, Elsevier, Amsterdam; London.

McCleaf, P., Englund, S., Ostlund, A., Lindegren, K., Wiberg, K. and Ahrens, L. 2017. Removal efficiency of multiple poly- and perfluoroalkyl substances (PFASs) in drinking water using granular activated carbon (GAC) and anion exchange (AE) column tests. Water Res. 120, 77-87.

McNamara, J.D., Franco, R., Mimna, R. and Zappa, L. 2018. Comparison of activated carbons for removal of perfluorinated compounds from drinking water. J. Am. Water Work Assoc. 110(1), E2-E14.

Mejia-Avendano, S., Munoz, G., Duy, S.V., Desrosiers, M., Benoit, P., Sauve, S. and Liu, J. 2017. Novel fluoroalkylated surfactants in soils following firefighting foam deployment during the Lac-Megantic railway accident. Environ. Sci. Technol. 51(15), 8313-8323.

Melzer, D., Rice, N., Depledge, M.H., Henley, W.E. and Galloway, T.S. 2010. Association between serum perfluorooctanoic acid (PFOA) and thyroid disease in the US national health and nutrition examination survey. Environ. Health Perspect. 118(5), 686-692.

Merino, N., Qu, Y., Deeb, R.A., Hawley, E.L., Hoffmann, M.R. and Mahendra, S. 2016. Degradation and Removal Methods for Perfluoroalkyl and Polyfluoroalkyl Substances in Water. Environmental Engineering Science 33(9), 615-649.

Millerick, K., Drew, S.R. and Finneran, K.T. 2013. Electron shuttle-mediated biotransformation of hexahydro-1,3,5-trinitro-1,3,5-triazine adsorbed to granular activated carbon. Environ. Sci. Technol. 47(15), 8743-8750.

Miyake, Y., Yamashita, N., Rostkowski, P., So, M.K., Taniyasu, S., Lam, P.K.S. and Kannan, K. 2007. Determination of trace levels of total fluorine in water using combustion ion chromatography for fluorine: A mass balance approach to determine individual perfluorinated chemicals in water. J. Chromatogr. A 1143, 98-104.

Mogensen, U.B., Grandjean, P., Nielsen, F., Weihe, P. and Budtz-Jørgensen, E. 2015. Breastfeeding as an Exposure Pathway for Perfluorinated Alkylates. Environmental Science & Technology 49(17), 10466-10473.

Moody, C.A., Hebert, G.N., Strauss, S.H. and Field, J.A. 2003. Occurrence and persistence of perfluorooctanesulfonate and other perfluorinated surfactants in

groundwater at a fire-training area at Wurtsmith Air Force Base, Michigan, USA. J. Environ. Monit. 5(2), 341–345.

Morales-Mcdevitt, M.E., Becanova, J., Blum, A., Bruton, T.A., Vojta, S., Woodward, M. and Lohmann, R. 2021. The Air That We Breathe: Neutral and Volatile PFAS in Indoor Air. Environmental Science & Technology Letters 8(10), 897-902.

Munoz, G., Duy, S.V., Labadie, P., Botta, F., Budzinski, H., Lestremau, F., Liu, J. and Sauve, S. 2016. Analysis of zwitterionic, cationic, and anionic poly- and perfluoroalkyl surfactants in sediments by liquid chromatography polarity-switching electrospray ionization coupled to high resolution mass spectrometry. Talanta 152, 447-456.

Nabb, D.L., Szostek, B., Himmelstein, M.W., Mawn, M.P., Gargas, M.L., Sweeney, L.M., Stadler, J.C., Buck, R.C. and Fasano, W.J. 2007. *In vitro* metabolism of 8-2 fluorotelomer alcohol: Interspecies comparisons and metabolic pathway refinement. Toxicol Sci 100(2), 333–344.

Nelson Jessica, W., Hatch Elizabeth, E. and Webster Thomas, F. 2010. Exposure to Polyfluoroalkyl Chemicals and Cholesterol, Body Weight, and Insulin Resistance in the General U.S. Population. Environmental Health Perspectives 118(2), 197-202.

NHANES (2014) *Fourth national report on human exposure to environmental chemicals (updated tables)*, Dept. of Health and Human Services Centers for Disease Control and Prevention, Atlanta, GA.

NIST 2018. Mass spectrum of pentadecafluorooctanoic acid https://webbook.nist.gov/cgi/cbook.cgi?ID=C335671&Units=SI&Mask=200#Mass-Spec (accessed December 2019).

Olsen, G.W., Burris, J.M., Ehresman, D.J., Froehlich, J.W., Seacat, A.M., Butenhoff, J.L. and Zobel, L.R. 2007. Half-Life of Serum Elimination of Perfluorooctanesulfonate,Perfluorohexanesulfonate, and Perfluorooctanoate in Retired Fluorochemical Production Workers. Environmental Health Perspectives 115(9), 1298-1305.

Pan, Y., Zhang, H., Cui, Q., Sheng, N., Yeung, L.W.Y., Sun, Y., Guo, Y. and Dai, J. 2018. Worldwide Distribution of Novel Perfluoroether Carboxylic and Sulfonic Acids in Surface Water. Environmental Science & Technology 52(14), 7621-7629.

Paul, A.G., Jones, K.C. and Sweetman, A.J. 2009. A first global production, emission, and environmental inventory for perfluorooctane sulfonate. Environ. Sci. Technol. 43(2), 386–392.

Place, B.J. and Field, J.A. 2012. Identification of novel fluorochemicals in aqueous film-forming foams used by the US military. Environ. Sci. Technol. 46(13), 7120–7127.

Poothong, S., Papadopoulou, E., Padilla-Sánchez, J.A., Thomsen, C. and Haug, L.S. 2020. Multiple pathways of human exposure to poly- and perfluoroalkyl substances (PFASs): From external exposure to human blood. Environment International 134, 105244.

Post, G.B., Cohn, P.D. and Cooper, K.R. 2012. Perfluorooctanoic acid (PFOA), an emerging drinking water contaminant: A critical review of recent literature. Environ. Res. 116, 93–117.

Prevedouros, K., Cousins, I.T., Buck, R.C. and Korzeniowski, S.H. 2006. Sources, fate and transport of perfluorocarboxylates. Environ. Sci. Technol. 40(1), 32–44.

Rahman, M.F., Peldszus, S. and Anderson, W.B. 2014. Behaviour and fate of perfluoroalkyl and polyfluoroalkyl substances (PFASs) in drinking water treatment: A review. Water Res. 50, 318-340.

Rappazzo, K., Coffman, E. and Hines, E. 2017. Exposure to Perfluorinated Alkyl Substances and Health Outcomes in Children: A Systematic Review of the Epidemiologic Literature. International Journal of Environmental Research and Public Health 14(7), 691.

Rice, E.W., Baird, R.B., Eaton, A.D. and Clesceri, L.S. (2012) Standard Methods for the Examination of Water and Wastewater, American Public Health Association, Washington, D.C.

Ross, I., Mcdonough, J., Miles, J., Storch, P., Thelakkat Kochunarayanan, P., Kalve, E., Hurst, J., S. Dasgupta, S. and Burdick, J. 2018. A review of emerging technologies for remediation of PFASs. Remediation Journal 28(2), 101-126.

Sagiv, S.K., Rifas-Shiman, S.L., Webster, T.F., Mora, A.M., Harris, M.H., Calafat, A.M., Ye, X., Gillman, M.W. and Oken, E. 2015. Sociodemographic and Perinatal Predictors of Early Pregnancy Per- and Polyfluoroalkyl Substance (PFAS) Concentrations. Environmental Science & Technology 49(19), 11849-11858.

Sahu, S.P., Qanbarzadeh, M., Ateia, M., Torkzadeh, H., Maroli, A.S. and Cates, E.L. 2018. Rapid degradation and mineralization of perfluorooctanoic acid by a new petitjeanite Bi3O(OH)(PO4)(2) microparticle ultraviolet photocatalyst. Environ Sci Tech Let 5(8), 533-538.

Sajid, M. and Ilyas, M. 2017. PTFE-coated non-stick cookware and toxicity concerns: A perspective. Environ. Sci. Pollut. Res. 24(30), 23436-23440.

Schaefer, L.A., Balan, S.A., Blum, A., Andrews, D.Q., Strynar, M.J., Dickinson, M.E., Lunderberg, D.M., Lang, J.R. and Peaslee, G.F. 2017. Fluorinated compounds in U.S. fast food packaging. Environ Sci Tech Let 4, 105-111.

Schmidt, M.W.I. and Noack, A.G. 2000. Black carbon in soils and sediments: Analysis, distribution, implications, and current challenges. Global Biogeochem Cy 14(3), 777–793.

Schröder, H.F. and Meesters, R.J.W. 2005. Stability of fluorinated surfactants in advanced oxidation processes – A follow up of degradation products using flow injection-mass spectrometry, liquid chromatography-mass spectrometry and liquid chromatography-multiple stage mass spectrometry. J. Chromatogr. A 1082(1), 110–119.

Schultes, L., Vestergren, R., Volkova, K., Westberg, E., Jacobson, T. and Benskin, J.P. 2018. Per- and polyfluoroalkyl substances and fluorine mass balance in cosmetic products from the Swedish market: implications for environmental emissions and human exposure. Environmental Science: Processes & Impacts 20(12), 1680-1690.

Shi, Y., Vestergren, R., Xu, L., Zhou, Z., Li, C., Liang, Y. and Cai, Y. 2016. Human Exposure and Elimination Kinetics of Chlorinated Polyfluoroalkyl Ether Sulfonic Acids (Cl-PFESAs). Environmental Science & Technology 50(5), 2396-2404.

Sinclair, E. and Kannan, K. 2006. Mass loading and fate of perfluoroalkyl surfactants in wastewater treatment plants. Environ. Sci. Technol. 40(5), 1408–1414.

Singh, R.K., Fernando, S., Baygi, S.F., Multari, N., Thagard, S.M. and Holsen, T.M. 2019. Breakdown products from perfluorinated alkyl substances (PFAS) degradation in a plasma-based water treatment process. Environ. Sci. Technol. 53(5), 2731-2738.

Skjemstad, J.O., Reicosky, D.C., Wilts, A.R. and McGowan, J.A. 2002. Charcoal carbon in U.S. agricultural soils. Soil Sci. Soc. Am. J. 66(4), 1249–1255.

Smithwick, M., Mabury, S.A., Solomon, K.R., Sonne, C., Martin, J.W., Born, E.W., Dietz, R., Derocher, A.E., Letcher, R.J., Evans, T.J., Gabrielsen, G.W., Nagy, J., Stirling, I., Taylor, M.K. and Muir, D.C. 2005. Circumpolar study of perfluoroalkyl contaminants in polar bears (*Ursus maritimus*). Environ. Sci. Technol. 39(15), 5517-5523.

Song, Z., Tang, H., Wang, N. and Zhu, L. 2013. Reductive defluorination of perfluorooctanoic acid by hydrated electrons in a sulfite-mediated UV photochemical system. J Hazard Mater 262, 332-338.

Steenland, K., Tinker, S., Shankar, A. and Ducatman, A. 2010. Association of perfluorooctanoic acid (PFOA) and perfluorooctane sulfonate (PFOS) with uric acid among adults with elevated community exposure to PFOA. Environ. Health Perspect. 118(2), 229–233.

Strynar, M., Dagnino, S., McMahen, R., Liang, S., Lindstrom, A., Andersen, E., McMillan, L., Thurman, M., Ferrer, I. and Ball, C. 2015. Identification of novel perfluoroalkyl ether carboxylic acids (PFECAs) and sulfonic acids (PFESAs) in

natural waters using accurate mass time-of-flight mass spectrometry (TOFMS). Environ. Sci. Technol. 49, 11622-11630.

Sunderland, E.M., Hu, X.D.C., Dassuncao, C., Tokranov, A.K., Wagner, C.C. and Allen, J.G. 2019. A review of the pathways of human exposure to poly- and perfluoroalkyl substances (PFASs) and present understanding of health effects. Journal of Exposure Science and Environmental Epidemiology 29(2), 131-147.

Takagi, S., Adachi, F., Miyano, K., Koizumi, Y., Tanaka, H., Watanabe, I., Tanabe, S. and Kannan, K. 2011. Fate of Perfluorooctanesulfonate and perfluorooctanoate in drinking water treatment processes. Water Res. 45(13), 3925–3932.

Tan, B., Wang, T., Wang, P., Luo, W., Lu, Y., Romesh, K.Y. and Giesy, J.P. 2014. Perfluoroalkyl substances in soils around the Nepali Koshi River: Levels, distribution, and mass balance. Environ Sci Pollut Res Int 21(15), 9201-9211.

Tang, H., Zhu, D., Li, T., Kong, H. and Chen, W. 2011. Reductive dechlorination of activated carbon-adsorbed trichloroethylene by zero-valent iron: carbon as electron shuttle. J Environ Qual 40(6), 1878-1885.

Tewari, P.K. and Singh, A.K. 2002. Preconcentration of lead with Amberlite XAD-2 and Amberlite XAD-7 based chelating resins for its determination by flame atomic absorption spectrometry. Talanta 56(4), 735-744.

Tharapiwattananon, N., Scamehorn, J.F., Osuwan, S., Harwell, J.H. and Haller, K.J. 1996. Surfactant recovery from water using foam fractionation. Separation Science and Technology 31(9), 1233-1258.

Tittlemier, S.A., Pepper, K., Seymour, C., Moisey, J., Bronson, R., Cao, X.-L. and Dabeka, R.W. 2007. Dietary Exposure of Canadians to Perfluorinated Carboxylates and Perfluorooctane Sulfonate via Consumption of Meat, Fish, Fast Foods, and Food Items Prepared in Their Packaging. Journal of Agricultural and Food Chemistry 55(8), 3203-3210.

Venkatesan, A.K. and Halden, R.U. 2013. National inventory of perfluoroalkyl substances in archived U.S. biosolids from the 2001 EPA National Sewage Sludge Survey. Journal of Hazardous Materials 252-253, 413-418.

Vestergren, R. and Cousins, I.T. 2009. Tracking the pathways of human exposure to perfluorocarboxylates. Environ. Sci. Technol. 43(15), 5565–5575.

Wang, F., Shih, K., Lu, X. and Liu, C. 2013. Mineralization behavior of fluorine in perfluorooctanesulfonate (PFOS) during thermal treatment of lime-conditioned sludge. Environ Sci Technol 47(6), 2621-2627.

Wang, J., Lin, Z., He, X., Song, M., Westerhoff, P., Doudrick, K. and Hanigan, D. 2022. Critical Review of Thermal Decomposition of Per- and Polyfluoroalkyl

Substances: Mechanisms and Implications for Thermal Treatment Processes. Environmental Science & Technology.

Wang, Y., Chang, W., Wang, L., Zhang, Y., Zhang, Y., Wang, M., Wang, Y. and Li, P. 2019. A review of sources, multimedia distribution and health risks of novel fluorinated alternatives. Ecotoxicology and Environmental Safety 182, 109402.

Wang, Y., Zhang, P.Y., Pan, G. and Chen, H. 2008. Ferric ion mediated photochemical decomposition of perfluorooctanoic acid (PFOA) by 254 nm UV light. J. Hazard. Mater. 160(1), 181-186.

Wang, Z., Boucher, J.M., Scheringer, M., Cousins, I.T. and Hungerbühler, K. 2017. Toward a Comprehensive Global Emission Inventory of C_4–C_{10} Perfluoroalkanesulfonic Acids (PFSAs) and Related Precursors: Focus on the Life Cycle of C_8-Based Products and Ongoing Industrial Transition. Environmental Science & Technology 51(8), 4482-4493.

Wang, Z., Cousins, I.T., Scheringer, M., Buck, R.C. and Hungerbühler, K. 2014. Global emission inventories for C4–C14 perfluoroalkyl carboxylic acid (PFCA) homologues from 1951 to 2030, Part I: production and emissions from quantifiable sources. Environment International 70, 62-75.

Washington, J.W., Jenkins, T.M. and Weber, E.J. 2015. Identification of unsaturated and 2H polyfluorocarboxylate homologous series and their detection in environmental samples and as polymer degradation products. Environ Sci Technol 49(22), 13256-13263.

Watanabe, N., Takata, M., Takemine, S. and Yamamoto, K. 2018. Thermal mineralization behavior of PFOA, PFHxA, and PFOS during reactivation of granular activated carbon (GAC) in nitrogen atmosphere. Environ Sci Pollut Res Int 25(8), 7200-7205.

Waters. 2011 An overview of the principles of MS^E, the engine that drives MS performance, pp. 1-6, Waters Corporation, Milford, MA.

Wei, C., Wang, Q., Song, X., Chen, X., Fan, R., Ding, D. and Liu, Y. 2018. Distribution, source identification and health risk assessment of PFASs and two PFOS alternatives in groundwater from non-industrial areas. Ecotoxicology and Environmental Safety 152, 141-150.

Whitehead, H.D., Venier, M., Wu, Y., Eastman, E., Urbanik, S., Diamond, M.L., Shalin, A., Schwartz-Narbonne, H., Bruton, T.A., Blum, A., Wang, Z., Green, M., Tighe, M., Wilkinson, J.T., Mcguinness, S. and Peaslee, G.F. 2021. Fluorinated Compounds in North American Cosmetics. Environmental Science & Technology Letters 8(7), 538-544.

Winkens, K., Koponen, J., Schuster, J., Shoeib, M., Vestergren, R., Berger, U., Karvonen, A.M., Pekkanen, J., Kiviranta, H. and Cousins, I.T. 2017. Perfluoroalkyl acids and

their precursors in indoor air sampled in children's bedrooms. Environmental Pollution 222, 423-432.

Wu, B., Hao, S., Choi, Y., Higgins, C.P., Deeb, R. and Strathmann, T.J. 2019a. Rapid Destruction and Defluorination of Perfluorooctanesulfonate by Alkaline Hydrothermal Reaction. Environmental Science & Technology Letters 6(10), 630-636.

Wu, B.R., Hao, S.L., Choi, Y.J., Higgins, C.P., Deeb, R. and Strathmann, T.J. 2019b. Rapid destruction and defluorination of perfluorooctanesulfonate by alkaline hydrothermal reaction. Environ Sci Tech Let 6(10), 630-636.

Xiao, F. 2017. Emerging poly- and perfluoroalkyl substances in the aquatic environment: A review of current literature. Water Res. 124, 482-495.

Xiao, F., Bedane, A.H., Zhao, J.X., Mann, M.D. and Pignatello, J.J. 2018a. Thermal air oxidation changes surface and adsorptive properties of black carbon (char/biochar). Sci Total Environ 618, 276-283.

Xiao, F., Golovko, S.A. and Golovko, M.Y. 2017. Identification of novel non-ionic, cationic, zwitterionic, and anionic polyfluoroalkyl substances using UPLC-TOF-MS(E) high-resolution parent ion search. Anal Chim Acta 988, 41-49.

Xiao, F., Gulliver, J.S. and Simcik, M.F. 2013a. Perfluorooctane sulfonate (PFOS) contamination of fish in urban lakes: A prioritization methodology for lake management. Water Res. 47(20), 7264–7272.

Xiao, F., Gámiz, B. and Pignatello, J.J. 2018b. Adsorption and desorption of nitrous oxide by raw and thermally air-oxidized chars. Sci. Total Environ. 643, 1436-1445.

Xiao, F., Halbach, T.R., Simcik, M.F. and Gulliver, J.S. 2012a. Input characterization of perfluoroalkyl substances in wastewater treatment plants: Source discrimination by exploratory data analysis. Water Res. 46(9), 3101–3109.

Xiao, F., Hanson, R.A., Golovko, S.A., Golovko, M.Y. and Arnold, W.A. 2018c. PFOA and PFOS are generated from zwitterionic and cationic precursor compounds during water disinfection with chlorine or ozone. Environ Sci Tech Let 5(6), 382-388.

Xiao, F., Jin, B., Golovko, S.A., Golovko, M.Y. and Xing, B. 2019. Sorption and desorption mechanisms of cationic and zwitterionic per- and polyfluoroalkyl substances in natural soils: Thermodynamics and hysteresis. Environ Sci Technol 53(20), 11818-11827.

Xiao, F. and Pignatello, J.J. 2015a. Interactions of triazine herbicides with biochar: Steric and electronic effects. Water Res 80, 179-188.

Xiao, F. and Pignatello, J.J. 2015b. π+–π interactions between (hetero)aromatic amine cations and the graphitic surfaces of pyrogenic carbonaceous materials. Environ. Sci. Technol. 49(2), 906–914.

Xiao, F. and Pignatello, J.J. 2016. Effects of post-pyrolysis air oxidation of biomass chars on adsorption of neutral and ionizable compounds. Environ. Sci. Technol. 50(12), 6276-6283.

Xiao, F., Sasi, P.C., Alinezhad, A., Golovko, S.A., Golovko, M.Y. and Spoto, A. 2021a. Thermal Decomposition of Anionic, Zwitterionic, and Cationic Polyfluoroalkyl Substances in Aqueous Film-Forming Foams. Environmental Science & Technology 55(14), 9885-9894.

Xiao, F., Sasi, P.C., Yao, B., Kubatova, A., Golovko, S.A., Golovko, M.Y. and Soli, D. 2020. Thermal stability and decomposition of perfluoroalkyl substances on spent granular activated carbon. Environ Sci Tech Let 7(5), 343-350.

Xiao, F., Sasi, P.C., Yao, B., Kubatova, A., Golovko, S.A., Golovko, M.Y. and Soli, D. 2021b. Thermal Decomposition of PFAS: Response to Comment on "Thermal Stability and Decomposition of Perfluoroalkyl Substances on Spent Granular Activated Carbon". Environ Sci Tech Let 8, 364–365.

Xiao, F., Simcik, M.F. and Gulliver, J.S. 2012b. Perfluoroalkyl acids in urban stormwater runoff: Influence of land use. Water Res. 46(20), 6601–6608.

Xiao, F., Simcik, M.F. and Gulliver, J.S. 2013b. Mechanisms for removal of perfluorooctane sulfonate (PFOS) and perfluorooctanoate (PFOA) from drinking water by conventional and enhanced coagulation. Water Res. 47(1), 49–56.

Xiao, F., Simcik, M.F., Halbach, T.R. and Gulliver, J.S. 2015. Perfluorooctane sulfonate (PFOS) and perfluorooctanoate (PFOA) in soils and groundwater of a U.S. metropolitan area: Migration and implications for human exposure. Water Res. 72, 64–74.

Xiao, F., Zhang, X., Penn, L., Gulliver, J.S. and Simcik, M.F. 2011. Effects of monovalent cations on the competitive adsorption of perfluoroalkyl acids by kaolinite: Experimental studies and modeling. Environ. Sci. Technol. 45(23), 10028–10035.

Yang, S.S., Fernando, S., Holsen, T.M. and Yang, Y. 2019. Inhibition of perchlorate formation during the electrochemical oxidation of perfluoroalkyl acid in groundwater. Environ Sci Tech Let 6(12), 775-780.

Yeung, L.W.Y., Miyake, Y., Taniyasu, S., Wang, Y., Yu, H.X., So, M.K., Jiang, G.B., Wu, Y.N., Li, J.G., Giesy, J.P., Yamashita, N. and Lam, P.K.S. 2008. Perfluorinated compounds and total and extractable organic fluorine in human blood samples from China. Environ. Sci. Technol. 42(21), 8140–8145.

Young, C.J., Furdui, V.I., Franklin, J., Koerner, R.M., Muir, D.C.G. and Mabury, S.A. 2007. Perfluorinated acids in arctic snow: New evidence for atmospheric formation. Environmental Science & Technology 41(10), 3455-3461.

Yu, J., Hu, J.Y., Tanaka, S. and Fujii, S. 2009a. Perfluorooctane sulfonate (PFOS) and perfluorooctanoic acid (PFOA) in sewage treatment plants. Water Res. 43(9), 2399–2408.

Yu, Q., Zhang, R., Deng, S., Huang, J. and Yu, G. 2009b. Sorption of perfluorooctane sulfonate and perfluorooctanoate on activated carbons and resin: Kinetic and isotherm study. Water Res 43(4), 1150-1158.

Zaggia, A., Conte, L., Falletti, L., Fant, M. and Chiorboli, A. 2016. Use of strong anion exchange resins for the removal of perfluoroalkylated substances from contaminated drinking water in batch and continuous pilot plants. Water Research 91, 137-146.

Zheng, G., Boor, B.E., Schreder, E. and Salamova, A. 2020. Indoor exposure to per- and polyfluoroalkyl substances (PFAS) in the childcare environment. Environmental Pollution 258, 113714.

Zhou, Q., Deng, S., Yang, B., Huang, J. and Yu, G. 2011. Efficient electrochemical oxidation of perfluorooctanoate using a Ti/SnO2-Sb-Bi anode. Environ. Sci. Technol. 45, 2973–2979.

Zhu, D.Q., Kwon, S. and Pignatello, J.J. 2005. Adsorption of single-ring organic compounds to wood charcoals prepared under different thermochemical conditions. Environ. Sci. Technol. 39(11), 3990–3998.

7. Appendix A: Supplementary information for Chapter 2

Table A1. PFAS chemicals used in this study.

PFCAs	Acronyms	Purity	Providers
Perfluorobutyric acid (C4)	PFBA	≥99.5	Sigma–Aldrich
perfluoropentanoic acid (C5)	PFPeA	97%	Sigma–Aldrich
Perfluoroheptanoic acid (C6)	PFHpA	≥98%	Fisher Scientific
Perfluorooctanoic acid (C8)	PFOA	95%	Sigma–Aldrich
Perfluorononanoic acid (C9)	PFNA	97%	Sigma–Aldrich
Perfluorodecanoic acid (C10)	PFDA	98%	Sigma–Aldrich
perfluoroundecanoic acid (C11)	PFUnDA	95%	Sigma–Aldrich
PFSAs	**Acronyms**	**Purity**	**Provider**
Perfluorobutanesulfonic acid potassium salt (C4)	PFBS	98.0%	Sigma–Aldrich
Perfluorohexanesulfonic acid potassium salt (C6)	PFHxS	≥98.0%	Sigma–Aldrich
Perfluorooctanesulfonic acid potassium salt (C8)	PFOS	≥98.0%	Sigma–Aldrich
PFECA (perfluoroalkyl ether carboxylic acid)	Acronym	Purity	Provider

2,3,3,3-tetrafluoro-2- (1,1,2,2,3,3,3-heptafluoropropoxy)propanoic acid (C3)	HFPO-DA (GenX)	97%	Fisher Scientific

Table A2. Arrhenius activation energy and enthalpy changes for thermal destabilization of PFOA and PFOS in different atmospheres.

	Arrhenius activation energy (kJ/mol)	**Enthalpy change (kJ/mol)**
PFOA (N_2)	112.5 (95% CI = 108.6–116.4)	109.2 (95% CI = 105.3–113.1)
PFOA (O_2)	104.8 (95% CI = 97.3–112.2)	101.4 (95% CI = 94.0–108.8)
PFOA (CO_2)	85.5 (95% CI = 78.3–92.7)	82.2 (95% CI = 75.0–89.3)
PFOS (N_2)	360.1 (95% CI = 333.7–386.6)	353.9 (95% CI = 327.5–380.4)
PFOS (O_2)	286.9 (95% CI = 261.8–312.0)	280.9 (95% CI = 255.8–306.0)
PFOS (CO_2)	286.8 (95% CI = 265.9–307.7)	280.7 (95% CI = 259.8–301.6)

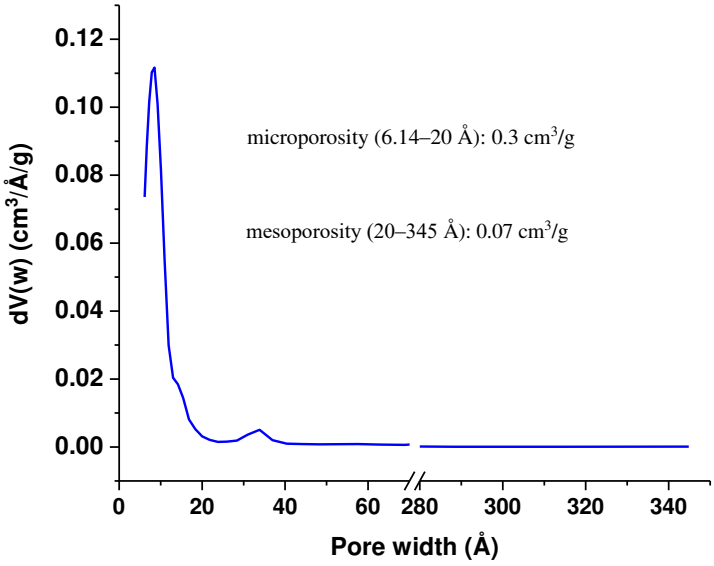

Figure A1. *Pore size distribution of Filtrasorb 200.*

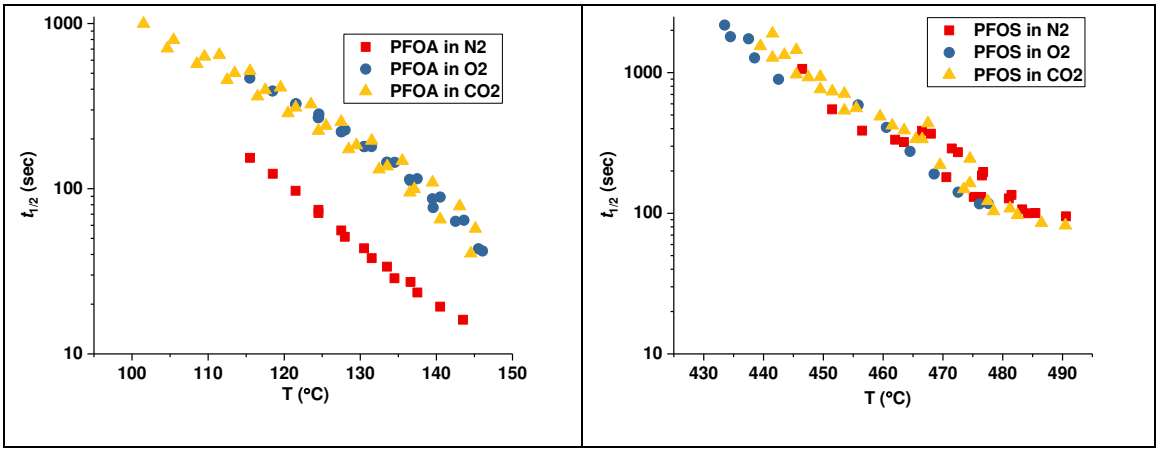

Figure A2. *Thermal destabilization half-lives of PFOA and PFOS calculated from first-order rate constants.*

8. Appendix B: Supplementary information for Chapter 3

Table B1. PFAS chemicals used in this study.

PFCAs	Acronyms	Purity	Providers
Perfluorobutyric acid (C4)	PFBA	≥99.5	Sigma–Aldrich
Perfluorooctanoic acid (C8)	PFOA	95%	Sigma–Aldrich
Perfluorononanoic acid (C9)	PFNA	97%	Sigma–Aldrich
Perfluorodecanoic acid (C10)	PFDA	98%	Sigma–Aldrich
perfluoroundecanoic acid (C11)	PFUnDA	95%	Sigma–Aldrich
PFSA	Acronyms	Purity	Provider
Perfluorooctanesulfonic acid potassium salt (C8)	PFOS	≥98.0%	Sigma–Aldrich
PFECA (perfluoroalkyl ether carboxylic acid)	Acronym	Purity	Provider
2,3,3,3-tetrafluoro-2-(1,1,2,2,3,3,3-heptafluoropropoxy)propanoic acid (C3)	HFPO-DA (GenX)	97%	Fisher Scientific

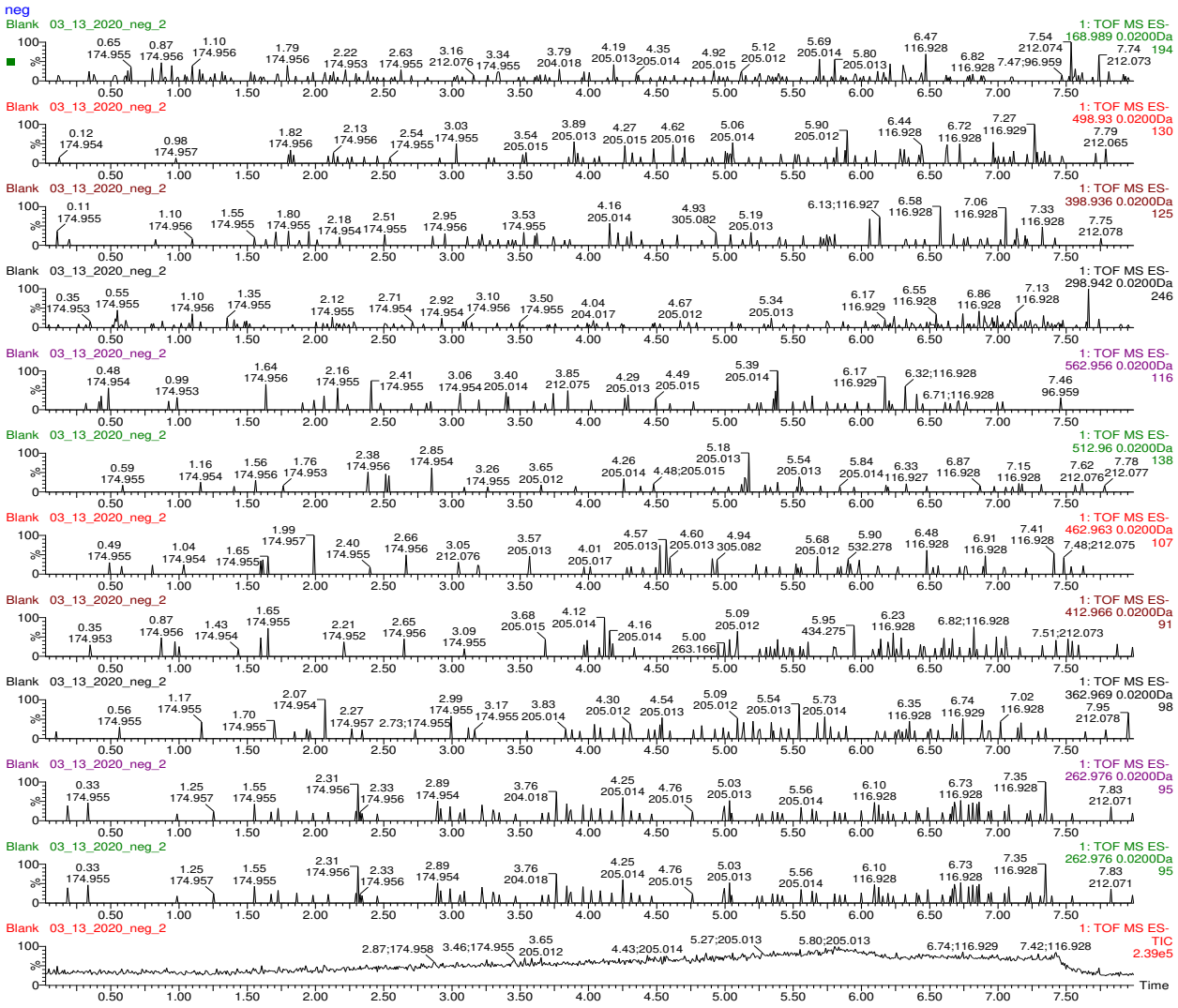

Figure B1. *UPLC–ESI⁻-ToF MS selected ion chromatograms of a blank sample for PFBA (m/z 168.989), PFOS (m/z 498.930), PFHxS (m/z 398.936), PFBS (m/z 298.942), PFUnDA (m/z 562.956), PFDA (m/z 512.960), PFNA (m/z 462.963), PFOA (m/z 412.966), PFHpA (m/z 362.969), and PFPeA (m/z 262.976) and the total ion current chromatogram (TIC).*

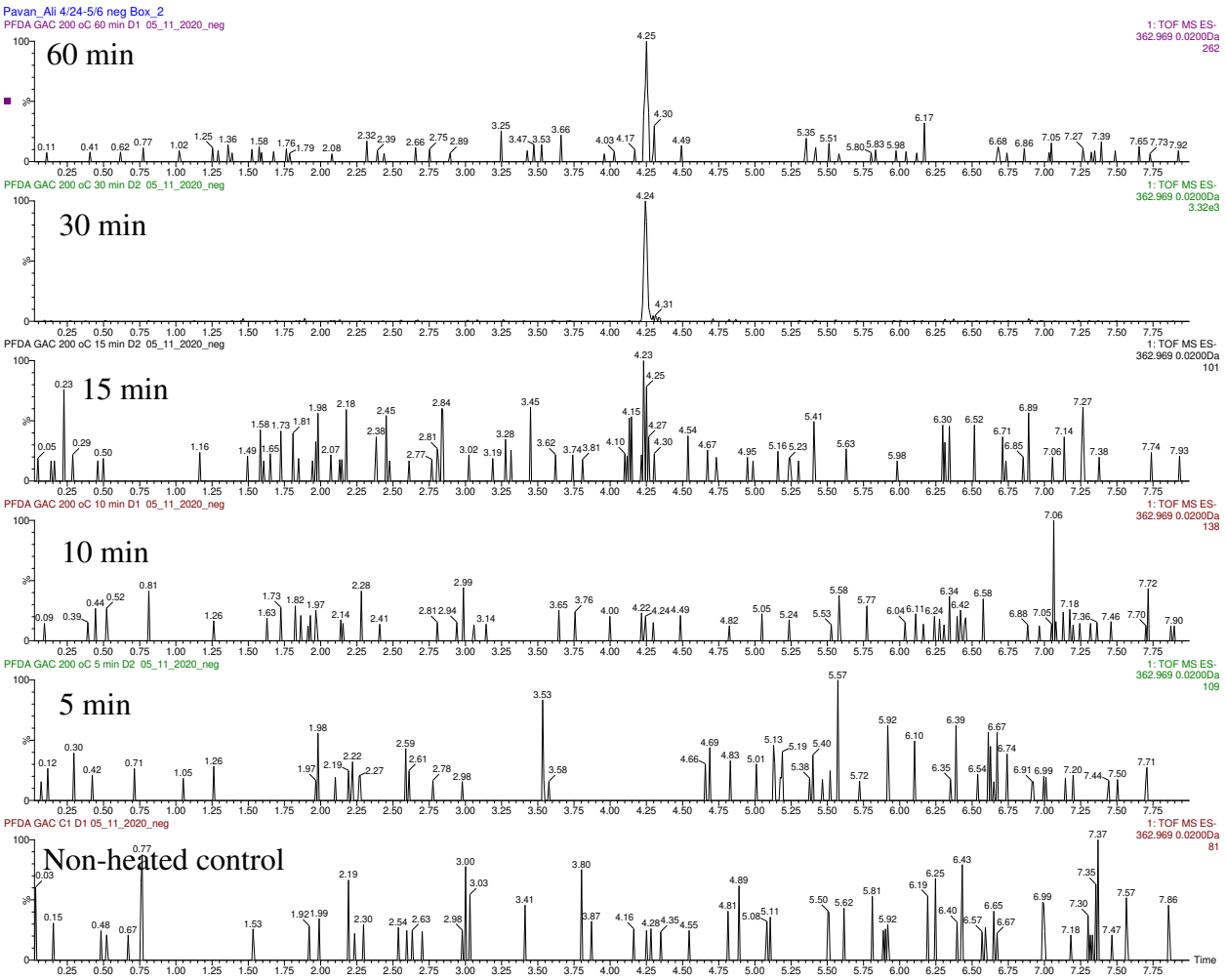

Figure B2. *UPLC–ESI⁻-ToF MS selected ion chromatograms on m/z 362.969 of methanol (with 100 mmol/L ammonium acetate) extracts of PFDA after T#2 (with the presence of GAC) thermal treatments at 200 °C for different times.*

The chromatograms show the generation and subsequent decomposition of PFHpA (m/z 362.969; RT = 4.24 min) during thermal treatments of PFDA at 200 °C.

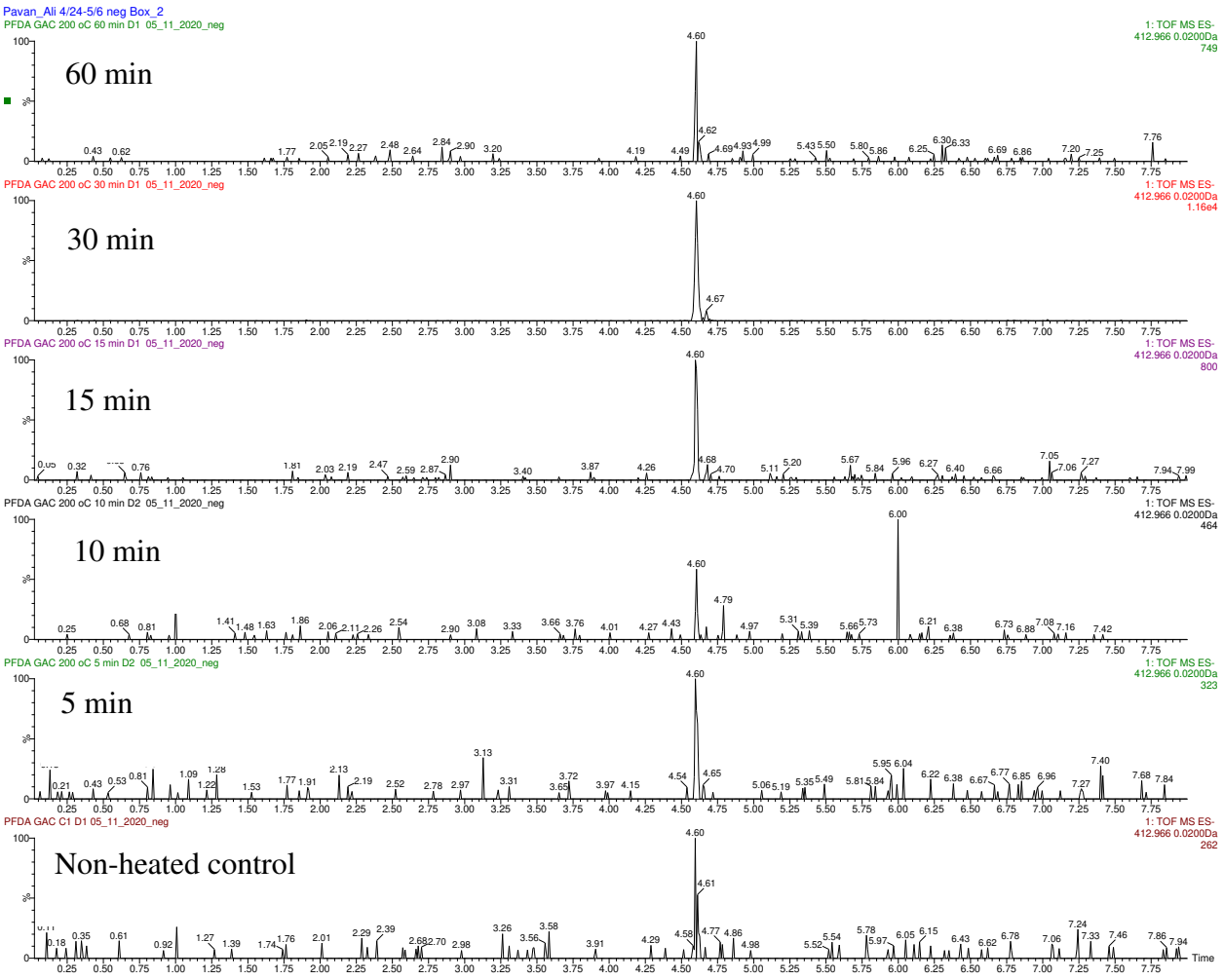

Figure B3. *UPLC–ESI-ToF MS selected ion chromatograms on m/z 412.966 of methanol (with 100 mmol/L ammonium acetate) extracts of PFDA after T#2 (with the presence of GAC) thermal treatments at 200 °C for different times.*

The chromatograms show the generation and subsequent decomposition of PFOA (m/z 412.966; RT = 4.60 min) during thermal treatments of PFDA at 200 °C.

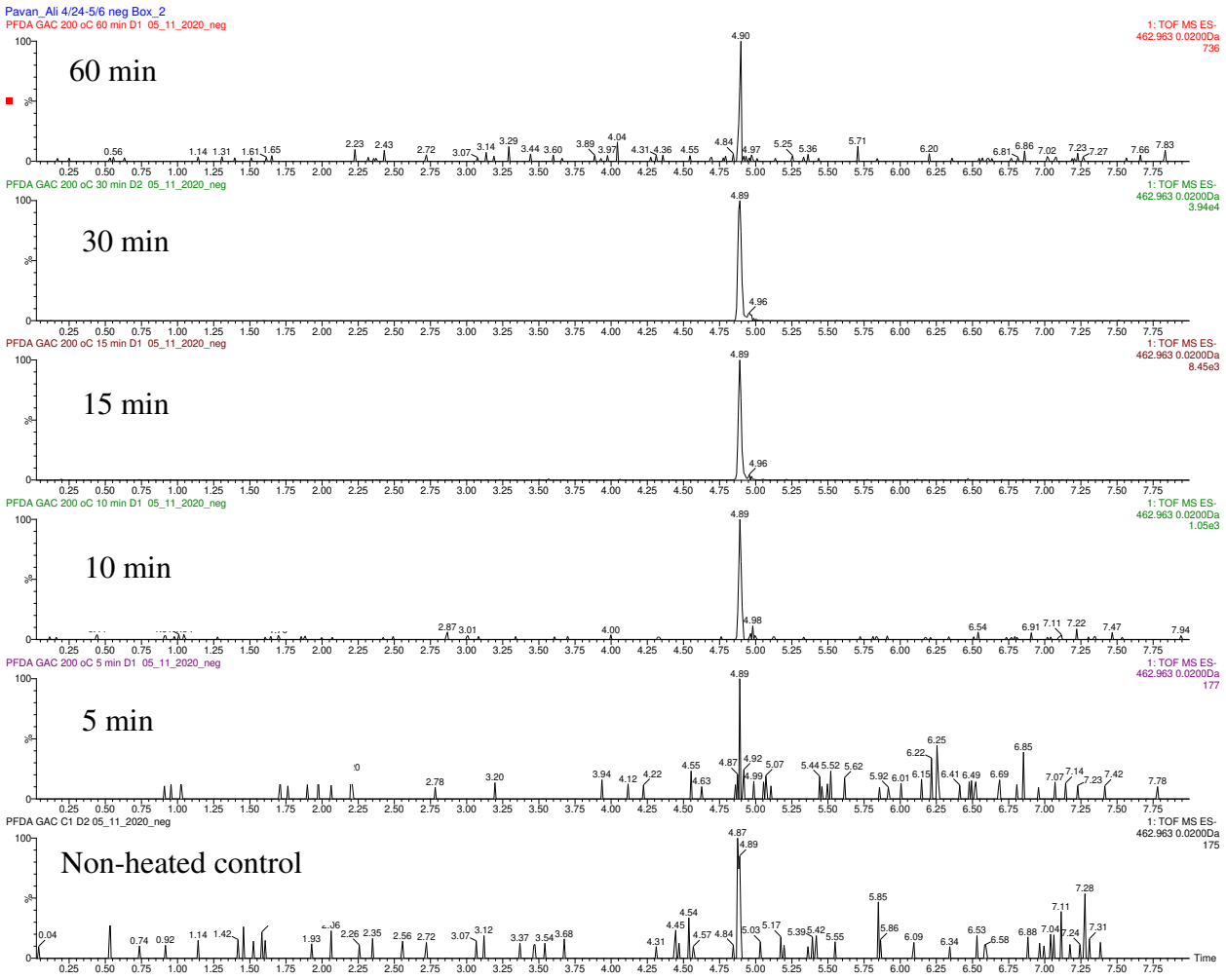

Figure B4. *UPLC–ESI-ToF MS selected ion chromatograms on m/z 462.963 of methanol (with 100 mmol/L ammonium acetate) extracts of PFDA after T#2 (with the presence of GAC) thermal treatments at 200 °C for different times.*

The chromatograms show the generation and subsequent decomposition of PFNA (m/z 462.963; RT = 4.89 min) during thermal treatments of PFDA at 200 °C.

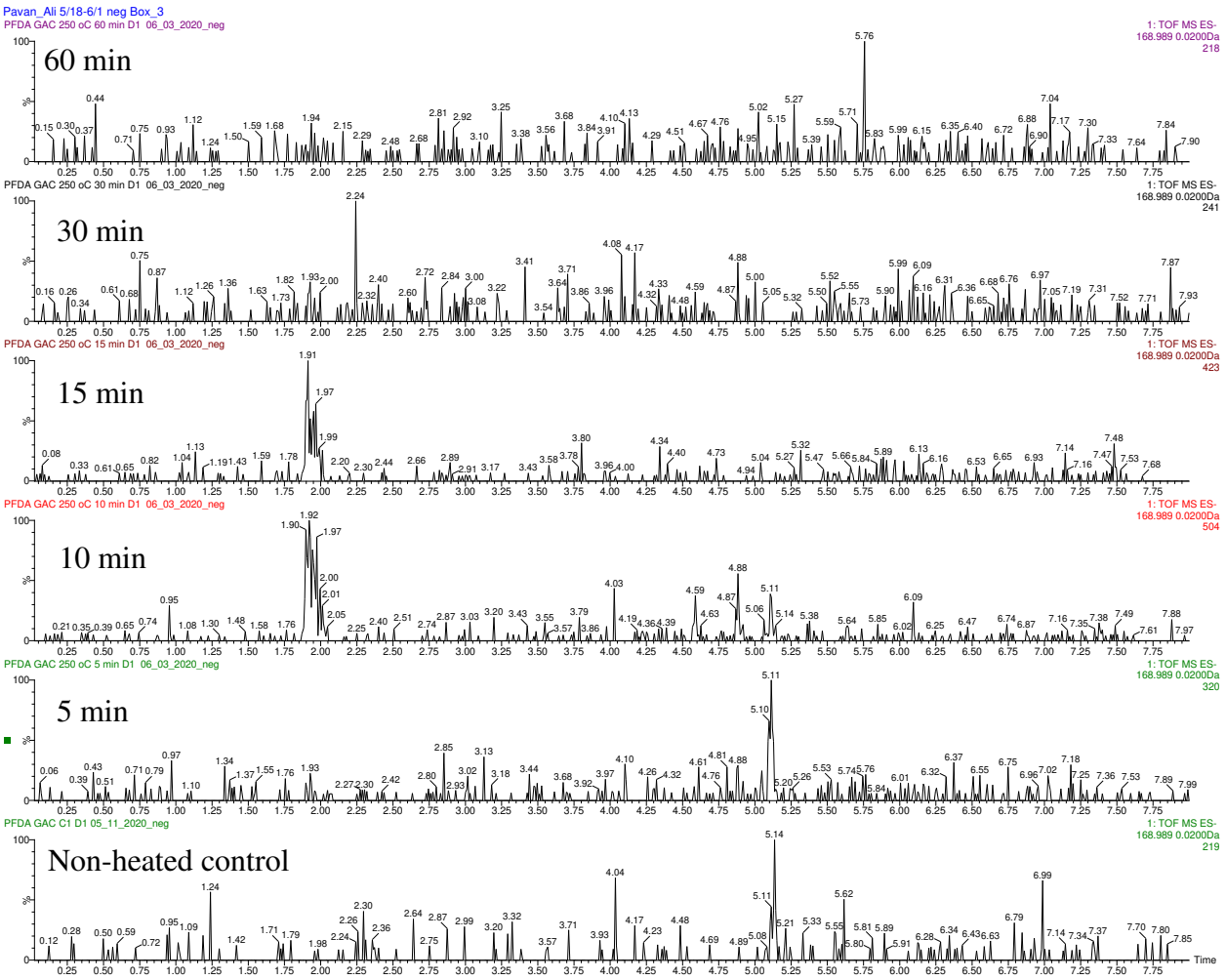

Figure B5. *UPLC–ESI⁻-ToF MS selected ion chromatograms on m/z 168.989 of methanol (with 100 mmol/L ammonium acetate) extracts of PFDA after T#2 (with the presence of GAC) thermal treatments at 250 °C for different times.*

The chromatograms show the generation and subsequent decomposition of PFBA (m/z 168.989; RT = 1.91 min) during thermal treatments of PFDA at 250 °C.

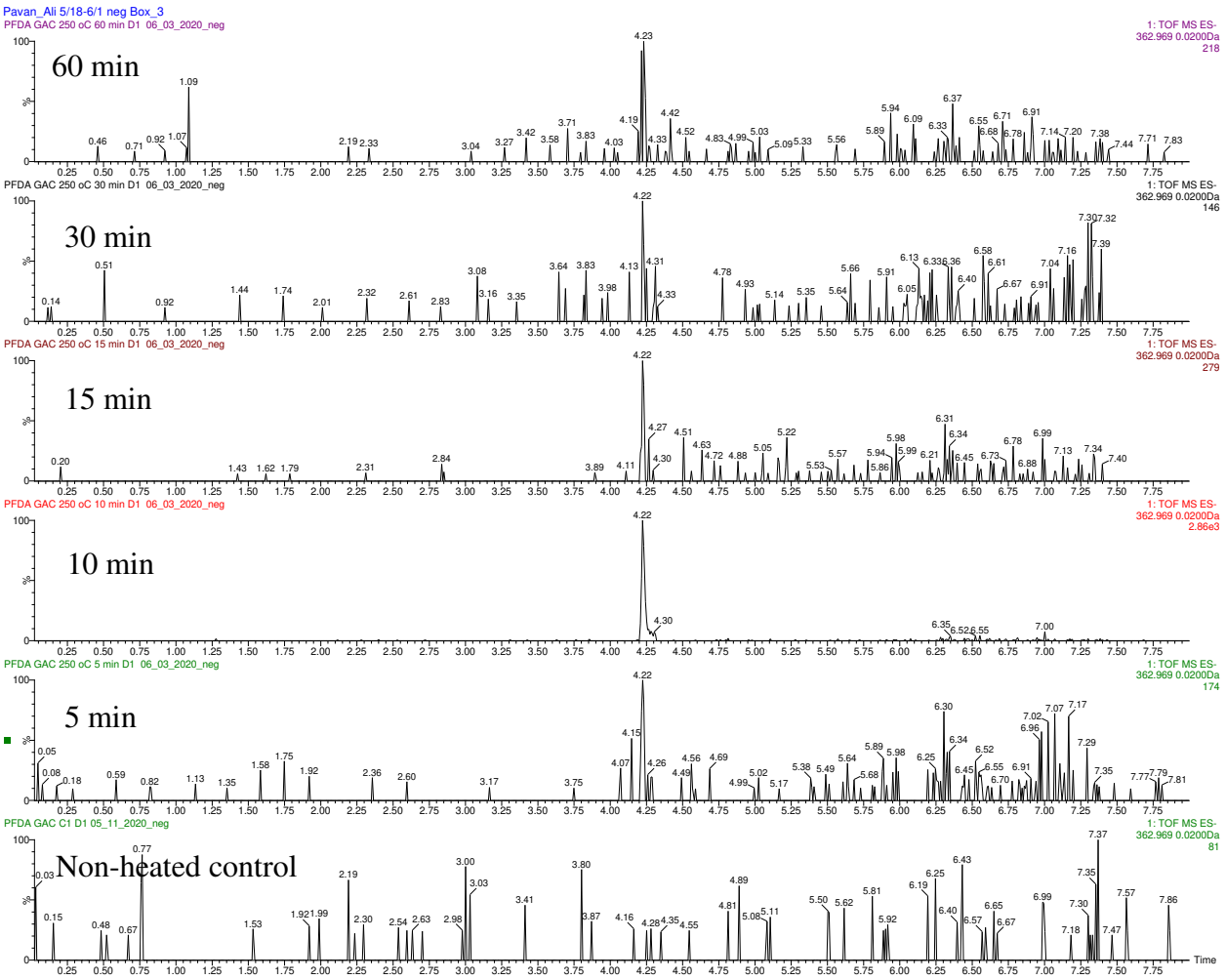

Figure B6. *UPLC–ESI⁻-ToF MS selected ion chromatograms on m/z 362.969 of methanol (with 100 mmol/L ammonium acetate) extracts of PFDA after T#2 (with the presence of GAC) thermal treatments at 250 °C for different times.*

The chromatograms show the generation and subsequent decomposition of PFHpA (m/z 362.969; RT = 4.22 min) during thermal treatments of PFDA at 250 °C.

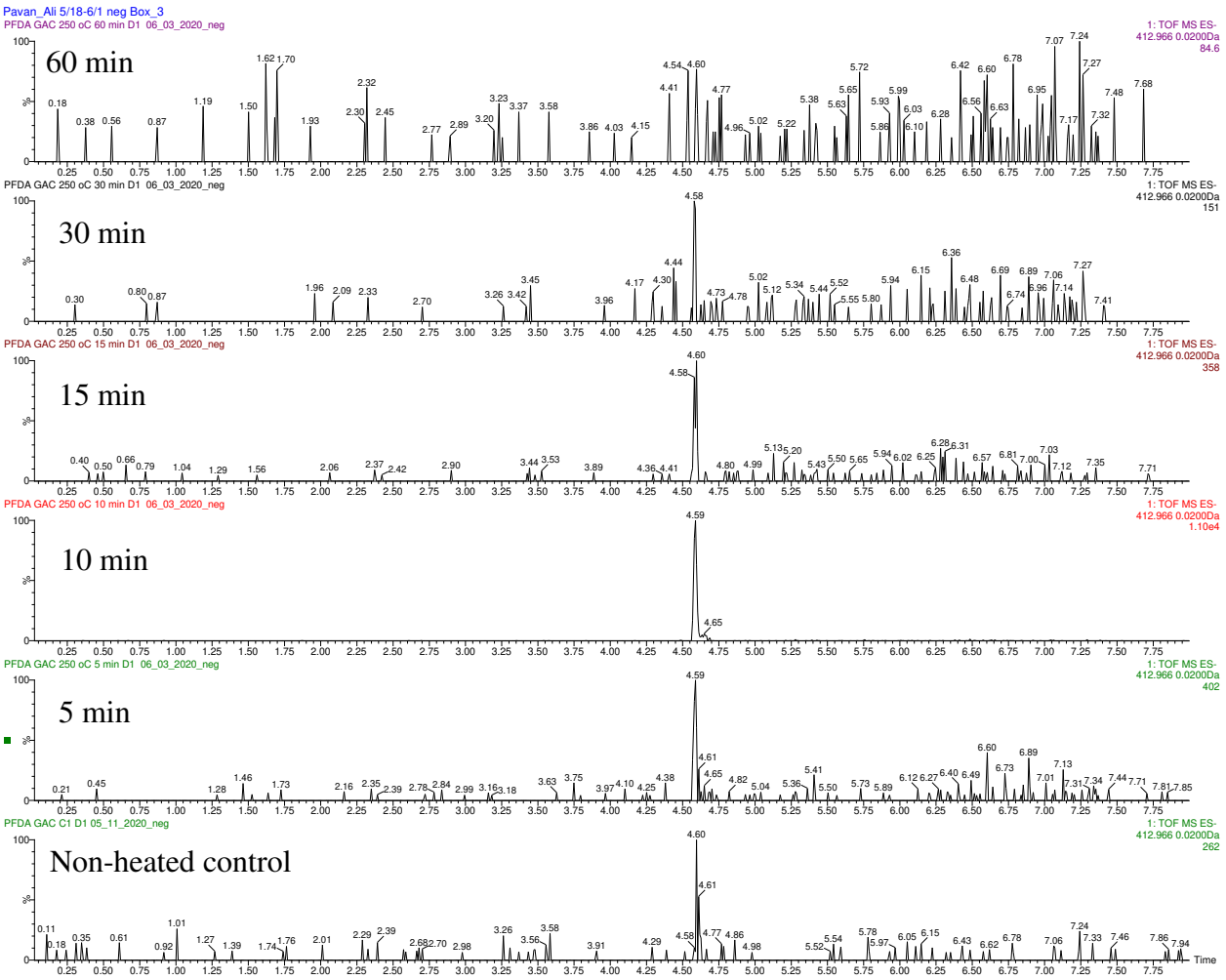

Figure B7. *UPLC–ESI⁻-ToF MS selected ion chromatograms on m/z 412.966 of methanol (with 100 mmol/L ammonium acetate) extracts of PFDA after T#2 (with the presence of GAC) thermal treatments at 250 °C for different times.*

The chromatograms show the generation and subsequent decomposition of PFOA (m/z 412.966; RT = 4.59 min) during thermal treatments of PFDA at 250 °C.

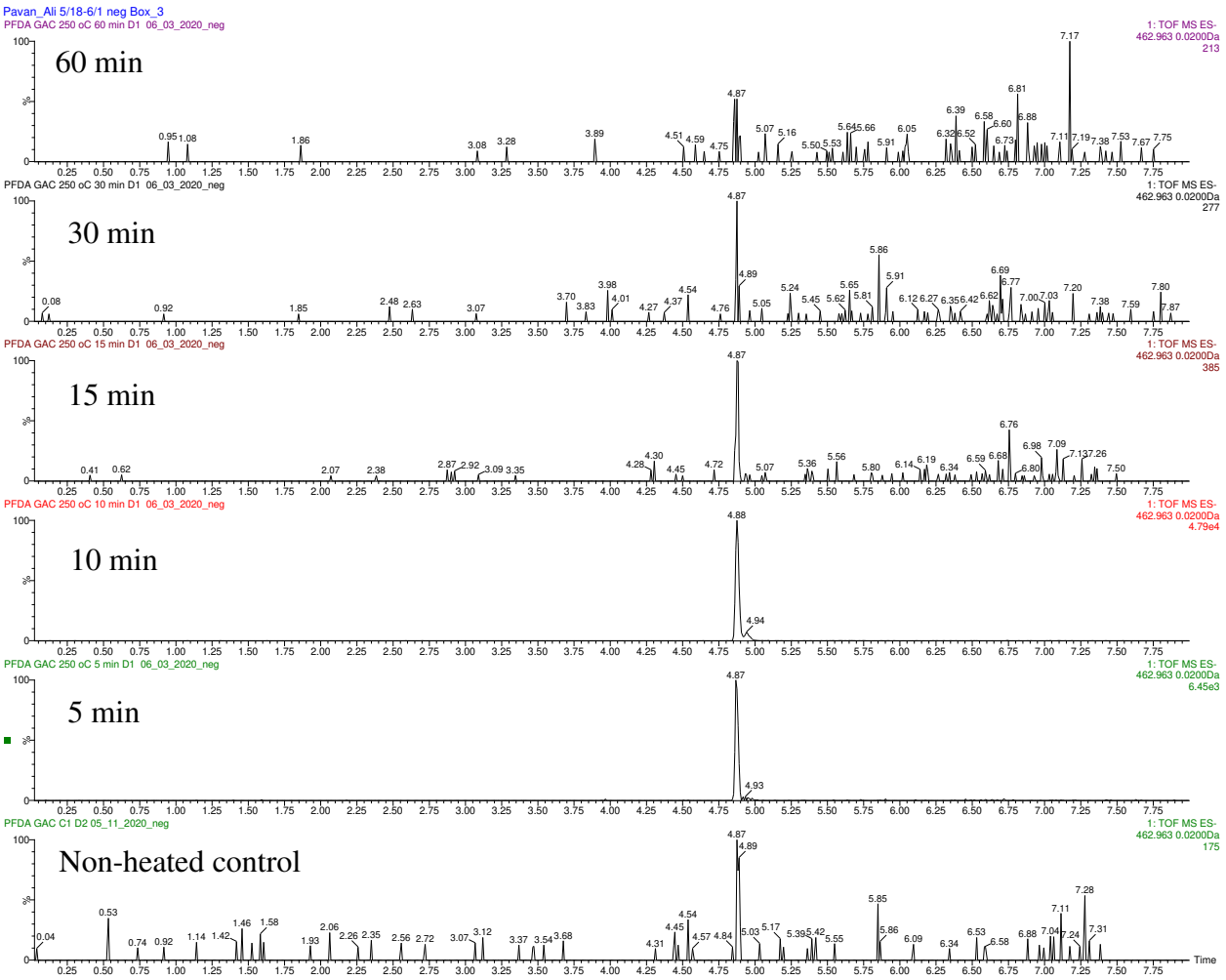

Figure B8. *UPLC–ESI-ToF MS selected ion chromatograms on m/z 462.963 of methanol (with 100 mmol/L ammonium acetate) extracts of PFDA after T#2 (with the presence of GAC) thermal treatments at 250 °C for different times.*

The chromatograms show the generation and subsequent decomposition of PFNA (m/z 462.963; RT = 4.87 min) during thermal treatments of PFDA at 250 °C.

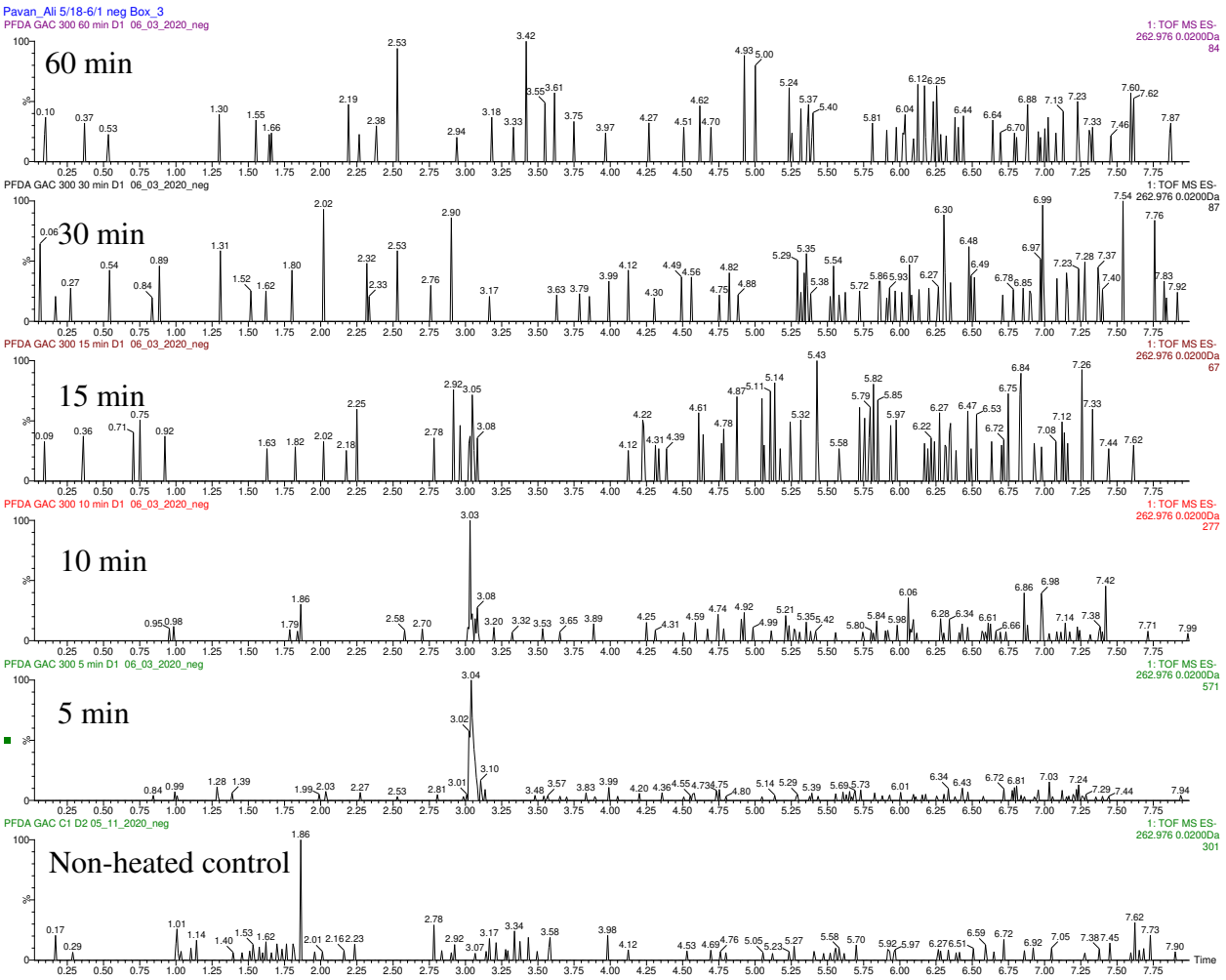

Figure B9. *UPLC–ESI⁻-ToF MS selected ion chromatograms on m/z 262.976 of methanol (with 100 mmol/L ammonium acetate) extracts of PFDA after T#2 (with the presence of GAC) thermal treatments at 300 °C for different times.*

The chromatograms show the generation and subsequent decomposition of PFPeA (m/z 262.976; RT = 3.03 min) during thermal treatments of PFDA at 300 °C.

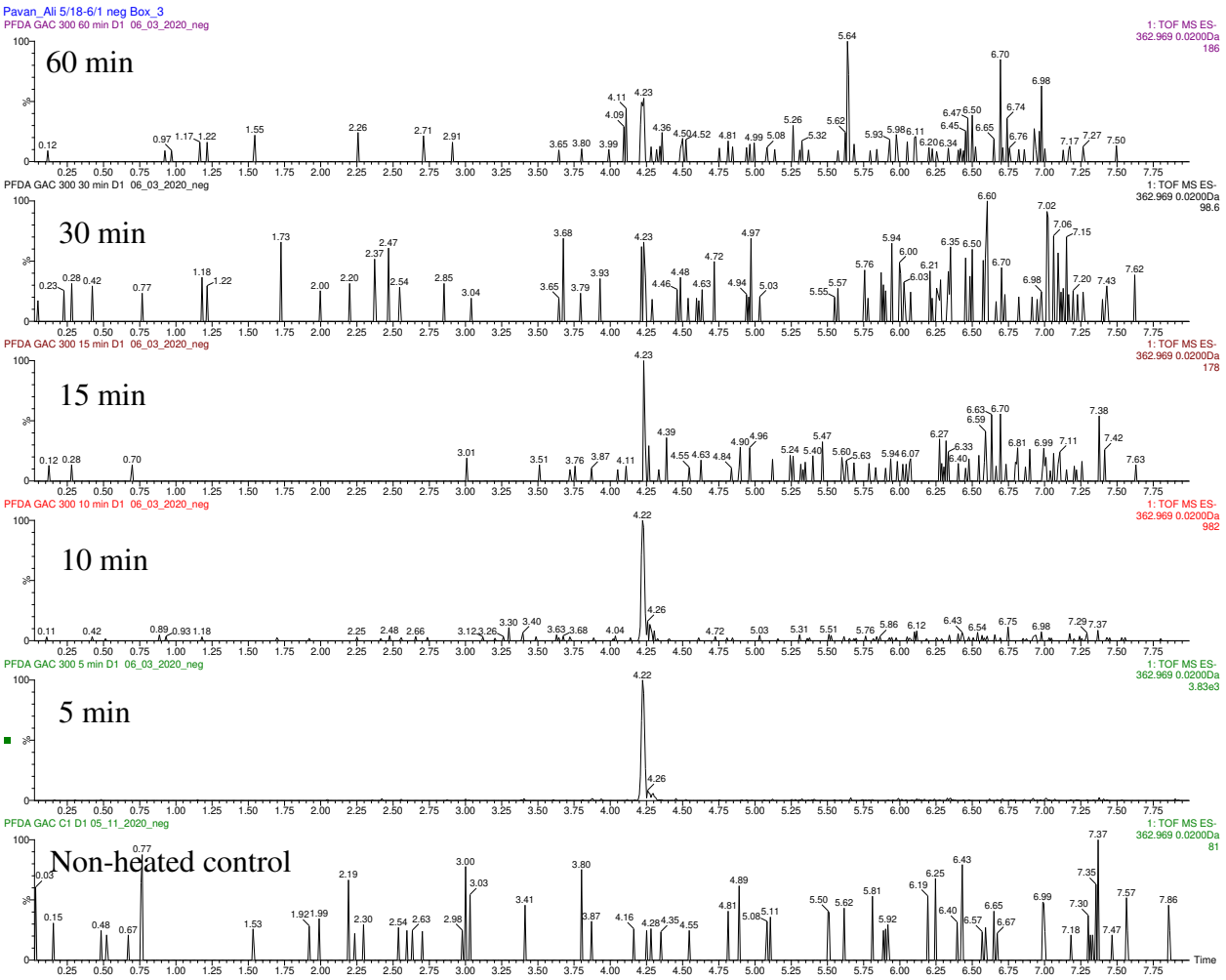

Figure B10. *UPLC–ESI⁻-ToF MS selected ion chromatograms on m/z 362.969 of methanol (with 100 mmol/L ammonium acetate) extracts of PFDA after T#2 (with the presence of GAC) thermal treatments at 300 °C for different times.*

The chromatograms show the generation and subsequent decomposition of PFHpA (m/z 362.969; RT = 4.22 min) during thermal treatments of PFDA at 300 °C.

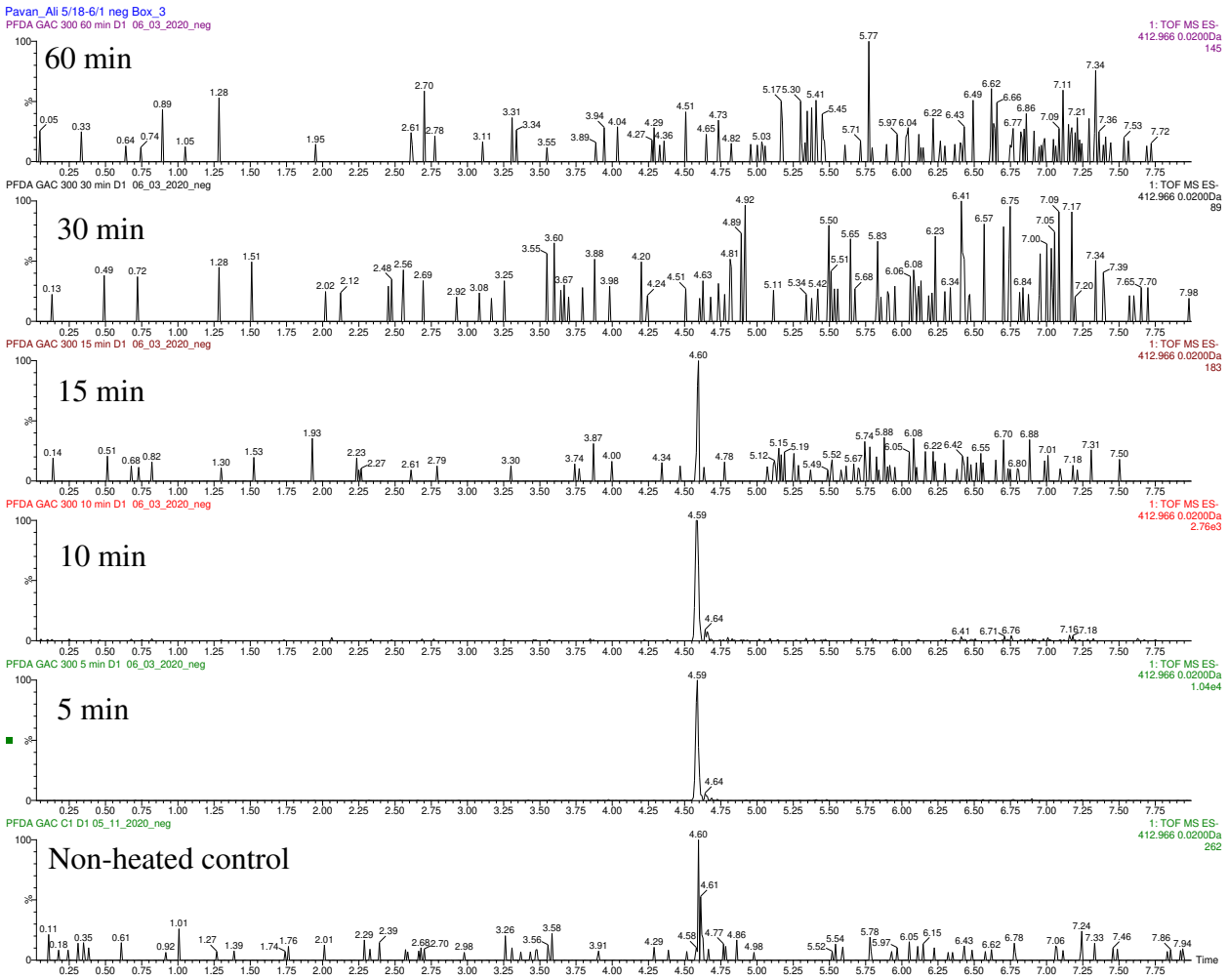

Figure B11. *UPLC–ESI⁻-ToF MS selected ion chromatograms on m/z 362.969 of methanol (with 100 mmol/L ammonium acetate) extracts of PFDA after T#2 (with the presence of GAC) thermal treatments at 300 °C for different times.*

The chromatograms show the generation and subsequent decomposition of PFOA (m/z 412.966; RT = 4.59 min) during thermal treatments of PFDA at 300 °C.

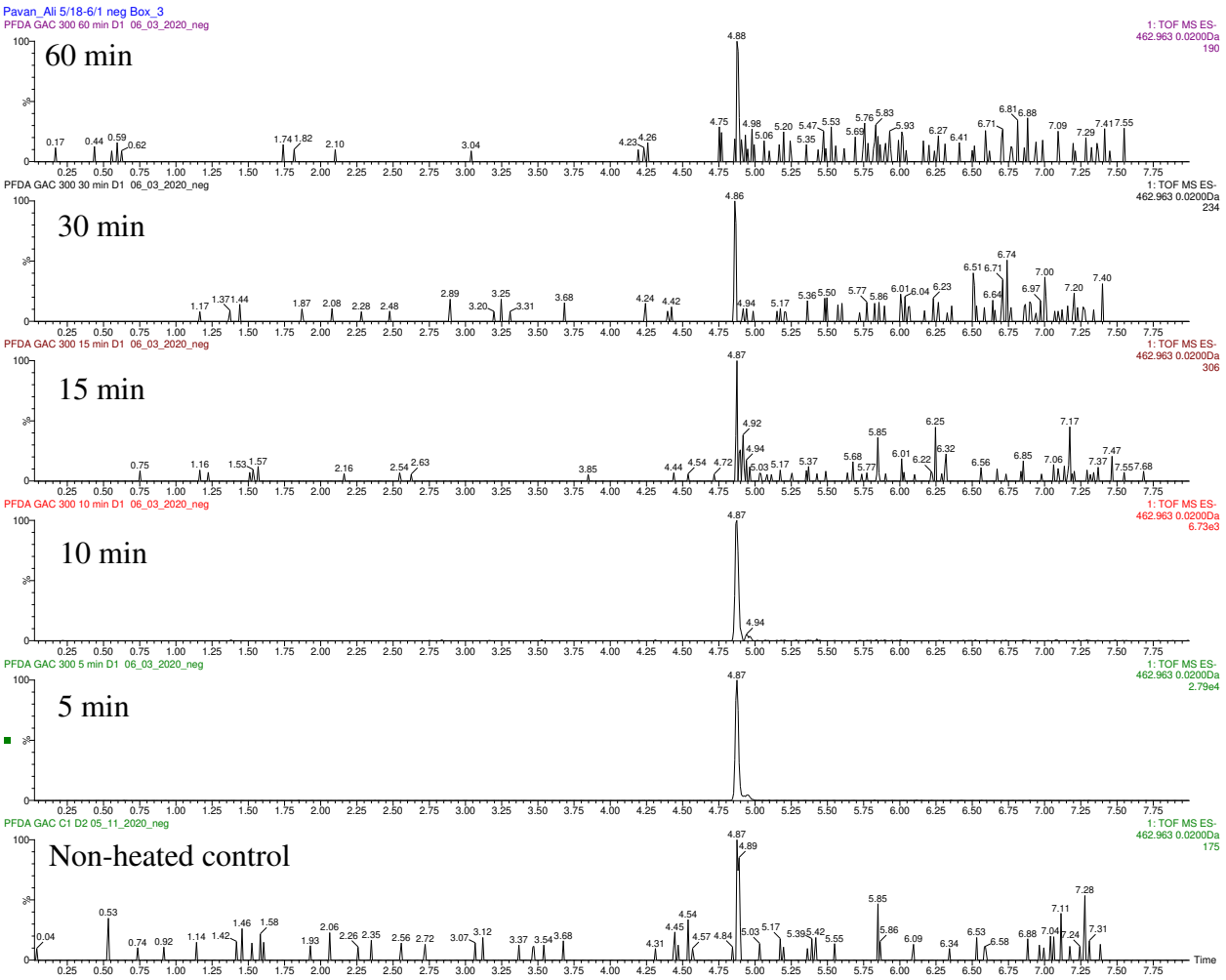

Figure B12. *UPLC–ESI⁻-ToF MS selected ion chromatograms on m/z 362.969 of methanol (with 100 mmol/L ammonium acetate) extracts of PFDA after T#2 (with the presence of GAC) thermal treatments at 300 °C for different times.*

The chromatograms show the generation and subsequent decomposition of PFNA (m/z 462.963; RT = 4.87 min) during thermal treatments of PFDA at 300 °C.

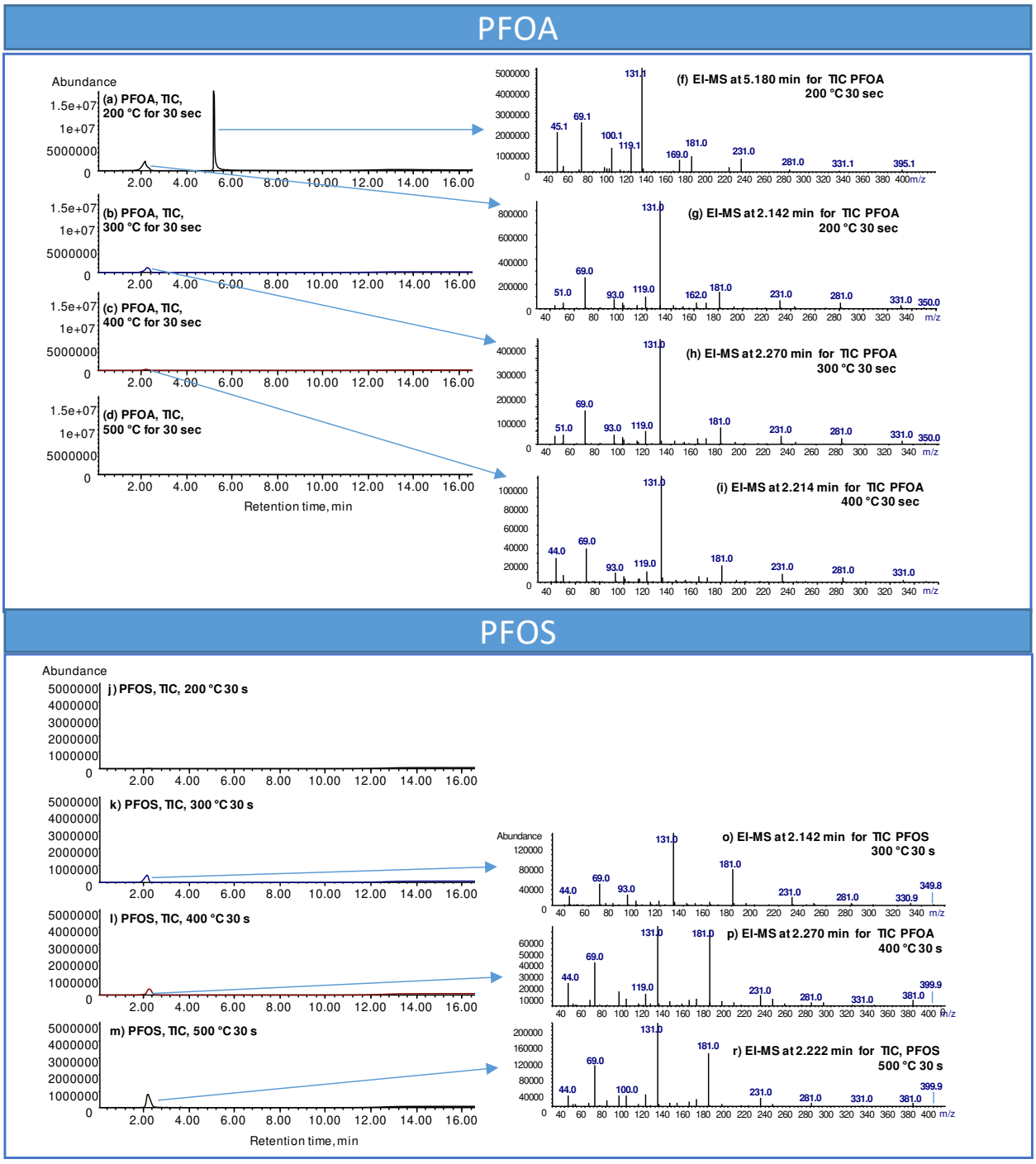

Figure B13. *TD–Pyr–GC–MS chromatograms (a–d and j–m) and mass spectra (f–i and o–r) of thermal decomposition products of PFOA (Xiao et al., 2020) and PFOS (this study) at different temperatures and predetermined durations.*

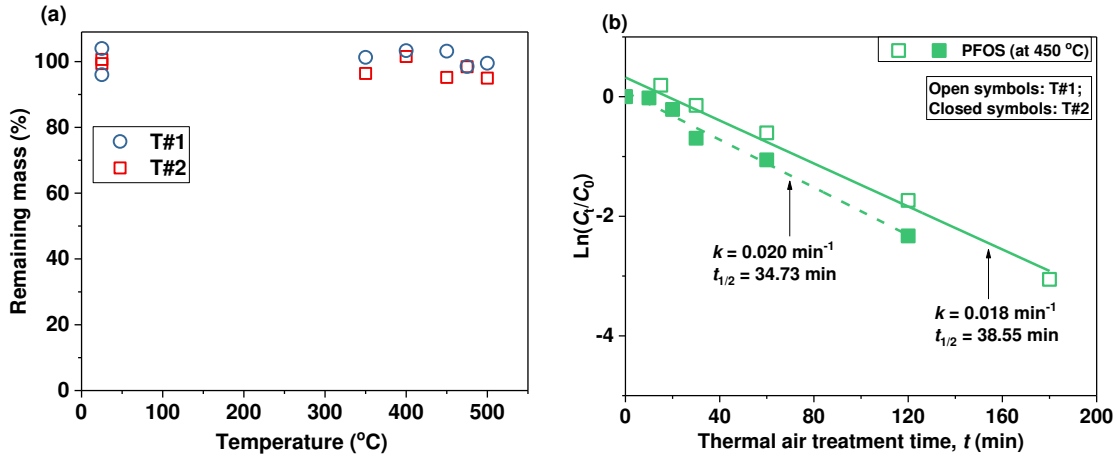

Figure B14. *(a) Decomposition of PFOS (1.2 × 10^{-5} mol) in a dynamic (10 °C/min) thermal environment. (b) Thermal decomposition of PFOS (1.2 × 10^{-5} mol) at 450 °C in T#1 and T#2 (with the presence of 0.1 g GAC) in a closed container.*

9. List of Publications

1. "*Effect of Granular Activated Carbon and Other Porous Materials on Thermal Decomposition of Per- and Polyfluoroalkyl Substances: Mechanisms and Implications for Water Purification*" ***Water Research***, 200, 117271, 2021. http://doi.org/10.1016/j.watres.2021.117271.
2. "*Thermal Decomposition of Anionic, Zwitterionic, and Cationic Polyfluoroalkyl Substances in Aqueous Film-forming Foams*" ***Environmental Science & Technology***, 55, pp. 9885–9894, 2021. https://doi.org/10.1021/acs.est.1c02125.
3. "*An Investigation of Thermal Air Degradation and Pyrolysis of PFAS and PFAS Alternatives in Soil*" ***ACS ES&T Engineering*** 2, 198–209, 2022. https://doi.org/10.1021/acsestengg.1c00335. (Supplementary Cover).
4. "*Thermal Decomposition of PFAS: Response to Comment on "Thermal Stability and Decomposition of Perfluoroalkyl Substances on Spent Granular Activated Carbon*" ***Environmental Science & Technology Letters***, 8, pp. 364–365, 2021. https://doi.org/10.1021/acs.estlett.1c00061.
5. "*Thermal Stability and Decomposition of Perfluoroalkyl Substances on Spent Granular Activated Carbon*" ***Environmental Science & Technology Letters*** 7, pp. 343–350, 2020.
6. "*Production of Granular Activated Carbon by Thermal Air Oxidation of Biomass Charcoal/Biochar for Water Treatment in Rural Communities: A Mechanistic Investigation*" ***Chemical Engineering Journal Advances***, 100035, 2020. doi.org/10.1016/j.ceja.2020.100035.